



National Library
of Canada

Bibliothèque nationale
du Canada

Acquisitions and
Bibliographic Services Branch

Direction des acquisitions et
des services bibliographiques

395 Wellington Street
Ottawa, Ontario
K1A 0N4

395, rue Wellington
Ottawa (Ontario)
K1A 0N4

Your file Votre référence

Our file Notre référence

NOTICE

The quality of this microform is heavily dependent upon the quality of the original thesis submitted for microfilming. Every effort has been made to ensure the highest quality of reproduction possible.

If pages are missing, contact the university which granted the degree.

Some pages may have indistinct print especially if the original pages were typed with a poor typewriter ribbon or if the university sent us an inferior photocopy.

Reproduction in full or in part of this microform is governed by the Canadian Copyright Act, R.S.C. 1970, c. C-30, and subsequent amendments.

AVIS

La qualité de cette microforme dépend grandement de la qualité de la thèse soumise au microfilmage. Nous avons tout fait pour assurer une qualité supérieure de reproduction.

S'il manque des pages, veuillez communiquer avec l'université qui a conféré le grade.

La qualité d'impression de certaines pages peut laisser à désirer, surtout si les pages originales ont été dactylographiées à l'aide d'un ruban usé ou si l'université nous a fait parvenir une photocopie de qualité inférieure.

La reproduction, même partielle, de cette microforme est soumise à la Loi canadienne sur le droit d'auteur, SRC 1970, c. C-30, et ses amendements subséquents.

UNIVERSITY OF ALBERTA

PROGRESS IN DEVELOPING TIME-OF-FLIGHT MASS
SPECTROMETRY FOR LIQUID CHROMATOGRAPHY
DETECTION

BY

ALAN PUI LING WANG



A thesis submitted to the Faculty of Graduate Studies and Research in partial
fulfillment of the requirements for the degree of Master of Science

DEPARTMENT OF CHEMISTRY

EDMONTON, ALBERTA

FALL 1992



National Library
of Canada

Bibliothèque nationale
du Canada

Canadian Theses Service Service des thèses canadiennes

Ottawa, Canada
K1A 0N4

The author has granted an irrevocable non-exclusive licence allowing the National Library of Canada to reproduce, loan, distribute or sell copies of his/her thesis by any means and in any form or format, making this thesis available to interested persons.

The author retains ownership of the copyright in his/her thesis. Neither the thesis nor substantial extracts from it may be printed or otherwise reproduced without his/her permission.

L'auteur a accordé une licence irrévocable et non exclusive permettant à la Bibliothèque nationale du Canada de reproduire, prêter, distribuer ou vendre des copies de sa thèse de quelque manière et sous quelque forme que ce soit pour mettre des exemplaires de cette thèse à la disposition des personnes intéressées.

L'auteur conserve la propriété du droit d'auteur qui protège sa thèse. Ni la thèse ni des extraits substantiels de celle-ci ne doivent être imprimés ou autrement reproduits sans son autorisation.

ISBN 0-315-77083-X

Canada

UNIVERSITY OF ALBERTA
RELEASE FROM

NAME OF AUTHOR: ALAN PUI LING WANG

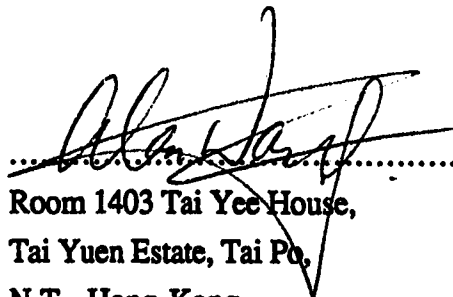
TITLE OF THESIS: PROGRESS IN DEVELOPING TIME-OF-
FLIGHT MASS SPECTROMETRY FOR LIQUID
CHROMATOGRAPHY DETECTION

DEGREE: MASTER OF SCIENCE

YEAR THIS
DEGREE GRANTED: 1992

Permission is hereby granted to the University of Alberta Library to reproduce single copies of this thesis and to lend or sell such copies for private, scholarly or scientific research purposes only.

The author reserves all other publication and other right in association with the copyright in the thesis, and except as hereinbefore provided neither the thesis nor any substantial portion thereof may be printed or otherwise reproduced in any material form whatever without the author's prior written permission.

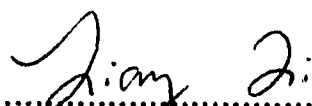

.....
Room 1403 Tai Yee House,
Tai Yuen Estate, Tai Po,
N.T., Hong Kong.

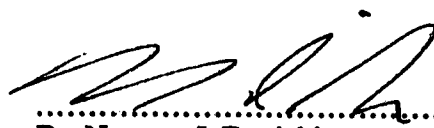
5/10/92


UNIVERSITY OF ALBERTA

FACULTY OF GRADUATE STUDIES AND RESEARCH

The undersigned certify that they have read, and recommend to the Faculty of Graduate Studies and Research for acceptance, a thesis entitled PROGRESS IN DEVELOPING TIME-OF-FLIGHT MASS SPECTROMETRY FOR LIQUID CHROMATOGRAPHY DETECTION submitted by ALAN PUI LING WANG in partial fulfillment of the requirements for the degree of MASTER OF SCIENCE.


.....
Dr. Liang Li (supervisor)


.....
Dr. Norman J. Dovichi


.....
Dr. Ronald T. Coutts

This work is dedicated to my parents, and my sister. Without their full support throughout the years, I would not have been able to go so far. I also dedicate this dissertation to my uncle and aunt for letting me have the opportunity to study in Canada.

Abstract

Multiphoton Ionization Mass Spectrometry (MPIMS) has been shown to be a powerful technique for analysis of biochemicals. When incorporated with Supersonic Jet Spectroscopy (SJS), a multidimensional detection scheme can be obtained. This SJS-MPIMS technique provides higher selectivity and higher sensitivity. Both soft and hard ionization can be obtained readily for molecular identification and structural analysis, respectively.

In the analysis of thermally labile and nonvolatile molecules in complex matrices, the combination of liquid chromatography with mass spectrometry (LC/MS) is normally used to obtain molecular and structural information. By combining SJS-MPI technique with time-of-flight mass spectrometry (TOFMS), a highly selective and sensitive detector for LC is available for the detection of thermally labile and nonvolatile molecules in complex mixtures.

In the first part of this thesis, the fundamental problems for SJ-MPIMS such as signal dilution along the axis of jet expansion and strong background build up in the ionization region have been examined. A solution to enhance signal intensity without degradation in mass resolution and supersonic jet cooling by using a cylindrical lens instead of spherical lens for ionization has been demonstrated. A method to reduce background signals in reflectron TOFMS based on different trajectories of signal ions and background ions attained on their way to the detector has been developed.

In the second part of this thesis, alternative methods for introducing thermally labile and nonvolatile molecules into supersonic jet expansions has been demonstrated. The first technique used here is fast atom bombardment (FAB). We have demonstrated that small biological molecules can be readily desorbed and entrained into a supersonic jet without significant thermal decomposition by using FAB. However, one of the advantages of this FAB method is that the FAB gun can be easily constructed and maintained at a low cost.

A second sample introduction method is interfacing time-of-flight mass spectrometry with conventional liquid chromatography. A pulsed sample introduction (PSI) interface has been developed which allows the coupling of LC to TOFMS. The construction of this PSI interface has been outlined and the performance of the PSI interface in terms of its applicability, reproducibility, sensitivity, quantitation, and transfer efficiency has been examined. The parameters that affect this PSI interface have also been evaluated. Finally, real applications of this PSI interface for on-line detection of LC/MS are shown.

Acknowledgments

I would like to take this opportunity to thank Dr. Liang Li for his guidance and encouragement throughout this work. I am also indebted to Dr. Li for his tremendous patience in teaching me the art of research. Without his enormous help, this work would not have been possible.

I also must thank all the personnel in the machine shop and the electronic shop of Chemistry Department, University of Alberta, for building and setting up the linear Time-of-Flight Mass Spectrometry and all the accessories for this work.

I also thank Dr. Horlick for his assistance in performing the numerical simulation program and Dr. Cantwell for his helpful comments in the LC work. I would like to thank David Gowanlock for performing the curve fitting program. I wish to thank Dr. F. Faraji for the proofreading of this thesis.

Finally, I would like to thank Chemistry Department, University of Alberta, the Natural Science and Engineering Research Council of Canada, and Alberta Environmental Research Trust for funding this work.

Table of Contents

Chapter	Page
1. Introduction	1
1.1. Multiphoton Ionization	2
1.2. Supersonic Jet Expansion	5
1.3. Interfacing Liquid Chromatography to Mass Spectrometry	11
1.4. TOFMS as a LC detector	16
2. Signal Enhancement and Background Reduction in a Supersonic Jet/Multiphoton Ionization Reflectron Time-of-Flight Mass Spectrometer	19
2.1. Introduction ..	19
2.2. Experimental	20
2.3. Results and Discussion	25
2.4. Conclusion	42
3. Pulsed Fast Atom Bombardment Sample Desorption with Multiphoton Ionization in a Supersonic Jet/Reflectron Time-of- Flight Mass Spectrometer	43
3.1. Introduction	43
3.2. Experimental	43
3.3. Results and Discussion	46
3.4. Conclusion	58
4. Pulsed Sample Introduction Interface for Combining Flow Injection Analysis with Multiphoton Ionization Time-of-Flight Mass Spectrometry	59
4.1. Introduction	59
4.2. Experimental	61

4.3. Results and Discussion	66
4.4. Conclusion	81
5. Liquid Chromatography/Time-of-Flight Mass Spectrometry with a Pulsed Sample Introduction Interface	84
5.1. Introduction	84
5.2. Experimental	85
5.3. Results and Discussion	85
5.4. Conclusion	101
6. Conclusion and Future Work	103
Bibliography	108

List of Tables

Table		Page
1.I.	LC-MS interfaces	14
1.II.	Characteristics of the most-widely used LC-MS interfaces	15
3.I.	Compounds Studied by the Fast Atom Bombardment/Supersonic Jet Multiphoton Ionization Technique	47
4.I.	Compounds Studied by FIA/MPI Mass Spectrometrywith the PSI Interface	66
5.I.	Sample Transfer Efficiency of the PSI Interface	97
6.I.	Publications	106

List of Figures

Figure	Page
1.1. Energy level diagram showing MPI transitions: (A) nonresonant MPI, (B) resonant two-photon ionization, (C) two-photon resonant REMPI.	3
1.2. Ladder switching mechanism.	6
1.3. A supersonic jet expansion.	8
1.4. Translational cooling process.	10
2.1. Schematic diagram of the main electrical elements in a reflectron time-of-flight mass spectrometer. Some dimensions are shown to indicate the size of the system.	21
2.2. Optics arrangement in the signal enhancement experiment. The shaded area between the extraction grid and repeller plate is the position where the beam size is measured.	23
2.3. The relative intensity of the molecular ion peak of aniline vs the laser beam size. I_p is the signal intensity of aniline peak obtained using a planar beam. I_c is the signal intensity of aniline peak obtained using a circular beam. Beam size refers to the diameter of the circular beam or the width of the planar beam (length=15 mm). The laser power density is about 5×10^6 W/cm ² and remains constant throughout the study.	26
2.4. The relations between mass resolution and the size of the laser beam for a planar and a circular beam.	28
2.5. Signal intensities of the molecular peaks of aniline(sample) and 9-methylanthracene(background) as a function of the delay time between the laser and the sample pulse with ion deflector voltages of (A) $V_{xy}=18$ V and (B) $V_{xy}=68$ V.	31

2.6.	Ion trajectories calculated by the Simion program with various deflector voltages(V_{xy}) of (A) -30 V, (B) 0 V, (C) 70 V, and (D) 130 V. Ions are simulated as being entrained into the field perpendicular to the flight tube axis with initial kinetic energies of (A) 0 eV, (B) 0.1 eV, (G) 0.2 eV, (D) 0.3 eV, and (E) 0.4 eV.	35
2.7.	Spatial separation of ions(Y-axis) with different initial kinetic energies as a function of the flight distance(X-axis) obtained by extrapolating the ion trajectories from Figure 2.6. Deflector voltages(V_{xy}) are (A) -30 V, (B) 0 V, (C) 70 V, and (D) 130 V. X-axis and Y-axis are defined as in Figure 2.1.	37
2.8.	Signal intensities of the molecular ion peaks of aniline(sample) and 9-methylanthracene(background) as a function of the ion deflector voltages in (A) a linear TOFMS with a 1-meter long flight tube and (B) a reflectron TOFMS. The time delay between the laser and the sample pulse is adjusted so that the laser ionizes the front portion of the sample pulse.	38
2.9.	MPI mass spectra of aniline sample and 9-methylanthracene background obtained with the ion deflector voltages of (A) 6 V, (B) 72 V, and (C) 126 V.	40
2.10.	MPI mass spectra of (A) aniline with background, (B) aniline and 9,10-dimethylanthracene with background, (C) aniline, and (D) aniline and 9,10-dimethylanthracene. Aniline is introduced into the jet directly with the expansion gas. 9,10-dimethylanthracene is introduced into the jet expansion by using laser desorption. The ion deflector voltage is 70 V for (A) and (B), 0 V for (C) and (D).	41
3.1.	Schematic of the experimental apparatus.	44

3.2.	Mass spectra of tryptophan obtained by the fast atom bombardment/supersonic jet multiphoton ionization technique at 266 nm. The ionization laser power density was (A) 1×10^6 W/cm ² , (B) 4×10^6 W/cm ² , and (C) 8×10^6 W/cm ²	48
3.3.	Mass spectrum of rubrene(molecular weight=532) obtained by FAB/SJMPI at 266 nm. The laser ionization power density was $\sim 1 \times 10^6$ W/cm ² . The molecular ion region is shown in the insert.	50
3.4.	Comparison of MPI mass spectra of Gly-Trp at 266 nm obtained by (A) using the fast atom bombardment method and (B) using the CO ₂ laser desorption method for sample introduction into the supersonic jet expansion. The ionization laser power density was about 1×10^6 W/cm ² . .	51
3.5.	Mass spectra of (A) 4-acetamidophenol and (B) Tylenol obtained by using the FAB/SJMPI technique. The ionization laser beam was a 266 nm radiation with its power density $\sim 1 \times 10^6$ W/cm ²	54
3.6.	MPI mass spectra of a mixture at 266 nm obtained by FAB/SJMPI: (A) tryptamine (M.W.=160) and indole-3-acetic acid (M.W.=175) (P= $\sim 4 \times 10^6$ W/cm ²); (B) tryptamine and indole-3-acetic acid plus NaOH (P= $\sim 5 \times 10^6$ W/cm ²); (C) tryptamine and indole-3-acetic acid plus NH ₄ OH (P= $\sim 4 \times 10^6$ W/cm ²).	56
4.1.	Schematic of the linear time-of-flight mass spectrometer for flow injection analysis.	62
4.2.	Schematic of the design of the pulsed sample introduction interface. Drawing is not to scale. The dimensions of the major components are given in the text.	64

4.3.	MPI mass spectra of (A) triphenylene, (B) 4-hydroxyl-3-methoxyphenylacetic acid(homovanillic acid), (C) 4-acetaminophenol, and (D) imipramine. The ionization laser beam was at 266 nm with its power density $\sim 1 \times 10^6$ W/cm ²	70
4.4.	MPI mass spectra of indole-3-acetic acid obtained by using (A) direct heating and (B) FIA with MPI. The ionization laser beam was at 266 nm with its power density $\sim 1 \times 10^6$ W/cm ²	71
4.5.	MPI mass spectra of (A) background, (B) aniline with background, (C) background with the LN2 trap filled, and (D) aniline with the LN2 trap filled. The ionization laser beam was at 266 nm with its power density $\sim 2 \times 10^6$ W/cm ²	74
4.6.	Flowgrams for repeated injections of different concentrations of indole-3-acetic acid.	76
4.7.	Calibration curves of tryptamine. The laser power density is 1×10^7 W/cm ² and the repeller voltage is 12.5 kV for (A). The laser power density is $\sim 1 \times 10^6$ W/cm ² and the repeller voltage is 5 kV for (B).	78
4.8.	Soft and hard MPI mass spectra of tryptamine obtained by FIA with MPI at 266 nm. The repeller voltages are 5 kV for (A) and (B), and 12.5 kV for (C) and (D). The ionization power densities are $\sim 1 \times 10^6$ W/cm ² for (A) and (C), and $\sim 1 \times 10^7$ W/cm ² for (B) and (D).	80
4.9.	MPI mass spectra of indole-3-acetic acid at different delay times: (A) Dt = 660 μ s and (B) Dt = 540 μ s. The ionization laser beam was at 266 nm with its power density $\sim 4 \times 10^6$ W/cm ²	82
5.1.	(A) UV chromatogram and (B) total ion chromatogram of a mixture of benzo[a]pyrene and triphenylene.	86

5.2.	(A) UV chromatogram and (B) total ion chromatogram of a mixture of indole-3-acetic acid, tryptamine, and tryptophol. The selected ion chromatograms of (C) indole-3-acetic acid, (D) tryptamine, and (E) tryptophol are obtained by monitoring the individual molecular ion peak only with the use of a boxcar integrator.	88
5.3.	Mobile phase flow rate dependence on the performance of the PSI interface. Indole-3-acetic acid is used as the test sample. Methanol is used as the mobile phase.	89
5.4.	Normalized peak area as a function of the water content in the methanol/water mobile phase. The flow rate is kept constant at 1 mL/min..	91
5.5.	Peak area as a function of the temperature of the sample vaporizer. Indole-3-acetic acid is used as the test sample. Methanol is used as the mobile phase at a flow rate of 1 mL/min.	93
5.6.	Peak area as a function of the temperature of the capillary tube. The LC conditions are the same as those used in Figure 5.5.	94
5.7.	Peak area as a function of the makeup gas flow rate. The LC conditions are the same as those used in Figure 5.5.	96
5.8.	A typical peak obtained by the LC/TOFMS system. The dot line is the experimental result from the injection of indole-3-acetic acid. The solid line is generated from the curve fitting program.	100

List of Abbreviations

CI - chemical ionization.

EI - electron impact.

FAB - fast atom bombardment.

FD - field desorption.

FI - field ionization.

FIA - flow injection analysis.

FWHM - full-width at half maximum.

GC - gas chromatography.

HPLC - high performance liquid chromatography.

IEV - ion-evaporation.

IP - ionization potential.

IR - infrared.

LC - liquid chromatography.

LD - laser desorption.

LDMS - laser desorption mass spectrometry.

LN2 - liquid nitrogen.

M⁺ - molecular ion.

MPI - multiphoton ionization.

MPIMS - multiphoton ionization mass spectrometry.

MS - mass spectrometry.

M.W. or MW - molecular weight.

PD - plasma desorption.

PAH - poly-aromatic hydrocarbon.

PC - personal computer.

PRH - pulsed rapid heating.

PSI - pulsed sample introduction.

REMPI - resonance enhanced multiphoton ionization.

R2PI - resonant two-photon ionization.

RSD - relative standard deviation.

SIMS - secondary ion mass spectrometry.

SJ - supersonic jet.

SJS - supersonic jet spectroscopy.

SJMPI - supersonic jet multiphoton ionization.

TC - thermocouple.

TOF - time-of-flight.

TOFMS - time-of-flight mass spectrometry.

TPRI - two-photon resonant ionization.

UV - ultraviolet.

VIS - visible.

Chapter 1

Introduction

Mass Spectrometry (MS) is one of the most important means amongst the various spectrometric techniques for chemical analysis. At present, MS remains the most sensitive method for molecular identification based on mass fragmentation patterns. These fragmentation patterns can be generated by methods such as electron bombardment or collision-induced dissociation, whereas other methods such as chemical ionization (CI), fast atom bombardment (FAB), plasma desorption (PD), matrix-assisted laser desorption (MALD), field desorption (FD), and secondary ion mass spectrometry (SIMS) can be used to obtain relatively soft ionization.

In the analysis of complicated mixtures, hyphenated methods are generally used to obtain sufficient discrimination among various components. These methods include gas chromatography/MS (GC/MS), liquid chromatography/MS (LC/MS), and tandem MS methods (MS/MS). These hyphenated techniques have become some of the most powerful tools for solving important problems including environmental trace analysis, pharmaceutical quality control, and structural analysis of biomolecules.

In this thesis, recent developments in combining multiphoton ionization (MPI) with mass spectrometry for the detection of biochemicals is reported. The progress of the development of a pulsed sample introduction (PSI) interface for interfacing liquid chromatography (LC) with time-of-flight mass spectrometry (TOFMS) is presented. For the first time we show the coupling of conventional liquid chromatography with time-of-flight mass spectrometry for the detection of thermally labile and nonvolatile chemicals in mixtures.

In this chapter, the basic concepts of multiphoton ionization and supersonic jet technique will be discussed and a brief review of different LC/MS interfacing techniques will also be included.

1.1. Multiphoton Ionization

The multiphoton ionization (MPI) technique involves the absorption of several photons by a molecule upon the irradiation with intense visible or ultra-violet (UV) light source [1- 49] resulting in the production of positive ions with the concurrent release of an electron. When the frequency of the excitation laser is tuned to a real intermediate electronic state, the cross-section of ionization is greatly enhanced. This technique is known as resonance-enhanced multiphoton ionization (REMPI). A molecule will ionize only if the sum of the absorbed photon energy exceeds the ionization potential of that molecule. However, if the laser frequency is not tuned to a real intermediate state, the probability of MPI will greatly reduce. Even though the ions are generated as the final product for the detection in mass spectrometry, the ion current obtained depends on the absorption cross-section of the molecule at the particular laser frequency. Thus, the plot of ion current as a function of laser frequency actually represents the absorption-excitation spectrum of the intermediate state. The uniqueness of MPI as an ionization source for mass spectrometry is that it can be employed as a means of achieving spectral selectivity of a target compound before mass analysis.

There are several means to induce MPI as shown in figure 1.1. The most commonly used MPI method in analytical chemistry is resonant-two photon ionization (R2PI) [23-47]. In this process, absorption of the first photon excites a molecule to an excited electronic state, i.e. $S_0 \rightarrow S_1$, and the second photon ionizes the molecule (see figure 1.1(B)). Thus, the sum of two photon energies must be greater than the ionization potential of the molecule for R2PI with the two photons either the same or different in frequencies. Since for most organic molecules, the ionization potentials (IP) are between 7 eV to 13 eV, a high-peak power, broadly tunable Nd:YAG laser or excimer-pumped frequency-doubled dye lasers in the UV region are commonly used for R2PI.

Other MPI processes such as two-photon resonant ionization (TPRI) or more generally, n-photon resonant ionization are possible. In these processes, two or more

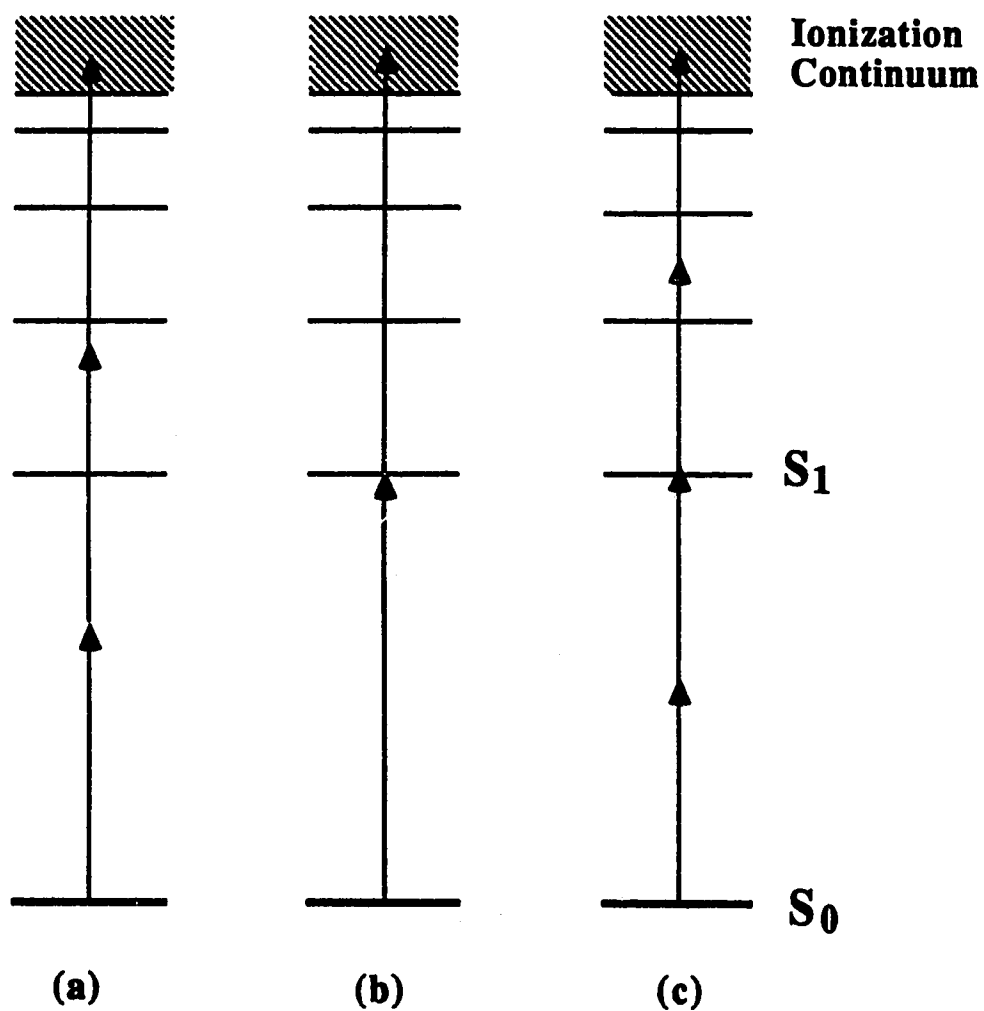


Figure 1.1. Energy level diagram showing MPI transitions: (A) nonresonant MPI, (B) resonant two-photon ionization, (C) two-photon resonant REMPI.

photons are required to reach the first resonance (see figure 1.1(C)). Since at least one photon is nonresonant and interacts with a short-lived virtual state ($< 10^{-15}$ sec), the efficiency for ionization in these processes is greatly reduced compared to the R2PI process. Totally nonresonant ionization is also feasible but requires higher laser power to drive this inefficient process (see figure 1.1(A)). In addition, the selectivity unique to the MPI process will be lost in this process.

R2PI has several unique features for mass spectrometry beside its potential for higher selectivity. R2PI is also amenable to the production of soft ionization in which only the molecular ion along with little or no fragmentation is obtained [17-21, 23-30, 33-36]. Although the full capability of this property has not been explored, soft ionization is generally obtained at moderate laser energies ($< 10^6$ W/cm²) for a wide range of organic compounds. For small aromatics such as aniline [23, 25, 28], benzene [8, 16, 21], and naphthalene [21, 28, 30], strong molecular ion peaks can be routinely obtained with little or no fragmentation. In more recent studies, relatively soft ionization have been obtained for other larger organic molecules, fragile biological molecules, and thermally labile molecules [28-30, 37]. The ability to generate only molecular ion peak can simplify the mass spectrum considerably and raises the possibility of identification according to molecular weight.

Although the parent molecular ion is the major product in most of the cases in R2PI at the laser power lower than 10^6 W/cm², this process is characterized by a high efficiency. Often ionization of up to several percent of the seeded molecules present in a molecular beam occurs without fragmentation [13, 14, 21, 29, 30, 33]. For aromatics such as aniline and naphthalene, ionization efficiencies ranging from 10 to 100 % have been estimated [21, 23, 26, 48]. This high ionization efficiency of R2PI contrasts sharply with that of the electron impact source which typically ionizes about 0.01 % of those molecules entering the ionization region in the mass spectrometer. Soft ionization with an electron beam can be obtained with a low electron beam energy, this will reduce the ionization cross-section

resulting in loss of ionization efficiency.

Multiphoton ionization can also produce extensive fragmentation by using higher laser power density or by varying the laser frequency for ionization. Zandee and co-workers [17-20], for example, have shown that C^+ is the dominant ion obtained from REMPI of benzene when the laser power density of about 10^9 W/cm^2 is used at 391.4 nm. When the laser power is varied, the fragmentation pattern will change accordingly, and different ratio of carbon fragments including $C_6H_n^+$, $C_5H_n^+$, $C_4H_n^+$, $C_3H_n^+$, $C_2H_n^+$, and CH_n^+ will be observed. Similar results were obtained in MPI as a function of laser power in the UV (300 - 260 nm) by numerous other investigators [10, 14, 21, 25-28]. The fragmentation process in these experiments occurs generally through ladder-switching processes (see figure 1.2) for most of organic molecules with a 10 ns laser pulse [49]. In this process, the molecular ion is initially produced by either R2PI or other MPI processes. When the laser power is increased, subsequent absorption of additional photons may take place and result in excitation to a state that dissociates, producing ionic and neutral fragments. These fragments can further absorb subsequent photons producing smaller fragments.

Therefore, the R2PI is a more versatile ionization technique for mass spectrometry that can produce soft ionization or very extensive fragmentation via successive up-pumping processes. This can be accomplished by simply changing the laser power. Moreover, the laser source can produce high appearance potential fragments with relative ease by increasing the laser energy and in some cases can produce unusual fragments that are not readily obtained with electron impact [39].

1.2. Supersonic Jet Expansion

One of the critical considerations in using MPI is the sample introduction because the handling of sample will affect the initial absorption contour of the molecules. For the early experiments, either bulks or effusive molecular beams were used. However, under

Ladder Switching

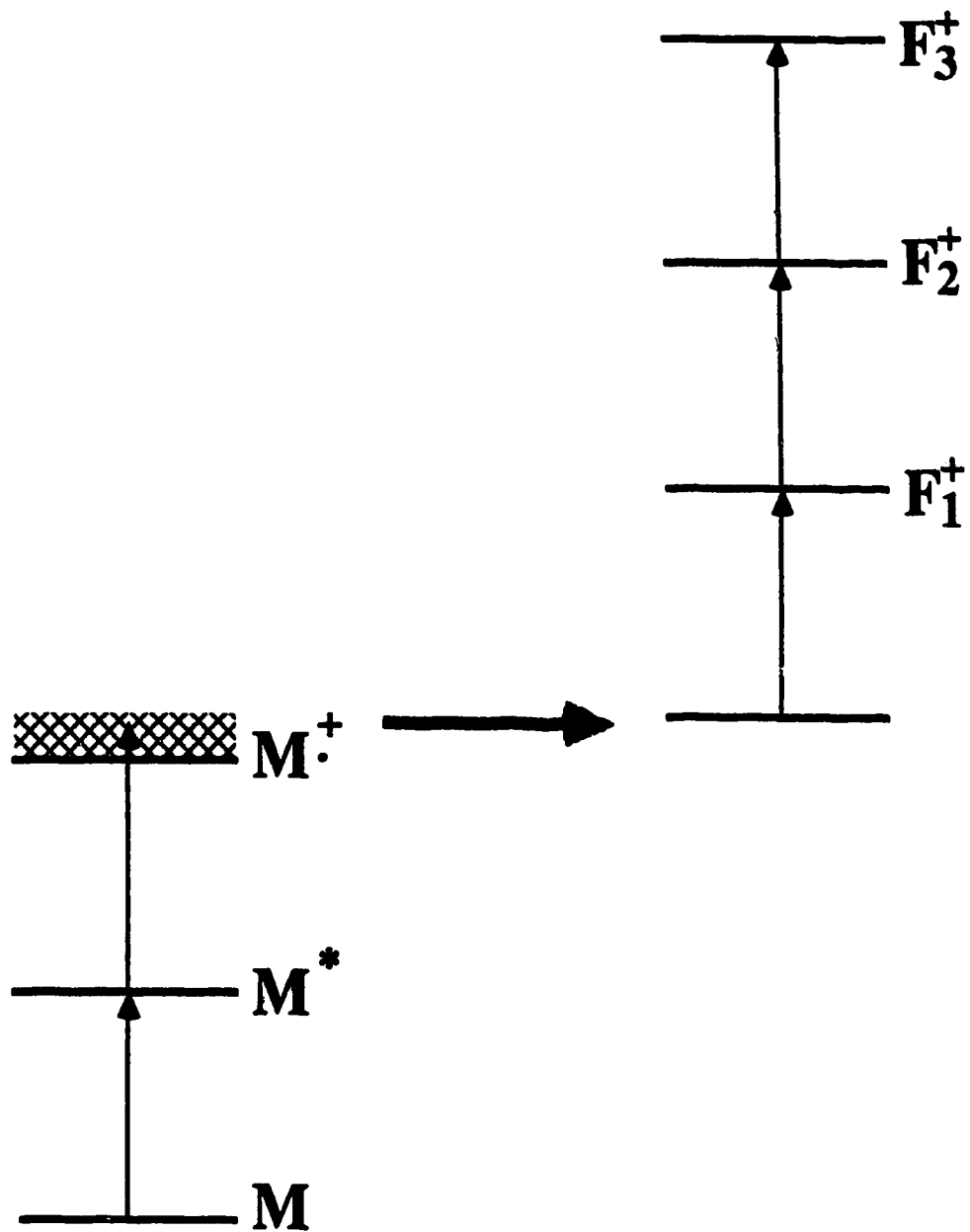
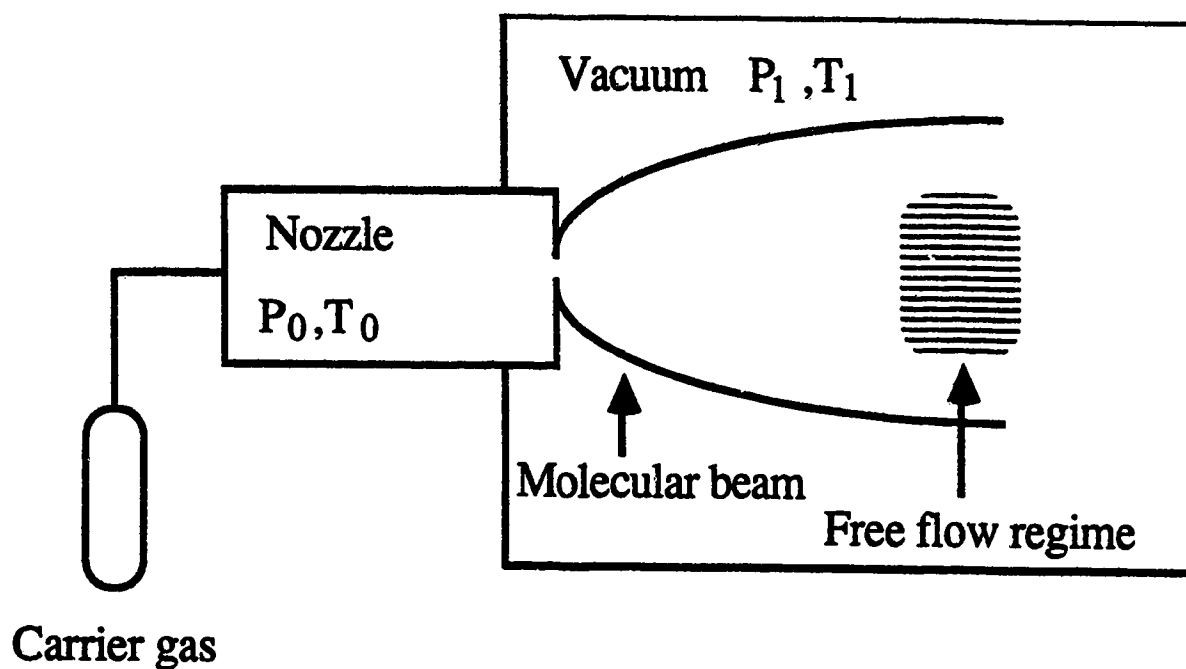


Figure 1.2. Ladder switching mechanism.

these situations, the laser probes a Boltzmann distribution of molecules, which is determined by the temperature of the source. One might expect that the potential selectivity of R2PI will be limited under this situation because the gas phase UV-visible spectra of larger polyatomic molecules are very broad and basically structureless due to the thermal population of a large manifold of internal states.

The supersonic jet technique can be used to enhance the selectivity of R2PI in the molecular systems since the broad contour observed due to the thermal conditions can be cooled down so that the structure collapses down to several sharp peaks. A supersonic jet is formed by expanding a carrier gas such as argon through a small orifice in a nozzle into a vacuum (see figure 1.3) [50-59]. There are two criteria for the generation of supersonic jet. First, there must be a large pressure gradient across the orifice. The typical pressure in the nozzle is about one atmosphere while the pressure in the vacuum is always lower than 10^{-4} torr. Another requirement for generating a supersonic jet is that the diameter of the orifice must be greater than the mean free path of the expanding gas in the nozzle so that a large numbers of collisions can take place during the expansion. If a small amount of sample is introduced into the nozzle and the mixture is expanded into the vacuum through the orifice, then a seeded molecular beam expansion is formed.

There are several salient features associated with supersonic jet expansion. The most important feature is translational cooling which takes place during the jet expansion. In the early stage of the expansion, the gas flow through and downstream of the orifice is a hydrodynamic process. This hydrodynamic process converts the random motions of the carrier gas into a directed mass flow. The translational temperature is defined by the width of the Maxwell-Boltzmann velocity distribution as shown in figure 1.4 (A). Before the expansion, the velocity distribution of the carrier gas is quite broad (see figure 1.4(B)) but after expansion, the velocity distribution in the direction of mass flow becomes narrow resulting in translational cooling (see figure 1.4(C)). The typical translational temperature of the expanding gas is less than 1° K [57, 58].



Features of Supersonic Jet Expansion

- Translational cooling
- Free flow regime without collision

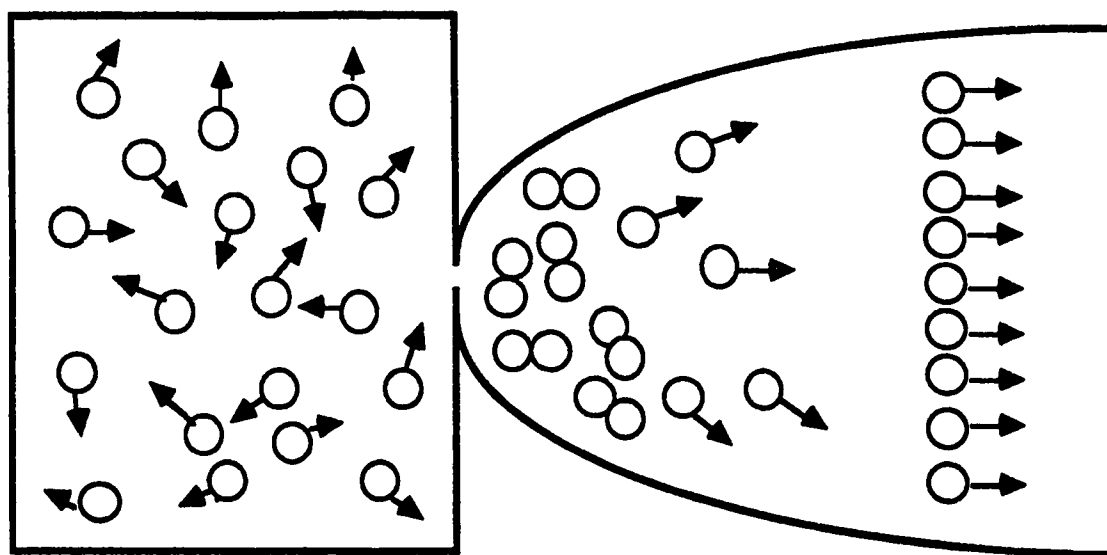
Figure 1.3. A Supersonic Jet Expansion.

Another important feature of supersonic jet expansion is that a "free flow" regime is obtained. As the expansion proceeds from the orifice, collisions between expansion gases and sample molecules continue, the translational temperature continues to drop as a function of the distance from the orifice. At some point, the density in the expansion becomes so low that no collision occurs to maintain cooling, and the free flow regime is reached. This free flow regime is basically collisionless and the final temperature is achieved. Most of the analytical measurements take place in this region because the matrix effect with complex mixture is eliminated.

For the supersonic jet experiment, a small amount of sample is mixed with a large quantity of the carrier gas and the mixture is then expanded through the small orifice to form the molecular beam. For each molecule, there are three motions: translational, vibrational and rotational motion. During the supersonic jet expansion, there are large number of collisions between the sample molecules and the carrier gas molecules resulting in the transfer of vibrational and rotational energy of the sample molecules to the carrier gas molecules. Since the energy exchange between molecular rotational motion and atomic translational motion is extremely fast, the molecular rotational temperature is similar to the atomic translational temperature of the carrier gas, that is, less than 1° K. On the other hand, the energy exchange between the molecular vibrational motion and the atomic translational motion is much slower, so the vibrational temperature of the molecule is above the translational temperature but well below the original temperature. The typical vibrational temperature of the molecule is less than 150 ° K [57]. Thus, the supersonic jet expansion can be used to prepare ultra cold, isolated gas phase molecules for spectroscopic applications.

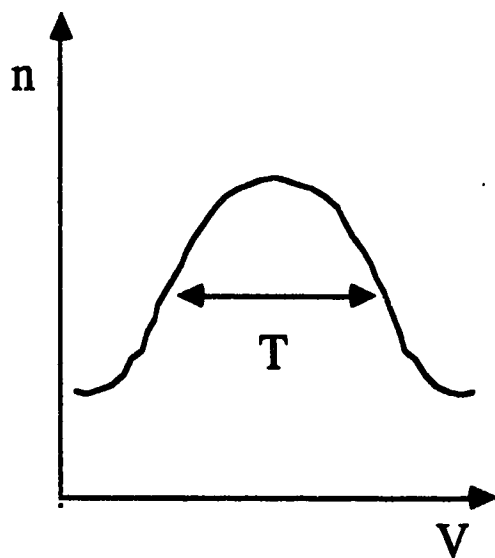
A key point of supersonic jet expansion is that a high on-axis intensity is achieved as a result of directed mass flow. This high on-axis intensity means enhancement of the sensitivity of detection for this technique. In typical supersonic jet expansion of Ar carrier gas, the on-axis density is generally 10^{14} to 10^{15} molecules/cc [21]. Although it is always

Translational cooling process

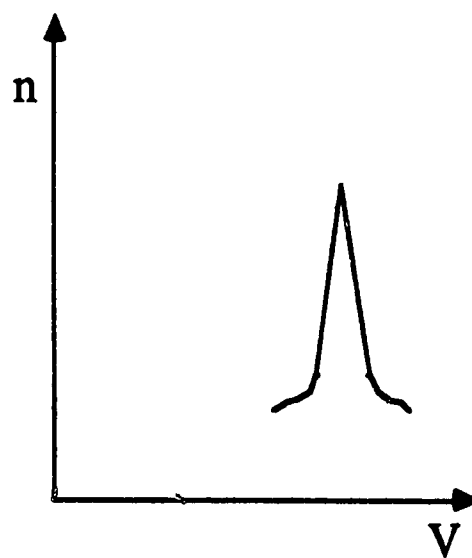


Nozzle

(a)



(b)



(c)

Figure 1.4. Translational cooling process.

desired to work with the free flow region to achieve selectivity, the on-axis density in the beam decrease as $1/X^2$, where X is the distance from the orifice, so it is necessary to balance between the need for sensitivity and selectivity for a particular real sample analysis.

1.3. Interfacing Liquid Chromatography to Mass Spectrometry

Combining chromatography with mass spectrometry offers the possibility of taking advantage of both chromatography as a separation method and mass spectrometry as an identification method. At present, the combination of high resolution gas chromatography and mass spectrometry (GC/MS) remains the most commonly used technique for the elucidation of structural information of the components in a complex mixture. However, only those compounds that are amenable to GC can be analyzed by GC/MS. Nonvolatile compounds such as larger polyatomic molecules, and thermally labile molecules cannot be analyzed by GC/MS readily. Thus, another chromatographic technique such as liquid chromatography (LC) is required to combine with mass spectrometry for the analysis of nonvolatile, and thermally labile compounds.

Combining LC with MS for the on-line analysis is not as simple as combining GC with MS. The difficulties in coupling LC with MS are well documented [60-63]. These problems include the amount of column effluent that has to be introduced into MS vacuum system, the composition of the eluent, and the type of analytes that must be analyzed. In order to solve these problems, different types of interfaces have been developed for specific separation problems as well as the specialized MS systems.

For interfacing LC with MS, both LC and MS point-of-view should be considered. In terms of LC operation, the interface should be able to handle any mobile phase composition and work under both isocratic and gradient elution. The interface should be able to handle additives in mobile phase such as volatile and nonvolatile buffers or ion-pair reagents without any difficulties. Of course, the most crucial requirement is the capability to handle mobile phase flow rate between 1 μ L/min to 2 mL/min. The interface itself

should have high sample transfer efficiency so that no or minimum analyte is lost. No additional peak broadening effect introduced by the interface is favorable. More important, the interface should not impose any degradation in resolution of eluted peaks from LC. The mass spectrometer that is used as detector for LC should provide qualitative information based on mass spectra for reliable molecular identification. The pumping capacity of the mass spectrometer should be high enough to handle large amount of liquid/gas introduced from LC and still maintain a low enough pressure in the source for ionization of analytes. Moreover, any interference from the solvent should be reduced to a minimum or completely eliminated so that it will not interfere with the analyte signal. In addition, the LC-MS system should be simple to operate, able to do quantitation, and have low detection limit.

During the progress in developing LC-MS interface, flow rate incompatibility of LC and MS is the most challenging problem. There are some solutions for handling high flow rate from conventional LC such as enlarging pumping capacity of MS system, removal of solvent or splitting prior to MS introduction, miniaturization of LC columns, and use of atmospheric-pressure ion source. With many interfacing development in the field, combination of various means are necessary. On the other hand, when LC column flow rate is too small, usually in nL/min range, then a make-up flow rate is introduced to maintain proper operation of the interface.

The mass spectrometers used in coupling with LC should combine several important analytical features. They include high sensitivity, selectivity, and applicability for most of organic compounds. The other important factor to determine the suitability of particular MS as a detector for LC work is the scanning rate or in more general terms, the rate to acquire data from eluted peak. In order to avoid loss in resolution of eluted peak, MS should obtain enough data points over the entire eluted profile of chromatographic peak for reconstructing the eluted peak. At present, the most commonly used MS systems for LC-MS are sector and quadrupole instruments [91, 101-113]. For scanning instrument,

scanning time depends on scanning mass range. In general, better mass resolution is obtained with longer scanning time [64] but loss of resolution of the eluted peaks are unavoidable. At present, a scan rate up to 1ms [65] per m/z -value is possible. However, when the mass range becomes larger, the limited scan rate will be a problem to obtain good resolution.

The most commonly used ionization techniques in LC-MS are electron impact (EI), chemical ionization (CI), fast atom bombardment (FAB), and ion evaporation (IEV). Except EI which is a hard ionization method that provides structural information for structural analysis, all the other techniques are soft ionization techniques which give only molecular information. For most of the interfaces developed over the years, only few of them can access to EI ionization and the rest of them are subjected to soft ionization techniques.

Over the past twenty years, starting in 1972 with the first LC-MS publication by the Russian group, Tal'roze *et al.* [66], the development of the LC-MS method has been continuous in the form of the introduction of different types of interfacing techniques. This has led to a vast number of papers on successful applications and to several successful commercially available LC-MS interfaces [91, 101-109]. Table 1.I shows a complete list of the interfaces reported in literature. The details of these interfacing techniques will not be discussed here and can be found in the literature [65].

Table 1.I LC-MS interfaces [65]

Year	Type of interface
1972	Stopped-flow
1972	Capillary inlet
1974	Moving belt
1974	Pneumatic nebulizer in atmospheric pressure source
1975	Solvent vapor separator membrane
1976	Liquid ion evaporation
1978	Crossed beam
1978	Jet separator
1979	Vacuum nebulizer
1980	Direct liquid introduction
1981	Conical tip
1981	Continuous sample preconcentration
1982	Rotating disk
1983	Helium
1983	Thermospray
1984	Monodisperse aerosol generator
1985	Electrospray
1985	Frit FAB
1986	Continuous-flow FAB
1986	Particle-beam
1986	Heated nebulizer
1987	Thermal beam
1987	Gas nebulized
1987	Ionspray
1988	Atmospheric-pressure spray
1989	Frit-EL/CI

From table 1.I, the development of LC-MS interfaces can be divided into three main streams: the development of an LC-MS interface that can handle 1 mL/min of aqueous column effluent, the development of analyte-enrichment interface, and the development of an interface that gives additional ionization possibilities. In order to get a clear picture of

the characteristics of these interfaces, a summary of the operation conditions of these interfaces is given in table 1.II.

Table 1.II Characteristics of the most-widely used LC-MS interfaces [65]

Interface	Max.flow rate($\mu\text{L}/\text{min}$)	Composition	Ionization technique
moving-belt	2000	NP	EI, CI, FAB
	500	RP	
direct liquid introduction	50	RP, B	LCI
thermospray	2000	RP, B	LCI, IEV
continuous-flow FAB	15	RP, B	FAB
frit FAB	5	RP	FAB
particle-beam	500	RP, NP, B	EI, CI, FAB
thermabeam/universal	1000	RP, NP, B	EI, CI, FAB
electrospray	10	RP, B	IEV, LCI
ionspray	100	RP, B	IEV, LCI
heated nebulizer	2000	RP, NP, B	APCI, IEV

NP=normal-phase chromatography with organic solvents, RP=reversed-phase chromatography with aqueous-organic solvent mixtures, B=volatile buffers.

EI=electron impact, CI=chemical ionization, LCI=solvent-mediated chemical ionization, IEV=ion evaporation, FAB=fast atom bombardment, APCI=atmospheric-pressure chemical ionization.

1.4. TOFMS as a LC detector

As mentioned before, for most of LC-MS experiments, a sector or quadrupole instrument is used. The main disadvantages of these instruments are limited mass range, lower ion transmission efficiency and lower scan rate. However, the use of a time-of-flight mass analyzer as a LC detector offers several unique advantages over these commonly used scanning mass spectrometers: higher ion transmission, able to obtain up to ten thousand complete mass spectra per second, and no mass limit. Moreover, the time-of-flight mass spectrometer is very simple to construct and yet inexpensive compared to other scanning mass spectrometers.

The time-of-flight mass spectrometer is well suited for pulsed operation, and detects ions in a discrete form. Higher ion transmission efficiency is attained by TOFMS since all ions generated in the ionization region are transmitted through a drift tube and subsequently detected by the microchannel plate detector. This higher ion transmission results in increasing detection sensitivity of TOFMS as a detector for LC.

One of the distinguished advantages of TOFMS as an ideal candidate for LC detector is its ability to obtain up to 10,000 complete mass spectra in a second [64]. This feature is extremely important for chromatographic detection. For conventional LC elution, the peak width of a particular chromatographic peak is normally in the range of about 20 seconds. Sufficient number of mass spectra per chromatographic peak must be obtained in order to retain eluted peak shape and resolution. With the use of TOFMS, theoretically 200,000 mass spectra can be acquired over the entire elution profile of a peak, which is sufficient to reconstruct the chromatographic peak without losing resolution of the eluted peak.

The other important feature of TOFMS is its ability to detect high mass. For most scanning mass spectrometers, mass range up to several thousand dalton can be obtained. TOFMS on the other hand has no ultimate mass limit. In fact, large proteins with molecular weights up to 300,000 Da. have been detected by TOFMS [67].

Besides all the advantages TOFMS offers, it also suffers some drawbacks as a LC detector. The most well known weakness of TOFMS is its poor mass resolution. Mass resolution of TOFMS is degraded by initial space and energy variations and the presence of metastable decomposition products in the ion optical path [54]. However, with the use of reflectron TOFMS, mass resolution up to 10,000 has been reported [74, 75].

The duty cycle of TOFMS is another limitation for it to be a effective chromatographic detector. The inability of TOFMS to detect the chromatographic effluent continuously causes a severe loss in sample sensitivity. In the light of fact that a TOFMS detects ions in a pulsed form, it is highly desirable to introduce chromatographic effluent into TOFMS in a pulsed form instead of continuous form in order to increase the duty cycle of TOFMS.

By using MPI as the ionization source, TOFMS becomes a more powerful method for LC detection. Some of the most outstanding characteristics of this system are: the ability to obtain both soft and hard ionization mass spectra, higher sensitivity, and higher selectivity.

The goal of our work is to develop a LC/TOFMS system that has the following characteristics.

- (1) Have high sensitivity with pg or low ng detection limits.
- (2) Have mass resolution above 2000.
- (3) Provide qualitative information based on laser ionization and/or electron impact mass spectra for reliable molecular identification.
- (4) Be able to perform on-line quantitation with high precision.
- (5) Be able to detect most compounds of interest in environmental samples.
- (6) Be reliable and convenient to operate.

In order to accomplish this goal, recently we developed a pulsed sample introduction (PSI) interface specifically suited for TOFMS. Since this PSI interface introduces sample in a pulse form instead of continuous form, the duty cycle of TOFMS

can be enhanced while still maintaining the low system pressure for ionization. This PSI interface can accept LC effluent of up to 1.6 mL/min without splitting and most of organic, aqueous or any combination of these solvents can be introduced into the system readily. The details of this PSI interface is given in Chapter 4 and successful applications of this PSI interface for on-line LC/MS detection of mixture is illustrated in Chapter 5.

Chapter 2

Signal Enhancement and Background Reduction in a Supersonic Jet/Multiphoton Ionization Reflectron Time-of-Flight Mass Spectrometer

2.1. Introduction

Supersonic Jet-Multiphoton ionization mass spectrometry (SJ-MPIMS) has been shown to be a very powerful technique for chemical analysis. In particular, when it is combined with various desorption techniques such as laser desorption (LD) [69,70], fast atom bombardment (FAB) [71], and pulsed rapid heating (PRH) [72] for sample vaporization, thermally labile and nonvolatile species can be studied. However, there are few problems associated with SJ-MPIMS. The first question arose when sample entrained into the supersonic jet and carried into the ionization region, sample dilution and expansion along with the jet expansion of the carrier gas are unavoidable and consequently reduces the ultimate sensitivity of the SJ-MPIMS technique. Associated with SJ-MPIMS with desorption techniques, another problem is the high-intensity background for sample vaporization. In FAB, PRH or LD/SJ-MPIMS, the nonvolatile molecules are first vaporized and then carried into the ionization region of the TOFMS. During this process, samples may condense on the wall of the vacuum chamber and the electric lens assembly of the TOFMS. These molecules and their decomposition products will eventually form the background for subsequent analyses. This cross-contamination can become quite severe because the turn-around-time of the system is usually very short, i.e., less than 5 minutes. Due to the possible overlap of the molecular ion and fragments with the background signals, the sensitivity for the detection of molecules of interest is often reduced, and also the structural information obtained from the mass fragmentation pattern suffers.

In this chapter, a simple technique for signal enhancement by using a cylindrical lens to provide a planar laser beam instead of a circular laser beam for ionization is

described. In MPI, the ionization signal is a function of the portion of the molecules intersected by the laser beam, thus using a larger size of a laser beam will result in signal enhancement of the analyte. We show that the use of a cylindrical lens to provide a planar laser beam instead of a circular beam enhances the signal from about 4 to 16 times depending on the laser beam sizes, i.e., the diameter of the beam for a spherical lens or the width of the beam for a cylindrical lens, without losing resolution. Even with a large planar beam (e.g., length=15mm, width=5mm), resolution above 2000 can be achieved. In addition, supersonic jet cooling can still be obtained.

Next, we describe a method for this background reduction in FAB, PRH and LD/SJ-MPIMS. This method involves (1) the use of an ion deflector in a supersonic jet/reflectron TOFMS, and (2) the optimization of the time delay between the sample pulse and the ionization laser pulse, to selectively detect the sample ions from background interference. If the sample in the jet expands to the ionization region at a velocity perpendicular to the acceleration field or ion flight axis, the ions generated from the sample (sample-ion-packet) will have different linear velocities from the ions originating from the background molecules (background-ion-packet). Thus they will travel to the detector with different trajectories. If there is a sufficient spatial separation between these two ion packets when they arrive at the detector, then, by selecting a proper ion deflector voltage, the sample-ion-packet can be selectively detected by the detector. We demonstrate here that the background can be significantly reduced by using the ion deflector in a reflectron TOFMS.

2.2. Experimental

The experimental setup for supersonic MPI is shown in Figure 2.1. The system consists of an angular reflectron time-of-flight mass spectrometer (R.M.Jordan Co., California) mounted vertically in a six-port cross pumped by a 6-in diffusion pump. A pulsed nozzle (R.M.Jordan Co., California) with a 50- μ s pulse width is used to form a

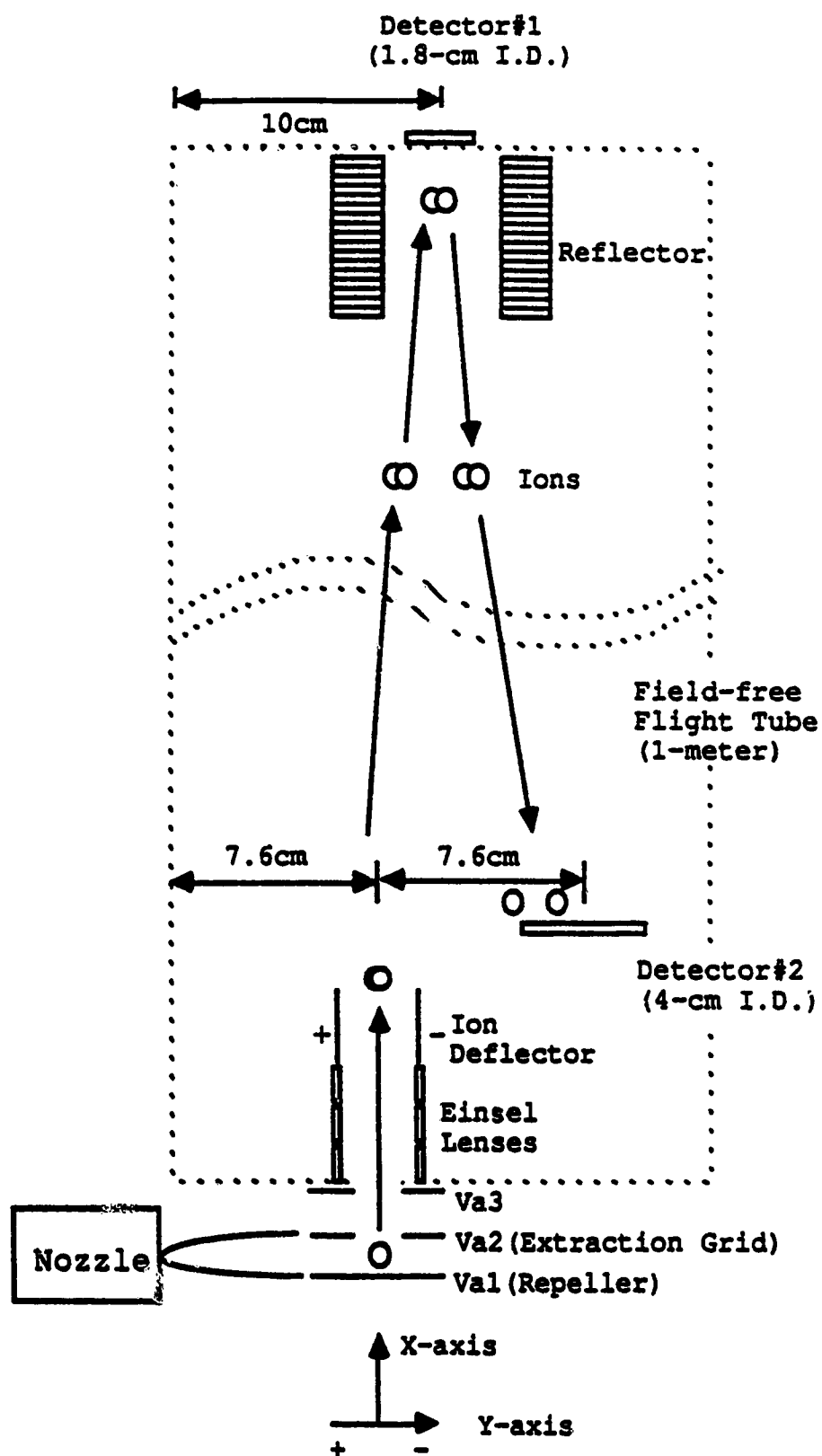


Figure 2.1. Schematic diagram of the main electrical elements in a reflectron time-of-flight mass spectrometer. Some dimensions are shown to indicate the size of the system.

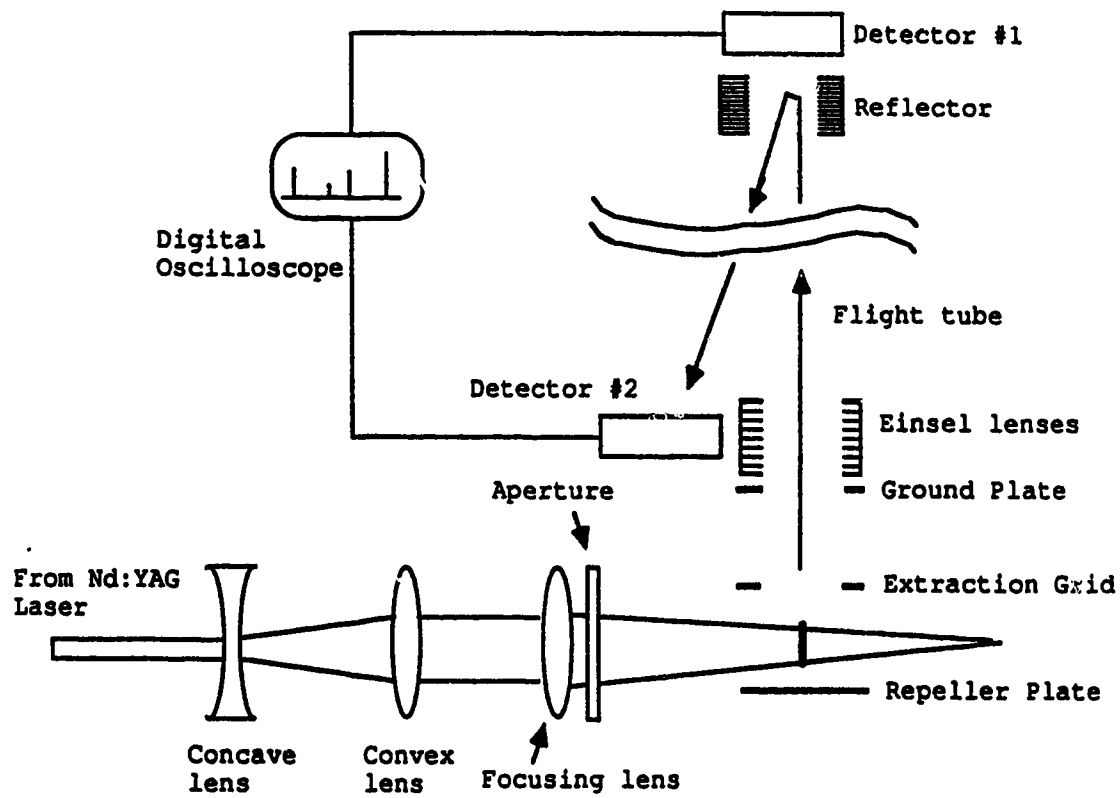


Figure 2.2. Optics arrangement in the signal enhancement experiment. The shaded area between the extraction grid and repeller plate is the position where the beam size is measured.

supersonic jet. CO_2 is used as the expansion gas throughout this work. The jet expands into the acceleration region of the TOF and a laser beam perpendicular to both the jet and flight tube ionizes the sample. The main test chamber is pumped by a 6-in diffusion pump (Varian Associates, Inc., Massachusetts). The flight tube is differentially pumped by a 4-in. diffusion pump (Varian Associates, Inc., Massachusetts). The pressure in the flight tube is usually below 2×10^{-7} Torr and the pressure in the ionization region is $< 10^{-6}$ Torr.

The ionization laser beam is a 266 nm radiation with a 7-ns pulse width from a frequency quadrupled Nd:YAG laser (GCR-3, Spectra-Physics, Mountain View, CA). The diameter of the beam directly from the laser is about 8 mm. A combination of one convex and one concave spherical lens is used to focus the laser beam to a 2-mm-diameter spot in most of the experiments and this beam can also be expanded up to 20 mm by using a combination of a concave and a convex lens (see Figure 2.2). The expanded laser beam is then focused into the ionization region of the TOFMS with either a cylindrical lens (focal length = 152 mm) to generate a planar beam or a spherical lens (focal length=150 mm) to generate a circular beam. The 25.4-mm-in-diameter cylindrical lens is made of UV grade fused silica (ESCO, Oak Ridge, NJ) and can be easily mounted to a regular lens holder used for a spherical lens. Different sizes of rectangular aperture or circular aperture are inserted in between the lens and the focal point to generate various sizes of laser beam. The length of the planar beam is fixed at 15 mm while the width of the beam can be varied. The planar beam is so aligned that the long direction (length = 15 mm) is parallel to the jet expansion direction. The focal point is located about 30 mm away from the center of the repeller plate to avoid local excess ionization. The laser beam size can be measured by using a heat-sensitive paper to display the beam profile. The beam size given below refers to the size of the laser beam at the plane passing through the centers of the repeller plate and the extraction grid. The diameter of the extraction grid is 1.5 cm. The laser power is measured with a Ophir Model 10A-MED-AN laser power/energy meter (Diamond Ophir Optics, Wilmington, MA).

Our mass spectrometer is so designed that immediately after ionization, ions will be repelled by the repeller plate and drawn through the extraction grid. A set of Einsel lenses placed just above the extraction grid can be used to focus the ions. A pair of deflection plates, i.e., the ion deflector, is placed above the Einsel lenses to control the trajectory of ions traveling towards the microchannel plate detector. Our system consists of two ion detectors. One is placed behind the reflecting field which is at the end of the flight tube so that this system will function the same as a linear TOFMS when the reflecting field is turned off. When the field is on, ions will be reflected. Thus the other detector is placed near the extraction grid at the other end of the flight tube. The mass resolution of aniline is about 300 and 2000 for linear and reflectron TOFMS. The mass spectrum is recorded by a LeCroy 9400A digital oscilloscope and data stored in an IBM compatible 386SX PC for processing.

LD/SJ-MPI study is carried out with a pulsed CO₂ laser (Allmark model 852, A-B lasers Inc., Acton, MA) which generates a 10.6 μm IR radiation with a 75-ns initial pulse and 2- μs tailing. The repetition rate of the laser can be adjusted from 0.1 Hz to 15 Hz, although 10 Hz is used here. In LD/SJ-MPI, a 1 cm diameter NaCl window in a 2" flange is used. The IR beam from the CO₂ laser is reflected by copper mirrors protected with gold coating (CVI Laser Corp., Albuquerque, NM) and focused on the sample probe by a germanium plano convex lens (Janos Technology Inc., Townshend, VT).

The actual sequence of events is controlled by several delay generators. The CO₂ laser beam is first turned on to desorb the sample, the pulsed nozzle opens to form a supersonic jet, and then the sample is entrained into the jet and carried into the ionization region of the TOFMS where the ionization proceeds.

All chemicals were purchased from Sigma Chemical Co., St. Louis, MO or Aldrich Chemical Co., Milwaukee, WI and used without further purification.

2.3. Results and Discussion

Signal Enhancement. Since the ionization signal intensity is directly related to the number of molecules within the interaction region between the laser beam and the molecular beam, any increase of the beam size will enhance the signal intensity. Indeed, we have found that the signal intensity increases with the increase of the diameter (D) of the circular beam for a spherical lens or the width (W) of the planar beam for a cylindrical lens. The use of a planar laser beam instead of a circular beam (when $D=W$) increases the ionization area. Thus signal enhancement by using a cylindrical lens can be obtained. Figure 2.3 shows the relative intensity between the molecular ion peak intensity when a cylindrical lens is used and that when a spherical lens is used at different laser beam sizes (D or W). This figure is obtained at a laser power density of about 5×10^6 W/cm [69]. When the laser power is slightly increased, fragment ions are observed. As Figure 2.3 shows, signal enhancement from about 4 to 16 times can be achieved depending on the size of the beam by simply using a cylindrical lens.

The signal enhancement which can be achieved seems to depend on the geometry of ion extraction and ion focusing. In particular, the number of ions extracted is limited by the size of the extraction grid. The larger the grid, the more ions can be transported to the flight tube and hence to the detector. Note that the ion detector in our system is quite large, 4 cm in diameter. Thus, even without Einsel lenses, which are placed just above the extraction grid, we can detect ions distributed in a 4-cm diameter area. Although the relative intensity versus beam size nearly follows the ratio of volumes in which molecules are ionized and ions are extracted for the two beams as Figure 2.3 indicates, there is a small deviation from the expected size dependence. With a 1.5-cm diameter grid used in our current system, the ratio of volumes for the two beams is expected to increase from 3 to 15 with the increase in beam sizes from 1 to 5 mm. Thus, the planar beam provides more signal enhancement than expected. This small deviation might be attributed to the fact that more ions are extracted and detected with the planar beam than expected.

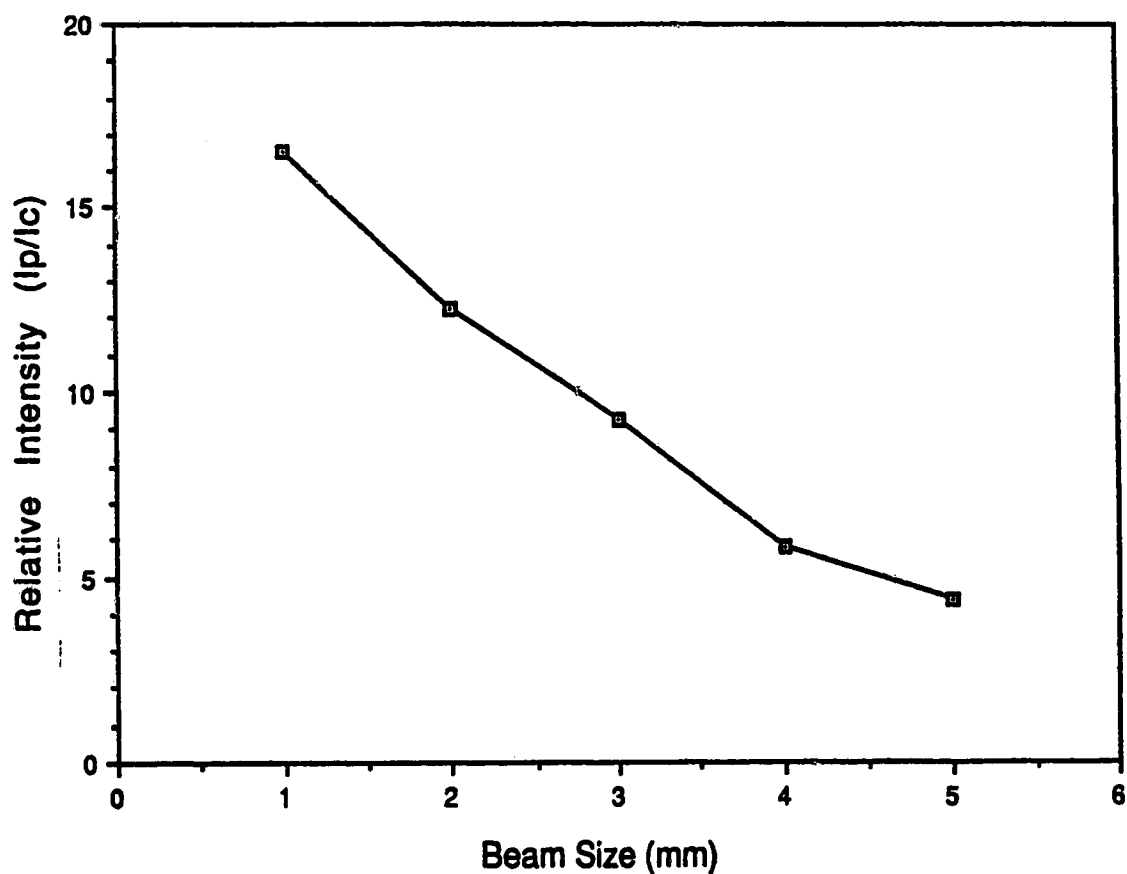


Figure 2.3. The relative intensity of the molecular ion peak of aniline vs the laser beam size. I_p is the signal intensity of aniline peak obtained using a planar beam. I_c is the signal intensity of aniline peak obtained using a circular beam. Beam size refers to the diameter of the circular beam or the width of the planar beam (length=15 mm). The laser power density is about 5×10^6 W/cm² and remains constant throughout the study.

It has been known that a TOFMS equipped with a reflectron field can improve mass resolution significantly over a simple linear TOFMS [73]. Mass resolution above 10,000 has been reported [74, 75]. Our system consists of two ion detectors. One is placed behind the reflecting field which is at the end of the flight tube so that this system will function the same as a linear TOFMS when the reflecting field is turned off. When the field is on, ions will be reflected. Thus the other detector is placed near the extraction grid at the other end of the flight tube. When the system is operated in a linear TOFMS mode, mass resolution is found to be about 300 for aniline at m/z 93 with a small size (1mm) of ionization laser beam.

When the beam size is increased, the resolution is so dramatically reduced that a reliable mass identification becomes very difficult. However, with a reflectron TOFMS, mass resolution above 2000 can be obtained even with a $5\text{mm} \times 15\text{mm}$ laser beam. Figure 2.4 shows the relation between the mass resolution and the beam size. This figure indicates that the use of a planar beam instead of a circular beam does not change the mass resolution. Thus, we can have net signal enhancement without losing resolution. Figure 2.4 also shows that the resolution decreases when the diameter or the width of the laser beam is increased. This suggests that our reflectron TOFMS can only partially compensate the initial spatial distribution.

We also examined the effect on supersonic jet cooling with use of a planar beam, instead of a circular beam. We have examined the cooling effect by examining the mass resolution in a linear TOFMS [37]. In a linear TOFMS, the mass resolution is directly related to the initial kinetic energy distribution of the sample molecules. The energy distribution will be very broad if there is no cooling or only partial cooling for the molecules in the jet [37]. This poor cooling will result in low resolution. By running our system in a linear TOFMS mode, we have found that mass resolution remains the same when a circular laser beam is replaced with a planar beam (here $D = W$). This indicates that the increase of the beam size in a direction parallel to the jet expansion axis does not affect

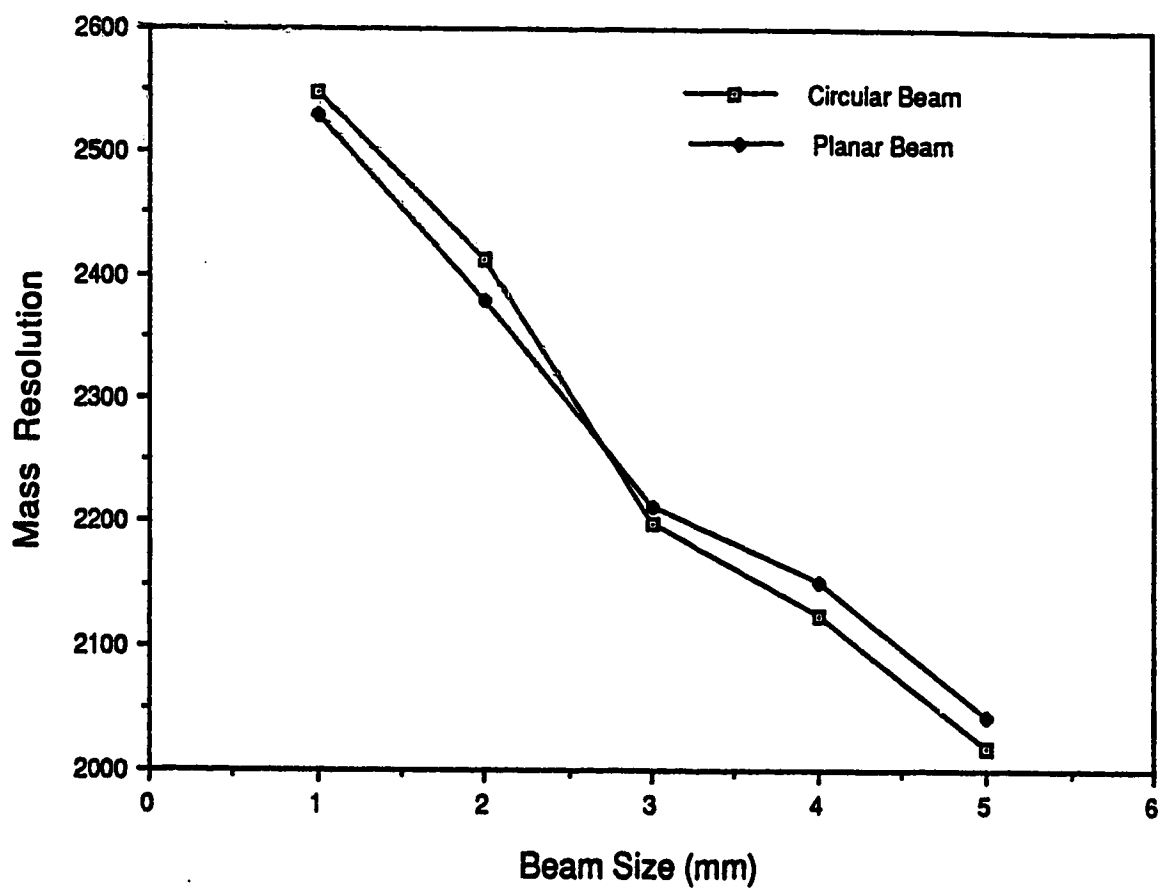


Figure 2.4. The relations between mass resolution and the size of the laser beam for a planar and a circular beam with reflectron/TOFMS.

the cooling significantly. Thus we conclude that the signal can be enhanced by the use of a planar beam without affecting the jet cooling. This result is very significant for the R2PI supersonic jet spectroscopy studies of biological molecules [76-78]. For most biological molecules, the use of high laser power will have two effects, i.e., severe fragmentation resulting in poor cooling and spectral peak saturation of the wavelength spectrum. The signal enhancement from 4 to 16 times will allow one to reduce the laser beam power about 2 to 4 times for R2PI while the overall signal intensity remains the same.

Background reduction. In FAB, PRH and LD/SJ-MPIMS, the high-intensity background is mainly from the ionization of the molecules condensed on the lens assembly. Although baking the vacuum chamber, a commonly used method for background reduction, could be employed here, the chamber cannot be kept at the baking condition during the experiment since the thermally labile sample molecules will be decomposed at high temperature. If the chamber is baked periodically between the runs, then the efficiency of the system will be greatly reduced. An alternative method is the use of liquid nitrogen (LN_2) to trap the background molecules [79]. Background reduction will be most efficient if the lens assembly, the chamber, and part of the flight tube are LN_2 -trapped. In a simple, linear-type TOFMS, this can be done with modest cost [79]. However, for a relatively complicated system such as Jordan's reflectron-type TOFMS [80], it would be difficult and expensive to use the LN_2 trap.

As indicated in the introduction, this background reduction method is based on the trajectory difference of the sample and background ions during the flight from the acceleration region to the detector. During the experiments, the sample molecules from the jet and background molecules are both ionized in the region between the repeller plate and extraction grid. The resulting ions are accelerated by V_{a2} and V_{a3} and enter the field-free flight tube. In here we first examined the velocity difference between the sample molecules from the jet and the background molecules.

For the sample molecules in the jet, the supersonic expansion not only reduces the initial velocity distribution but also forces these molecules to travel in one direction, i.e., perpendicular to the flight tube axis (see Figure 2.1). After the molecules are ionized by the laser, the ions will retain the molecular flight trajectories. Therefore the ions in this ion packet will have relatively uniform velocities and have a net linear velocity moving along the jet expansion axis. Since the jet-cooled sample molecules travel at almost the same velocity as the expanding gas, the linear velocity of the molecules can be experimentally determined by measuring their flight time from the nozzle to the ionization region. To determine the velocity, the aniline sample is directly introduced into the nozzle and mixed with CO₂. The mixture expands into the TOFMS to form a jet. The distance between the nozzle and the ionization region was varied from 10 cm up to 20 cm in a 2.5 cm increment, the corresponding flight time of the aniline sample changed from 130 μ s to 256 μ s. From the linear relationship of the travel distance with the flight time, the linear velocity of the jet-cooled sample molecules was determined to be about 7.7×10^4 cm/sec. This velocity is consistent with the results reported by others [81].

The linear velocities of other molecules, i.e., hot sample molecules and background molecules in the system, are more difficult to determine with high accuracy. However, by examining the pulse profiles of these molecules, we can estimate the velocities or provide an indication about their velocity differences from the cooled sample molecules. Figure 2.5 shows the pulse profiles of sample and background obtained by monitoring the molecular ion intensities of aniline (sample) and 9-methylanthracene (background) as a function of time delay between the nozzle and the ionization laser. The ion deflector voltage (V_{xy}) was set at 18 volts for Figure 2.5(A) and 68 volts for Figure 2.5(B) with the reflectron TOFMS. At $V_{xy}=18$ V, a background signal is observed along with a strong signal from the jet-cooled sample. When V_{xy} is below 18V, the background signal decreases. If the voltage is adjusted to above 18V, then the background signal increases and the shape of the sample pulse becomes broader. As Figure 2.5(B) shows, at $V_{xy}=68$ V, background can

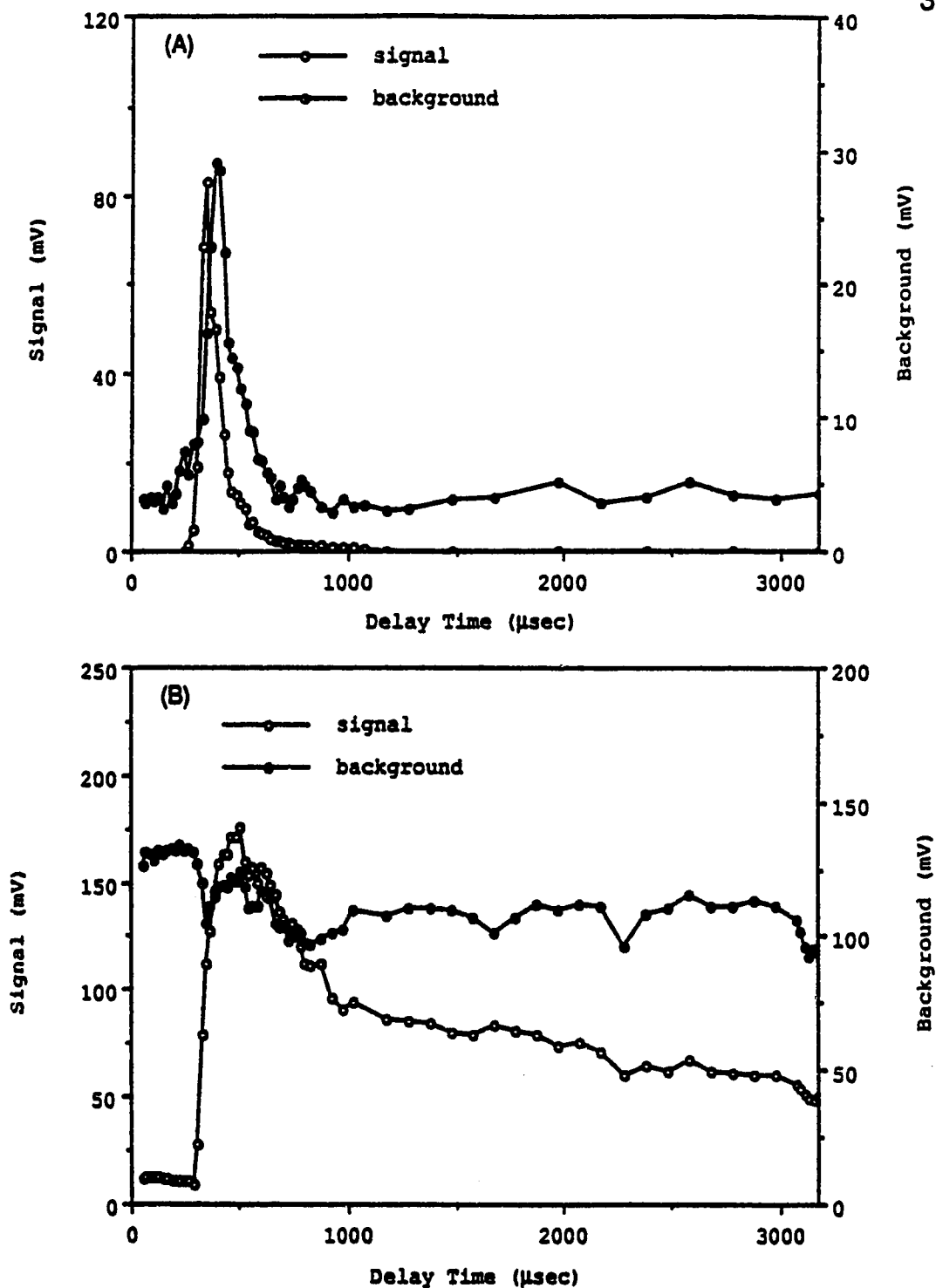


Figure 2.5. Signal intensities of the molecular peaks of aniline (sample) and 9-methylanthracene (background) as a function of the delay time between the laser and the sample pulse with ion deflector voltages of (A) $V_{xy}=18$ V and (B) $V_{xy}=68$ V.

be detected no matter what the time delay is and the sample pulse becomes very broad.

Figure 2.5(A) also shows that the width of the sample pulse is about $75\ \mu\text{s}$, which is close to the gas pulse width data, i.e., $\sim 50\ \mu\text{s}$, provided by the manufacture. The velocities of the sample molecules in Figure 2.5(A) are the highest compared with the background and the portion of samples in Figure 2.5(B). Moreover, from the mass resolution studies of the molecular ion peak of the sample [99], we found that the molecules from the pulse in Figure 2.5(A) are cooler than those in Figure 2.5(B). Thus, we may conclude that the sample ions detected at $V_{xy}=18\text{V}$ are from the jet-cooled molecules. Interestingly, the background in Figure 2.5(A) also gives a pulse profile, which has a similar shape as the sample pulse but with a slight time-shift. This indicates that some background molecules are entrained into the jet near the nozzle and become cold. However, due to insufficient collisions with the expanding gas, the background molecules are not as cold as the sample and have a smaller velocity. Therefore, by optimizing the time delay between the nozzle and the laser, one can selectively ionize the jet-cooled molecules when a proper V_{xy} is used. For supersonic jet spectroscopy, this result suggests that one should use the laser to intersect the front portion of the sample pulse to reach the optimal cooling if the background is the same as the sample molecules. Indeed, this was true for the resonant two-photon ionization jet spectroscopy studies of biological molecules with laser desorption sample entrainment into the jet [76, 77].

In contrast to Figure 2.5(A), the sample pulse shown in Figure 2.5(B) is very broad. Moreover, the velocity of the sample ion packet is reduced to less than $5 \times 10^4\ \text{cm/sec}$ as indicated by the prolonged delay time. These results, along with the fact that the sample molecules at the tail of the pulse are not as cold as those in the front of the pulse and those in Figure 2.5(A), lead us to believe that part of the jet-cooled sample molecules has been warmed up during the course of traveling from the nozzle to the center of the ionization region due to their collisions with the background molecules en route, particularly the high intensity background molecules in the ionization region. In addition,

these collisions tend to reduce the linear velocities of sample molecules, and some background molecules may gain momenta or velocities moving towards the center of the ionization region during the course of collisions. However, the velocities of background molecules should be much lower than those of samples because of the incomplete collisions. Note that the intensity of the background signal remains high before the sample pulse arrives at the ionization region, which suggests that the background molecules from the center of the ionization region with zero initial linear velocity are pushed away by the sample pulse when the pulse arrived at that region. This further indicates that the background molecules have some linear velocities in the same direction as the jet expansion, although they are moving at much smaller velocities than the jet-cooled molecules.

From this pulse profile study, we can conclude that the jet-cooled molecules have the highest velocity along the expansion axis, i.e., about 7.7×10^4 cm/sec in our experimental setup. In addition, the linear velocities of the background molecules in the ionization region at the time of sample arrival are much lower, but not zero. Next we want to examine the spatial separation of the sample and background ions when they arrive at the detector and also the effect of the ion deflector on the ion trajectory and the spatial separation. In an attempt to illustrate these facts, we performed a computer simulation on the ion trajectories.

The numerical simulation program, Simion (MacSimion, version 1.0, Montech Pty Ltd, Australia), was used to model the electrostatic lenses and calculate the ion trajectories in the TOFMS. Due to the large dimension of the TOFMS system and the limited size of matrix available in the Simion program, it was difficult to perform the complete simulation of the system with high accuracy. However, we show here that it is possible to simulate the ion trajectory with high accuracy in the important part of the system, i.e., the extraction and acceleration region, the Einzel lenses, the ion deflector, and a small portion of the field-free region. Based on this ion trajectory, the positions of the ions striking at the detector

can be calculated by extrapolating the trajectory with a curve fitting program in the computer. In the simulation, the geometry of each electrical element (see Figure 2.6) is first modeled after the experimental setup. A voltage is then assigned to each element. The voltages applied to extraction and acceleration plates are determined by the experiment. We found that optimal sensitivity and mass resolution of the system could be achieved when $V_{a1}=1948\text{V}$, $V_{a2}=1220\text{V}$ and $V_{a3}=0\text{V}$. Thus in this calculation, V_{a1} , V_{a2} and V_{a3} were set at these values. Although other sets of voltages can be used for optimizing the background reduction, they tend to reduce the sensitivity and give poorer mass resolution. Since the molecules are ionized in a relatively small area compared with the large size of our detector and the ions generated by the laser have a fairly uniform energy distribution in the supersonic jet experiments, the effect of Einsel lenses on the sensitivity was found to be negligible. Thus, these lenses were set at zero voltages in this study. Because the program is not capable of performing simulation with both cylindrical and noncylindrical elements simultaneously, the Einsel lenses were treated as noncylindrical elements similar to the parallel plates. We believe that this assumption will not affect the accuracy of defining the electrostatic field significantly since there are no voltages applied to Einsel lenses. A plate (modeled as a detector) with zero voltage is placed 25 cm away from the repeller plate. We found that the small variation of the distance (e.g. the distance is changed to 20 cm) does not change the ion trajectory. This indicates that ion trajectory may not alter significantly in the field-free region and will follow the original path to the detector.

Next the initial conditions of the ions are defined for the calculation of ion trajectories in the electrostatic field described above. Here the important parameters affecting the ion trajectory are the initial kinetic energy and the entrance angle with respect to the field. The initial kinetic energy of an individual ion can be calculated according to $E=1/2mv^2$, where m is the mass of the ion and v is the linear velocity. For the majority of the ions from the cold sample molecules (aniline) in the jet, they have the kinetic energies in the range of flight 0.3eV ($v\sim 7.7\times 10^4\text{ cm/sec}$) and entrain into the field perpendicular to

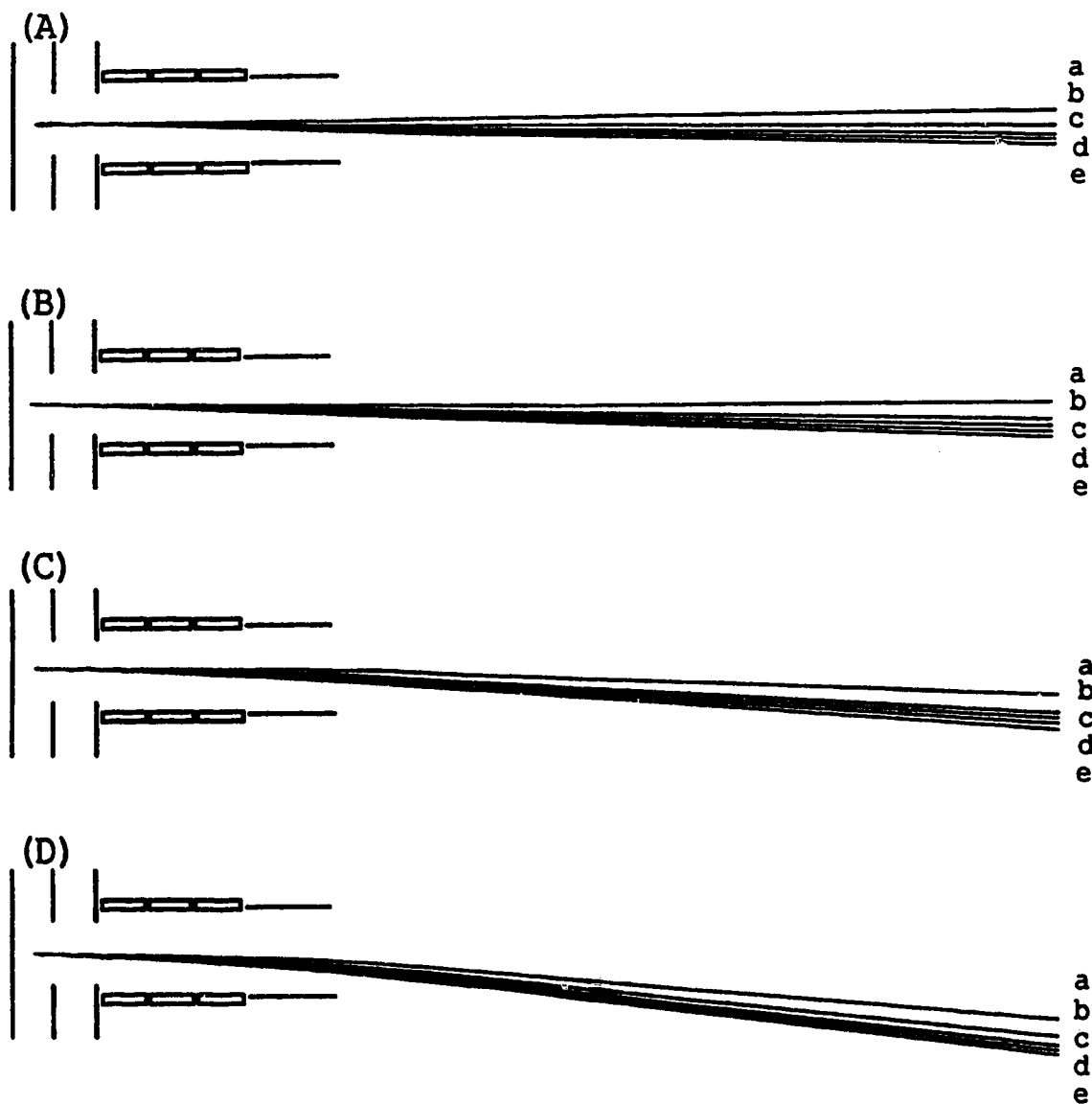


Figure 2.6. Ion trajectories calculated by the Simion program with various deflector voltages(V_{xy}) of (A) -30 V, (B) 0 V, (C) 70 V, and (D) 130 V. Ions are simulated as being entrained into the field perpendicular to the flight tube axis with initial kinetic energies of (a) 0 eV, (b) 0.1 eV, (c) 0.2 eV, (d) 0.3 eV, and (e) 0.4 eV.

the tube axis. Now in the case of the background molecules in the supersonic jet experiments, they do have some linear velocity, but this velocity is much lower than that of the cooled sample molecules. In addition, the mass difference between the sample and background is relatively small. Thus we can conclude that the initial kinetic energy of the background ion packet in the jet expansion direction is much lower than that of the sample ion packet.

Figure 2.6 shows the ion trajectories calculated by the Simion program at various deflector voltages. Ions are simulated as being entrained into the field with initial kinetic energies ranging from 0 to 0.4 eV in a step of 0.1 eV. Figure 2.7 shows the spatial separation of ions (Y-axis) with different initial kinetic energies arriving the detector by extrapolating the ion trajectories from Figure 2.6. As Figure 2.7 indicates, the spatial separation between the ion with no initial kinetic energy and the ion with 0.3eV energy at the detector in the linear TOFMS is about 2.8cm. This suggests that if all background molecules had zero initial energies in the jet expansion axis, a detector with 18-mm in diameter target area would selectively detect the sample ions when a proper voltage is applied to the ion deflector (Figure 2.7(B)). The experimental result for the signal profiles obtained by monitoring the molecular ion peak intensities of aniline (sample) and 9-methylanthracene (background) as a function of the deflector voltage in the 1-meter linear TOFMS is shown in Figure 2.8(A). As Figure 2.8(A) shows, it is not possible to selectively detect the sample ions. Note that the background ion profile shown in Figure 2.8(A) is broader than the sample profile. This can be attributed to the fact that background ions enter the acceleration field with various velocities according to the Maxwell-Boltzmann distribution with a mean velocity corresponding to the linear velocity of the background-ion-packet and with various entrance angles, whereas the sample ions enter the field with more uniform velocities and entrance angles. Figure 2.8(A) also shows that the center of the sample ion profile is different from the background profile and a small deflector voltage is needed to alter the sample ions flight path to ensure that the ions arrive at the

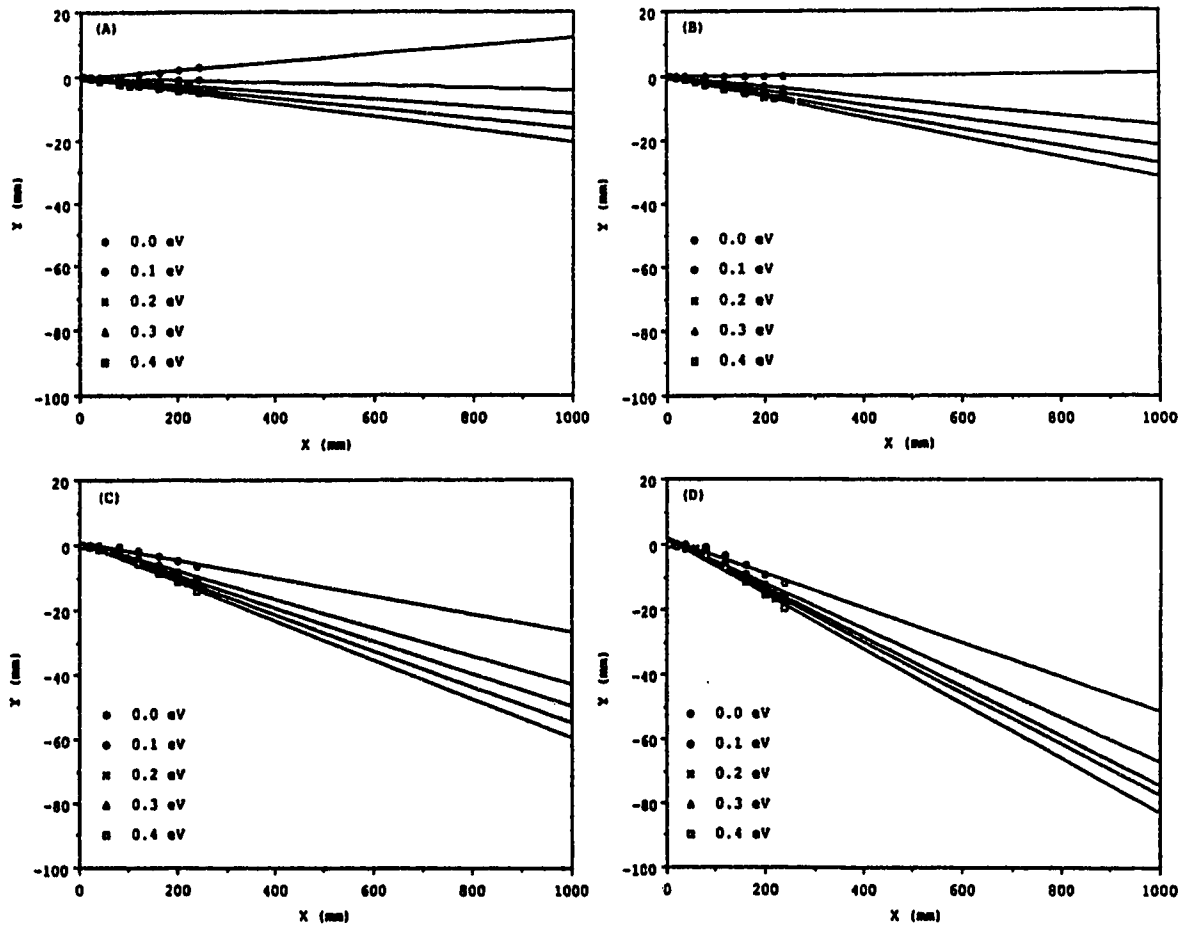


Figure 2.7. Spatial separation of ions (Y-axis) with different initial kinetic energies as a function of the flight distance (X-axis) obtained by extrapolating the ion trajectories from Figure 2.6. Deflector voltages (V_{xy}) are (A) -30 V, (B) 0 V, (C) 70 V, and (D) 130 V. X-axis and Y-axis are defined as in Figure 2.1.

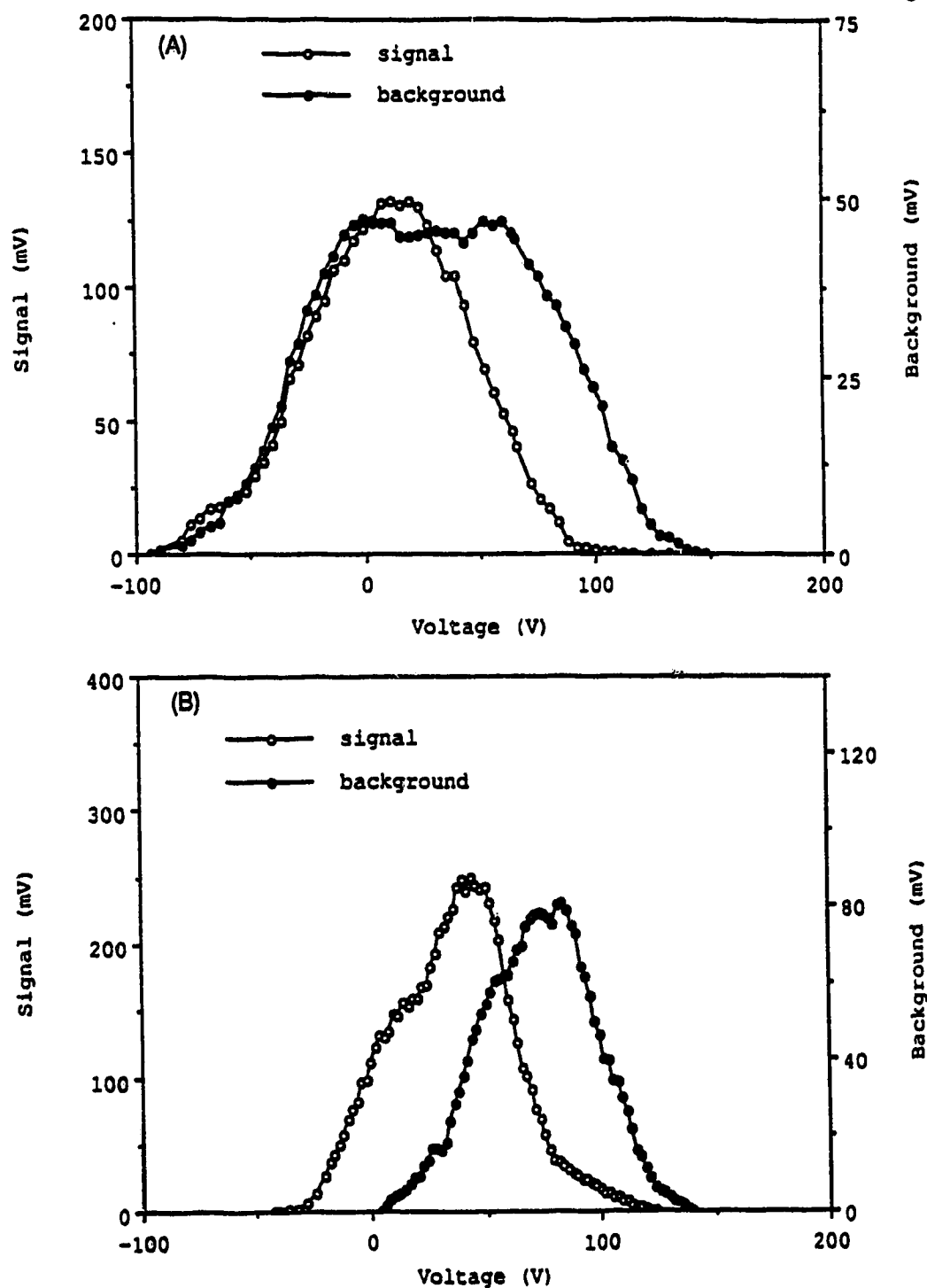


Figure 2.8. Signal intensities of the molecular ion peaks of aniline (sample) and 9-methylanthracene (background) as a function of the ion deflector voltages in (A) a linear TOFMS with a 1-meter long flight tube and (B) a reflectron TOFMS. The time delay between the laser and the sample pulse is adjusted so that the laser ionizes the front portion of the sample pulse.

detector. Unfortunately, after the ions travel about 1 meter and strike the detector, the spatial separation between the sample-ion-packet and the background-ion-packet is not large enough to allow the selective detection of sample ions.

Now according to our simulation, if the flight length is doubled, then the spatial separation will also be nearly doubled, which may allow us to use the detector to selectively detect the sample ions. To do this, we can either increase the length of the flight tube in a linear TOFMS or use a reflectron TOFMS to double the flight length. However, the use of a reflectron TOFMS also provides a means of compensating the initial energy distribution of the isomass ions, resulting in a less-diffused sample-ion-packet [73-75]. The effective flight length in our reflectron TOFMS is about 2 meters. Figure 2.8(B) shows the ion profiles of sample and background obtained by operating the TOFMS in a reflectron mode. The time delay between the laser and the sample pulse is adjusted so that the laser intersects the front portion of the sample pulse. Note that the spatial separation between the sample and background ions are now clearly obtained. Therefore, it is now possible to selectively detect the sample molecules by applying a proper deflector voltage to alter the ion trajectory so that only sample ions arrive at the detector. Note that the background can be completely eliminated at $V_{xy}=0V$ or below, although the signal intensity is reduced to about one third of its highest peak. Figure 2.9 shows the mass spectra of aniline and 9-methylanthracene obtained by MPI at 266 nm with different voltages applied to the ion deflector. At $V_{xy}=6V$, aniline is selectively detected. At $V_{xy}=72V$, the background, 9-methylanthracene along with aniline is detected. At $V_{xy}=126V$, the background is detected because now the ion trajectory of the aniline ions is so altered by the deflector that no aniline ions will arrive at the detector.

The application of this background reduction method for FAB and LD/SJ-MPIMS is illustrated in figure 2.10. Figure 2.10(A) is the mass spectrum of aniline ($m/z=93$) and background obtained by using laser ionization at 266 nm with the ion deflector voltage of 70V. Figure 2.10(B) shows the mass spectrum of 9,10-dimethylanthracene obtained by

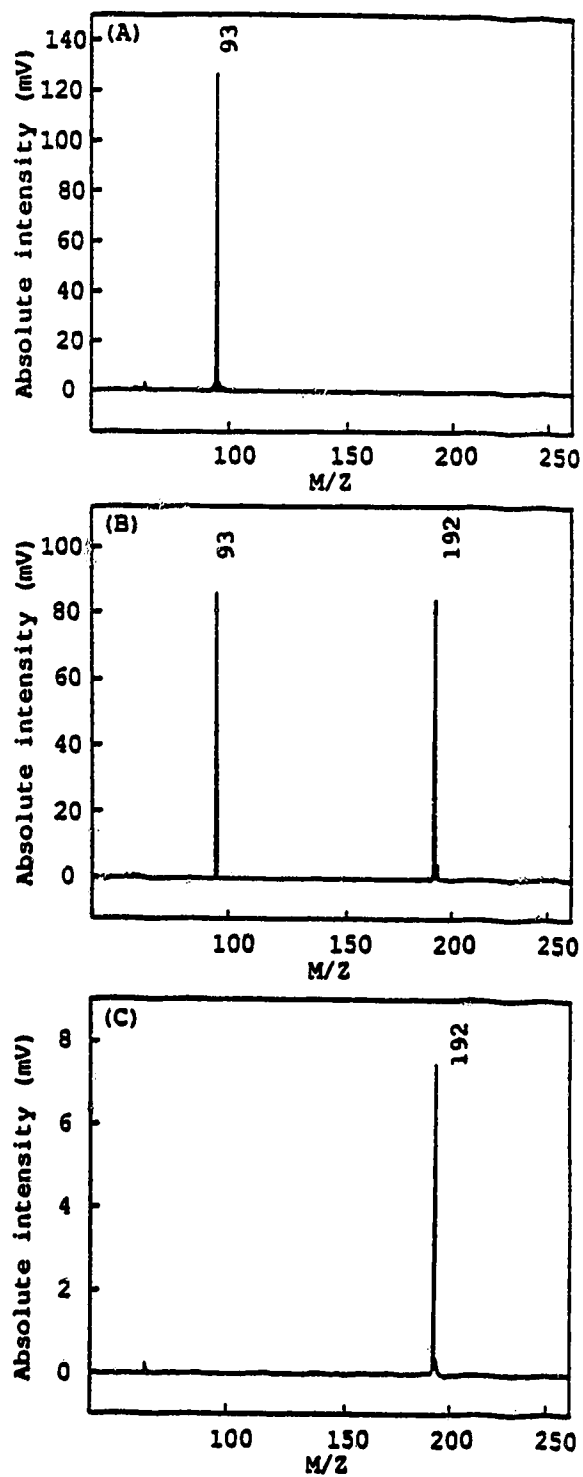


Figure 2.9. MPI mass spectra of aniline sample and 9-methylantracene background obtained with the ion deflector voltages of (A) 6 V, (B) 72 V, and (C) 126 V.

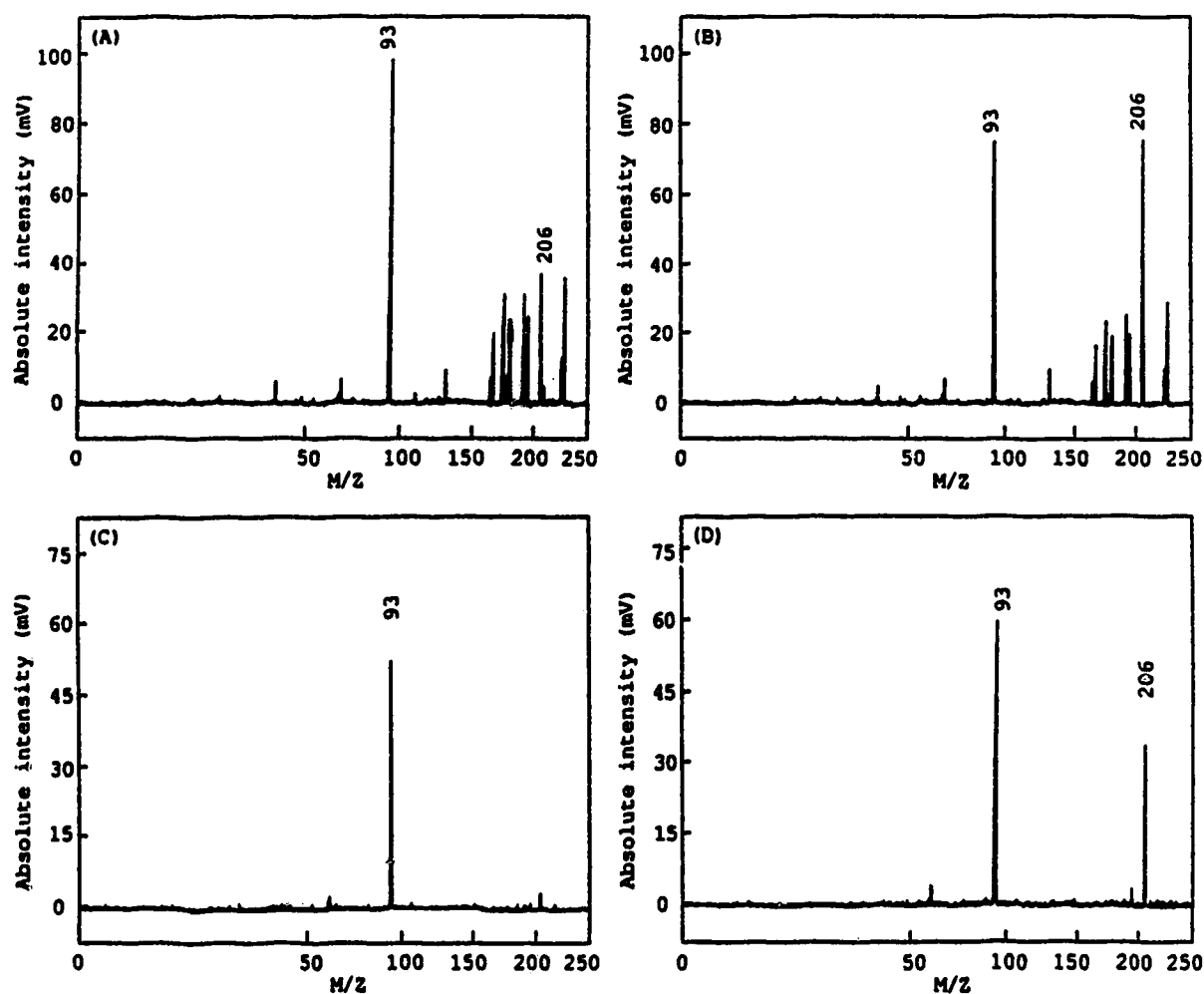


Figure 2.10. MPI mass spectra of (A) aniline with background, (B) aniline and 9,10-dimethylantracene with background, (C) aniline, and (D) aniline and 9,10-dimethylantracene. Aniline is introduced into the jet directly with the expansion gas. 9,10-dimethylantracene is introduced into the jet expansion by using laser desorption. The ion deflector voltage is 70 V for (A) and (B), 0 V for (C) and (D).

Chapter 3

Pulsed Fast Atom Bombardment Sample Desorption with Multiphoton Ionization in a Supersonic Jet/Reflectron Time-of-Flight Mass Spectrometer

3.1. Introduction

In the past, SJS/MPIMS has been used for the detection of volatile chemicals. To extend this SJS/MPIMS technique for the study of thermally labile biological molecules, several methods including supercritical fluid injection [82] and thermospray/heating [83] have been attempted to introduce these molecules into the supersonic jet. More recently, laser desorption (LD) [84,76] has been successfully used to entrain biological molecules into jet expansions .

In this chapter, an alternative method for introducing thermally labile and nonvolatile molecules into supersonic jet expansions is described. The technique used herein is fast atom bombardment (FAB) [85]. Instead of using photons from a high-power laser, we have used a FAB gun to generate fast atoms to desorb the sample molecules. We demonstrate that small biological molecules can be readily desorbed and entrained into a supersonic jet without significant thermal decomposition by using FAB. However, one of the advantages of this FAB method is that the FAB gun can be easily constructed and maintained at a low cost.

3.2. Experimental

The experimental setup for fast atom bombardment/supersonic jet multiphoton ionization (FAB/SJMPI) is shown in Figure 3.1. The system is a reflectron type Time-of-Flight mass spectrometer and has been described in detail in Chapter 2.

A saddle-field FAB gun [86, 87] is constructed to fit into the test chamber through a 5 cm flange and placed close to the nozzle orifice. The distance between the FAB gun

using laser desorption for sample volatilization with MPI at 266 nm. The deflector voltage is also set at 70V. Note that the molecular ion peak ($m/z=206$) is superimposed with the background. This makes quantitation difficult. The mass spectra shown in Figure 2.10(C) and (D) are obtained at the same conditions as in Figure 2.10(A) and (B), respectively, except that the ion deflector voltage is set at 0V. As Figure 2.10(C) and (D) shows, the background is now significantly reduced, and the small fragment ion ($m/z=191$) from the loss of CH_3 from the molecular ion peak can be clearly identified. This example represents a typical experiment for background reduction performed in FAB and LD/SJMPI studies of nonvolatile chemicals. This method has now been routinely used in our lab.

2.4. Conclusion

Signal enhancement from 4 to 16 times in a SJS/MPI can be easily achieved by using a planar ionization laser beam. The use of a planar beam does not affect mass resolution and supersonic jet cooling. This should be found useful for sensitive detection of organic and biological molecules and for obtaining supersonic jet spectra of biochemicals.

We have also demonstrated that the background signal can be significantly reduced with the use of an ion deflector and the proper adjustment of the time delay between the laser and the sample pulse in the reflectron TOFMS. We show that there are some linear velocities for the background molecules moving along the jet expansion axis in the supersonic jet experiments. However, the velocities of the jet-cooled sample molecules are much larger than those of the background molecules. A computer simulation indicates that it is possible to selectively detect the sample ions based on this linear velocity difference, if a sufficient flight distance is provided. In FAB and LD/SJ-MPIMS, the linear TOFMS with a 1-meter-long flight tube is found to be incapable of reducing the background signals. However, with a reflectron TOFMS, the combination of longer flight length and less diffused sample-ion-packet allows us to reduce the background significantly.

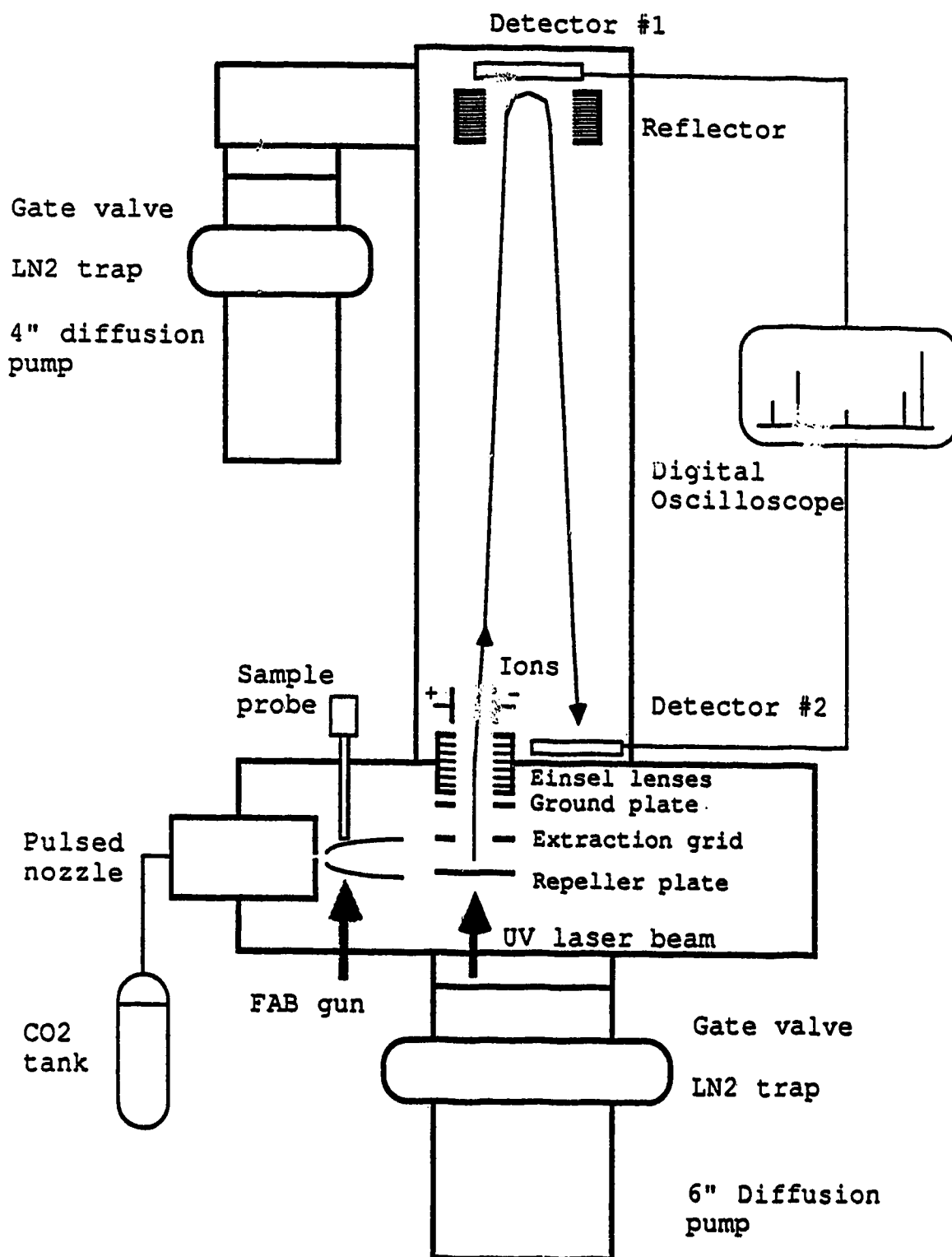


Figure 3.1. Schematic of the experimental apparatus.

outlet and the nozzle orifice is about 40 mm. The distance between the FAB gun and the center axis of the jet is also about 40 mm. A 5-mm or 10mm-in-diameter sample probe made of machinable Macor ceramic is located at about 20 mm away from the center axis of the jet. About 100 μ g sample is generally used and placed on the sample probe directly by either wetting or dissolving the compound in a solvent (i.e. methanol) and coating on the surface with the use of a spatula. Although glycerol can be used as a matrix, we have found that in this study sample desorption can be performed and mass spectra obtainable over a short period of time (more than 100 pulses) without the use of glycerol. Thus, for the compounds studied herein, glycerol was not used.

Argon or xenon is used in the saddle-field discharge for the FAB gun. The anode potential is fixed at 10 kV and, by adjusting the pressure in the gun, the discharge current varies from 1 to 5 mA. We have found that for chemicals with a high melting point it is necessary to use a higher discharge current in order to desorb a sizeable amount of neutrals for laser postdesorption ionization. The size of the FAB beam is approximately 1.5 mm in diameter as determined by examining the dark image created on a thermal-sensitive paper after the paper has been briefly exposed to the FAB beam. The high voltage power supply for the FAB gun is Spellman Model RH5R15PN60 and can be operated in a continuous mode or a pulsed mode using an external trigger system.

The actual sequence of events is controlled by several delay generators. The FAB gun is first turned on to desorb the sample, the pulsed nozzle opens to form a supersonic jet, and then the sample is entrained into the jet and carried into the ionization region of the TOFMS where the ionization proceeds. The selection of the repetition rate of the experiment ranging from 0.1 to 20 Hz is mainly dependent on the pulse width of the FAB power supply. For most of the compounds we have reported herein, the pulse width is adjusted to be 300 ms with a 100- μ s rise-time and 100- μ s fall-time. Thus the repetition rate of the experiment is optimized at 3 Hz.

One of the parameters which we have not optimized for the current system is the

duty cycle. There are several factors affecting the overall duty cycle. With a TOFMS, the ion detection duty cycle is very high since all ions can be detected in one single pulse. However, the duty cycle for the generation of ions is dependent on the pulse widths and repetition rates of the ionization laser beam and FAB. It also depends on the pulse profile of the neutral molecules desorbed by FAB. One of the major factors limiting the duty cycle of our current system is the pulse width (~300 ms) of the FAB gun.

All chemicals were purchased from Sigma Chemical Co., St. Louis, MO or Aldrich Chemical Co., Milwaukee, WI and used without further purification.

3.3. Results and Discussion

The mass spectra of tryptophan obtained by using fast atom bombardment sample desorption with multiphoton ionization at different laser power densities are shown in Figure 3.2. Tryptophan is known to be thermally labile [88]. However, Figure 3.2 demonstrates that a molecular ion peak can be readily obtained with no thermal decomposition products. This shows that although the actual mechanism for the generation of neutrals is not completely understood, the rapid heating/sputtering induced by FAB can be used to introduce thermally labile biological molecules into a supersonic jet for multiphoton ionization. Other molecules including amino acids, carboxylic acids, catecholamines, neuroleptic drugs, pineal indoles, small peptides and polycyclic aromatic hydrocarbons (PAHs) studied by this technique are shown in Table 3.I. In these experiments, sample molecules are desorbed by a pulsed FAB beam in a 1.5 mm diameter spot and postdesorption ionization is performed by a 266 nm laser beam. The pulsed power supply for the FAB gun is adjusted so that the potential is 10 kV and the discharge current ranges from 1 to 5 mA. Although the actual power density of fast atoms impinging on the sample probe is unknown, we believe that the atom flux is very intense ($>10 \mu\text{A}/\text{cm}^2$) [87]. As Figure 3.2 illustrates, the molecular ion, with no or little fragmentation, can be observed if the laser power is low. When the laser power density is increased,

**Table 3.I Compounds Studied by the Fast Atom Bombardment/
Supersonic Jet Multiphoton Ionization Technique**

1. Amino acids:	6. Peptides:
(1). Phenylalanine	(1). Trp-Ala
(2). Tryptophan	(2). Trp-Gly
(3). Tyrosine	(3). Trp-Leu
2. Carboxylic acids:	(4). Gly-Trp
(1). Anthranilic acid	(5). Tyr-Ala
(2). 3-Amino-4-hydroxybenzoic acid	(6). Tyr-Gly
(3). Indole-3-acetic acid	(7). Tyr-Leu
3. Catecholamines:	(8). Phe-Gly
(1). Dopa	(9). Trp-Gly-Gly
(2). Dopamine	(10). CBZ-Gly-Leu
(3). Synephrine	(11). CBZ-Ala-Gly
4. Neuroleptic drugs:	(12). Gly-Tyr-amide
(1). Chlorpromazine	7. PAHs:
(2). Desipramine	(1). 2-aminoanthracene
(3). Imipramine	(2). 9-Aminophenanthrene
5. Pineal indoles:	(3). Benzo[e]pyrene
(1). Harmaline	(4). Carbazole
(2). Melatonin	(5). 2-Chloroanthracene
(3). Tryptamine	(6). Chrysene
	(7). Decacyclene
	(8). Perylene
	(9). Rubrene
	(10). Triphenylene

a mass spectrum with fragment ions can be obtained, which can be used for structural analysis. This important feature of MPI is also observed for most of the compounds studied herein. Note that the axis of signal intensity in Figure 3.2 is plotted as an actual scale in mV, rather than normalized percentage scale. This shows that the overall signal intensity decreases when the laser power is reduced. This finding is consistent with the results reported [77, 89].

Another key result is that, as shown in Table 3.I, PAHs can readily be studied by FAB/SJMPL. Figure 3.3 shows the MPI mass spectrum of rubrene (molecular

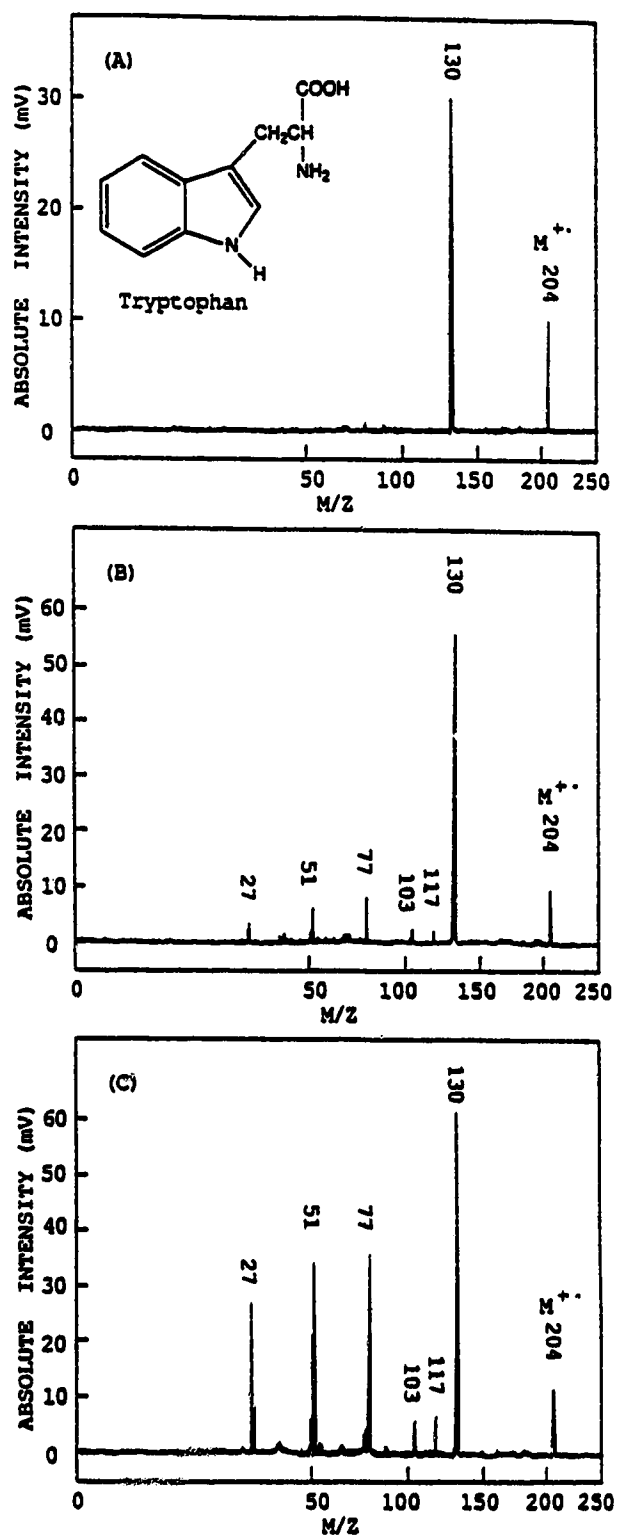


Figure 3.2. Mass spectra of tryptophan obtained by the fast atom bombardment/supersonic jet multiphoton ionization technique at 266 nm. The ionization laser power density was (A) $1 \times 10^6 \text{ W/cm}^2$, (B) $4 \times 10^6 \text{ W/cm}^2$, and (C) $8 \times 10^6 \text{ W/cm}^2$.

weight=532; m.p.>315°C) obtained by using about 100 µg sample with FAB desorption sample introduction. The ionization laser power density is about 1×10^6 W/cm² at 266 nm. Since the mass resolution is generally above 2000, the isotope composition can be easily revealed (see the insert in Figure 3.3). The peak at m/z 455 is the fragment from the molecular ion minus one benzene radical (M-77)⁺. The fragment ion peak at m/z 378 arises from the molecular ion by the loss of two benzene radicals (M-154)⁺. Note that due to the nonpolar nature of PAHs, mass spectra of PAHs are extremely difficult to obtain by direct FAB ionization [90]. Combining with a HPLC (for instance, via a continuous flow FAB probe [91]), this technique seems to be a promising method for the detection of high molecular weight or thermally labile PAHs, which are not currently amenable to GC/MS or direct FAB.

Table 3.I also lists some dipeptides we have studied with the FAB/SJMPI technique. These peptides are also examined by laser desorption/supersonic jet MPI(LD/SJMPI). LD/SJMPI study is carried out with a pulsed CO₂ laser (Allmark model 852, A-B lasers Inc., Acton, MA) which generates a 10.6 µm IR radiation with a 75-ns initial pulse and 2-µs tailing. The repetition rate of the laser can be adjusted from 0.1 Hz to 15 Hz, although 10 Hz rep-rate is used here. In LD/SJMPI, the FAB gun is replaced by a 1 cm diameter NaCl window in a 2" flange. The IR beam from the CO₂ laser is reflected by copper mirrors protected with gold coating (CVI Laser Corp., Albuquerque, NM) and focused on the sample probe by a germanium plano convex lens (Janos Technology Inc., Townshend, VT).

Figure 3.4 shows the mass spectra of Gly-Trp obtained by FAB/SJMPI (Figure 3.4(A)) and by LD/SJMPI (Figure 3.4(B)) along with proposed fragmentation patterns. Interestingly, for some of the dipeptides studied by FAB/SJMPI, as an example shown in Figure 3.4(A), the molecular ion peak (M⁺) is rather small (generally <20%); but the ion peak at 18 mass units lower, M-18, is the dominant ion in the mass spectrum. Note that small peptides have been previously studied by LD/SJMPI [70, 39, 78, 92, 93] and, in

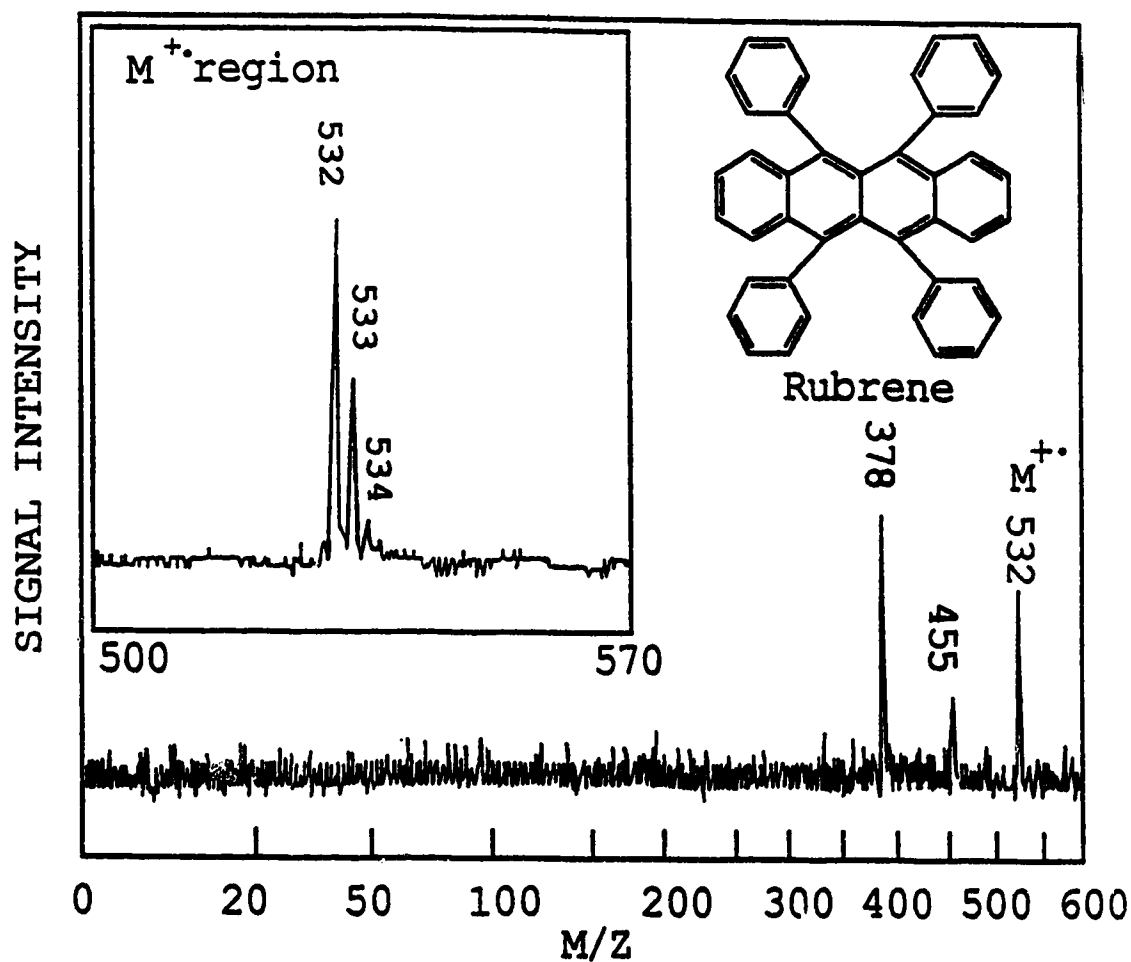


Figure 3.3. Mass spectrum of rubrene (molecular weight=532) obtained by FAB/SJMPI at 266 nm. The laser ionization power density was $\sim 1 \times 10^6$ W/cm². The molecular ion region is shown in the insert.

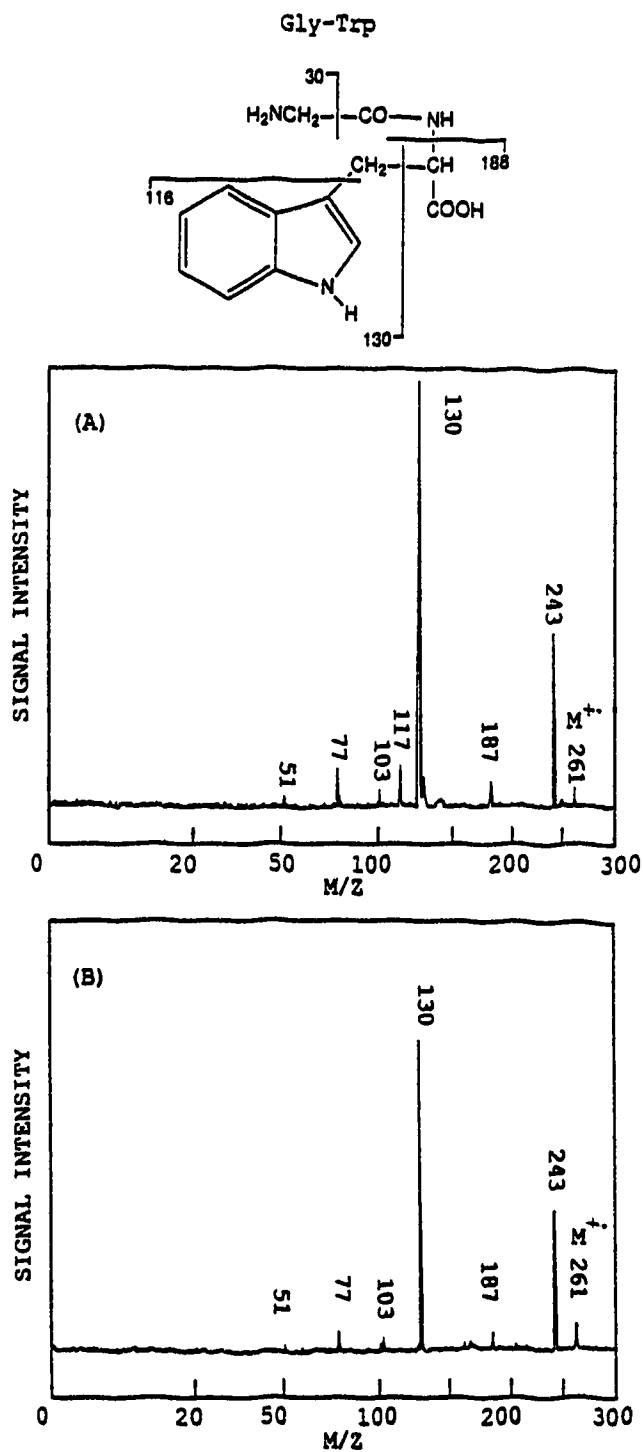


Figure 3.4. Comparison of MPI mass spectra of Gly-Trp at 266 nm obtained by (A) using the fast atom bombardment method and (B) using the CO₂ laser desorption method for sample introduction into the supersonic jet expansion. The ionization laser power density was about 1×10^6 W/cm².

some cases, the M-18 peak was also found to be the dominant one. The M-18 peak was carefully examined [92] and believed to be from the thermal decomposition product, i.e., cyclo-dipeptide, during the laser desorption process. This study shows that the generation of M-18 peak is not unique to the IR laser desorption experiment and suggests that the cyclo-dipeptide is not generated by the IR laser photo-dissociation process. However, in LD/SJMPI, the M-18 peak can often be reduced by using a thin film of the sample and avoiding multiple desorption in the same sample spot [92]. Here, we have found that it is generally more difficult to avoid the M-18 peak in FAB/LDMPI. This probably can be attributed to the fact that the FAB pulse width or the sputtering time (~ 300 ms) in our current system is much longer than the CO_2 laser beam ($< 2 \mu\text{s}$). Thus, in our current FAB/SJMPI experiments, the thermal decomposition process may compete with the desorption process for some compounds such as dipeptides [94]. Nevertheless, for most of compounds listed in Table 3.I, MPI mass spectra from LD and FAB experiments are essentially the same.

Next we have studied the sensitivity of this FAB/SJMPI method. In the past several years, direct desorption mass spectrometry techniques such as LDMS, FABMS, plasma desorption (PD), and secondary ion mass spectrometry (SIMS) have been widely used for the analysis of organic molecules. However, it is believed that the secondary ions generated by these techniques are only a very small fraction ($< 10^{-4}$) of the total sputtered material [95]. Thus electron ionization [96], chemical ionization [95, 97, 98], and multiphoton ionization [37, 41, 43] techniques have been employed to post-ionize the sputtered neutrals in order to increase the overall sensitivity. To provide an estimate of the sensitivity of this FAB/SJMPI method, a set of sample standard solutions are prepared. Various amounts of sample solution were placed on the 5-mm-diameter sample probe by using a microliter syringe. A higher power was applied to the FAB gun in order to completely desorb the sample in a single pulse. The peak height of the molecular ion peak was recorded and a corresponding plot of the peak height versus concentration was used to

estimate the lower limit of detection. The detection limits at a signal-to-noise ratio of 2 for indole-3-acetic acid ($m/z=175$) and triphenylene ($m/z=228$) are 26 ng and 21 ng, respectively. Although the detection limit shown here is not nearly as low as the tens of picogram detection limit achieved with LD/SJMFI [77], we believe that a similar detection limit (picogram regime) should be expected when the ionization laser wavelength and supersonic jet cooling are fully optimized.

One of the important aspects of using MPI as an ionization technique for mass spectrometry is its high selectivity. With multiphoton ionization in a supersonic jet, there are at least two ways to improve the selectivity. First of all, a molecule will be efficiently ionized only if the laser wavelength is in resonance with a real intermediate electronic state and the sum of the energy of the photons absorbed exceeds the ionization potential of the molecule. Therefore, MPI is an almost ideal ionization method for the sputtered neutrals by FAB. This is because the matrix such as glycerol, which is commonly used in FABMS, does not contribute to the background noise since glycerol does not ionize at 266 nm [76]. Figure 3.5(A) shows the MPI mass spectrum of 4-acetamidophenol at 266 nm and Figure 3.5(B) shows the mass spectrum of a Tylenol tablet. The tablet is purchased from a local drug store and contains corn starch and other components according to the label. About 100 μg of a ground-up tablet is mixed with a drop of methanol and the mixture directly placed onto the sample probe. The FAB gun is used to desorb/sputter the sample and the neutrals are entrained into a CO_2 jet and then ionized by a laser beam at 266 nm with a laser power density at 1×10^6 . As Figure 3.5 shows, the mass spectrum of the Tylenol tablet is almost identical to that of 4-acetamidophenol. Other major components such as corn starch are not ionized. This demonstrates that we can selectively ionize the active substance in pharmaceutical dosage forms with very little sample preparation by using FAB/SJMFI.

Another method to enhance the selectivity of this technique is to combine supersonic jet spectroscopy (SJS) with MPIMS. MPIMS combined with SJS has been demonstrated as a very powerful analytical tool for isomer discrimination and isotope

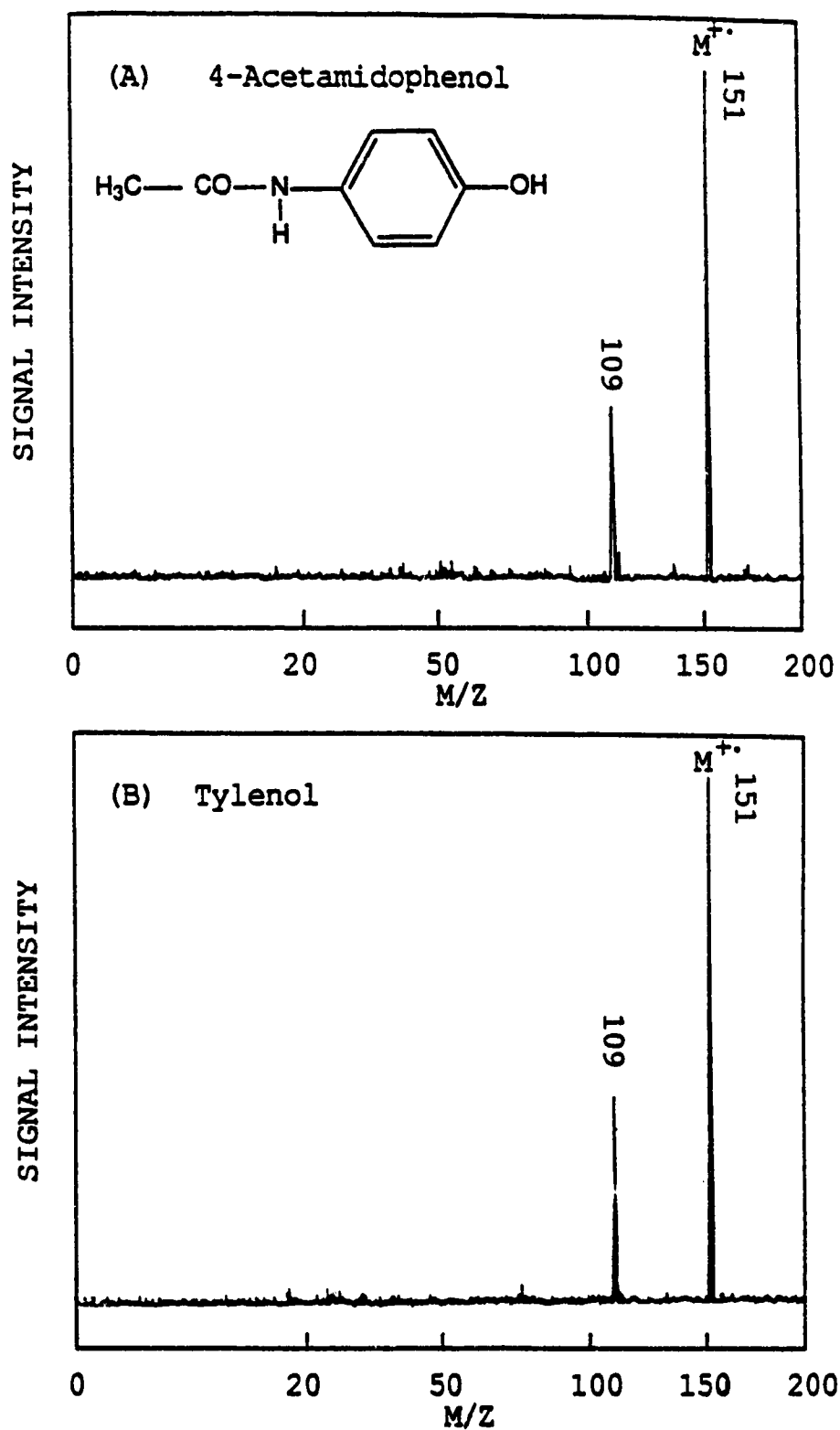


Figure 3.5. Mass spectra of (A) 4-acetamidophenol and (B) Tylenol obtained by using the FAB/SJMPI technique. The ionization laser beam was a 266 nm radiation with its power density $\sim 1 \times 10^6$ W/cm².

selective detection [33, 35, 59, 82]. More recently, jet-cooled wavelength spectra for biological molecules have also been obtained with the use of laser desorption technique for sample volatilization and the analytical applicability of MPIMS/SJS for the selective detection of biological molecules has been studied [69]. Here we believe that fast atom bombardment might be an inexpensive and simple alternative for the volatilization and entrainment of thermally labile and nonvolatile molecules into a supersonic jet.

We have examined the cooling effect by examining the mass resolution in a linear TOFMS [37, 90]. In a linear TOFMS, the mass resolution is directly related to the initial kinetic energy distribution of the sample molecules. The energy distribution will be very broad if there is no cooling or only partial cooling for the molecules in the jet. This poor cooling will result in low resolution. By running our system in a linear TOFMS mode, we have found that the mass resolution of molecules such as indole-3-acetic acid which is volatilized by FAB and entrained into the jet expansion is about 375 at m/z 175. However, the background molecules which are not cooled by the jet give mass resolutions less than 200. Thus we believe that the jet cooling is obtained with FAB sample entrainment into jet expansions.

Finally, the effect of the sample chemical properties on the detectability of molecules of interest in a mixture is examined. The spatial and temporal separation of desorption and ionization processes in this FAB/SJMPI allows one to uniquely study and control the two individual events. Here we find that, for organic molecules, chemical properties of the sample may play a very important role on the two processes. Figure 3.6 shows the MPI mass spectra of a mixture of indole-3-acetic acid and tryptamine with and without the addition of NaOH or NH_4OH . Figure 3.6(A) is obtained by using a mixture of indole-3-acetic acid and tryptamine in a solvent of 50% methanol/50% water. Figure 3.6(B) is the mass spectrum for the same mixture but with the addition of NaOH until the $\text{pH} > 12$. In Figure 3.6(C), NH_4OH was used to adjust the pH instead of NaOH. Note that the molecular ion peak for indole-3-acetic acid in Figure 3.6(B) is absent and no peak

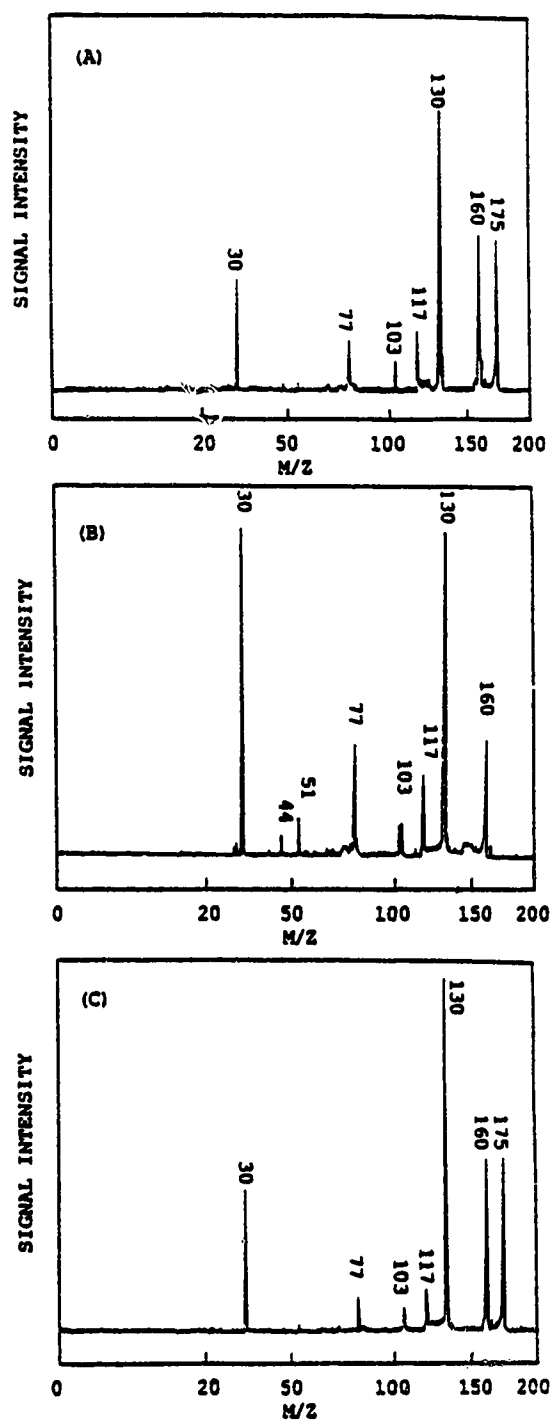


Figure 3.6. MPI mass spectra of a mixture at 266 nm obtained by FAB/SJMPI: (A) tryptamine (M.W.=160) and indole-3-acetic acid (M.W.=175) ($P = \sim 4 \times 10^6$ W/cm²); (B) tryptamine and indole-3-acetic acid plus NaOH ($P = \sim 5 \times 10^6$ W/cm²); (C) tryptamine and indole-3-acetic acid plus NH₄OH ($P = \sim 4 \times 10^6$ W/cm²).

corresponding to sodium indole-3-acetate is obtained. The same results are obtained at even higher laser power density although more fragments are observed as expected, but no indole-3-acetic acid and/or sodium indole-3-acetate peaks. This might be attributed to the low ionization efficiency of sodium indole-3-acetate. Although the melting point of the organic salt, i.e. sodium indole-3-acetate, is expected to be higher than the indole-3-acetic acid, the desorption of the salt appears to be complete by examining the sample probe after it has been bombarded by FAB. The fact that no peaks are observed from the possible decomposition products such as indole leads us to believe that most of sodium indole-3-acetate molecules are desorbed intact. Note that direct FAB has been used for determination of dissociation constants of weak acids in solution by Caprioli [100]. In his study, sodium salts of a variety of organic acids have also been desorbed intact and detected as $(\text{NaA}+\text{H})^+$ and $(\text{NaA}+\text{Na})^+$. In addition, the electronic absorption (checked by UV spectrum in solution) for sodium indole-3-acetate and indole-3-acetic acid do not differ significantly in terms of absorption bands and absorptivity. These results indicate that sodium indole-3-acetate may not be ionized efficiently by MPI due to its low ionization cross section at 266 nm in the gas phase. To our best knowledge, there is no report on MPI studies of organic salts involving metal cations in the gas phase (possibly because most organic salts are unstable upon heating). Now in the case of the ammonium salt, the salt may decompose into indole-3-acetic acid and NH_3 during the FAB desorption process. Similar results are also obtained with other organic acids such as biphenyl phosphoric acid. For analytical applications, this preliminary study indicates that (1) the selective detection of molecules of interest can sometimes be achieved by using simple sample preparation; (2) in the cases where the pH is important, such as buffered biological chemical samples and organic acids, NH_4OH is a better choice for adjusting the pH.

3.4. Conclusion

Fast atom bombardment is a powerful means of desorbing thermally labile biological molecules into the gas phase for analysis by multiphoton ionization mass spectrometry. A variety of biological molecules can be desorbed without significant thermal decomposition. Polycyclic aromatic hydrocarbons can also be studied. At present, the detection limit achieved is typically in the low nanogram regime. The selectivity of this method has also been studied. We have shown that it is possible to use this technique to selectively ionize the active substance in a drug tablet with no sample preparation. We demonstrate that FAB can be used to introduce samples into supersonic jet expansions without affecting the jet cooling. In addition, we have shown that tryptamine can be selectively desorbed from a mixture of indole-3-acetic acid and tryptamine by adding NaOH to the mixture.

Chapter 4

Pulsed Sample Introduction Interface for Combining Flow Injection Analysis with Multiphoton Ionization Time-of-Flight Mass Spectrometry

4.1. Introduction

As shown in Chapter 3, SJ-MPIMS combined with desorption sample vaporization methods such as FAB can be a power technique for the detection of pure chemicals or relatively simple mixtures. However, for real sample analysis, it is often necessary to separate the complex mixture prior to the sample injection into a mass spectrometer. Thus, there is a great deal of interest to combine chromatography techniques such as high performance liquid chromatography (HPLC) to a mass spectrometer for on-line detection and quantitation. The great challenge here is to develop suitable interfaces for introducing the liquid flow into the mass spectrometer without significant compromise in the operating conditions of either the HPLC or the mass spectrometer. To our best knowledge, however, no suitable LC interfaces have yet been developed for SJS and MPI mass spectrometry.

There are some reports on the studies of combining HPLC or liquid injection into a supersonic jet with laser-induced fluorescence spectroscopy for molecular detection [111, 112]. Unfortunately, those interfaces are generally not suitable for laser ionization work. This is because a TOFMS, commonly used in the laser ionization work, must be operated at the pressure less than 10^{-5} torr whereas in the SJS/fluorescence detection experiments the pressure can be in the range of 0.02 to 0.005 torr [113]. In related work, Lubman and co-workers have developed an interface for supercritical fluid injection into a supersonic beam mass spectrometer [82, 116]. Although this interface may not be suitable for HPLC experiments, their work provides valuable information for the future development of LC/MPI mass spectrometry in terms of mass spectrometer system designing and the

general applicability of the MPI technique.

The ultimate goal of this research is to develop a convenient interface for combining conventional HPLC with a TOFMS, and here we report an interface to introduce the liquid flow into a time-of-flight mass spectrometer with MPI. This chapter is mainly focused on the development of flow injection analysis (FIA) [114, 115] with supersonic jet spectroscopy and multiphoton ionization mass spectrometry. It should be noted that for the simplest FIA system such as the one used here, one can view the flow injection analyzer as a HPLC system without a column. The operating conditions for its interface to a TOFMS is similar to those introducing the effluent of HPLC to a mass spectrometer. Thus, the study of FIA/TOFMS would provide some information on the performance of the interface for the future work of LC/TOFMS. In addition, there are several advantages of using FIA for SJS and MPI. FIA has the capability of introducing small-volume samples into the system in a rapid, precise way [114]. As demonstrated here, quantitation, which is not an easy task in desorption/MPI techniques [72], can be readily performed with FIA. Using FIA, there is also a potential to automate the sample injection process. Moreover, it is possible to perform on-line sample derivatization [114] such as the addition of an absorption center to a molecule of interest. This unique feature should prove useful for MPI in the detection of molecules that possess no absorption centers at the chosen wavelength.

The interface described here differs from most reported interfaces for LC/MS in which the sample molecules are introduced continuously into a quadrupole or sector mass spectrometer [91, 101-113]. In light of the fact that a TOFMS detects ions in a discrete manner, continuous sample introduction into a TOFMS will reduce the sample utilization efficiency. Thus, the work described here utilizes a pulsed sample introduction (PSI) interface to introduce the sample vapor into the TOFMS in a pulsed form. Compared with a continuous sample introduction technique, PSI allows us to use a much larger diameter orifice to introduce a larger amount of sample vapors in a short pulse into the mass

spectrometer without overloading the pumping system.

This PSI interface consists of two major parts: a heated capillary tube and a high temperature pulsed nozzle. In the experiment, sample and liquid carrier are transported through a heated capillary tube to form aerosol droplets. These aerosols are entrained into the sample vaporizer of the nozzle where the sample is thermally vaporized. The nozzle allows the vapor to be injected into the TOFMS at a repetition rate determined by the ionization source.

4.2. Experimental

Figure 4.1 shows the schematic diagram of the experimental set-up of flow injection analysis with SJS and MPI mass spectrometry. It consists of a linear Time-of-Flight mass spectrometer mounted vertically in a six-port cross pumped by a 6-in. diffusion pump (Varian Associated, Inc., Lexington, MA). The 1 m long flight tube is differentially pumped by a 4-in. diffusion pump (Varian). A liquid nitrogen (LN₂) trap assembly is used to cool part of the flight tube and the entire acceleration lens assembly (see Figure 4.1). The trap was manufactured by R.M.Jordan Co (Grass Valley, CA) to our specifications. All other vacuum components were constructed in house.

The ionization laser source is a 266 nm laser beam from a frequency-quadrupled Nd:YAG laser (GCR-3, Spectra-Physics, Mountain View, CA). The laser is operated at a repetition rate of 10 Hz. A combination of a concave and a convex lens is generally used to produce a beam 2-3 mm in diameter for ionization. The ions generated by the laser beam are extracted to the acceleration region, and then are accelerated to the drift tube. Voltages up to 15 kV can be applied to both the repeller and the acceleration grid through high voltage vacuum feedthroughs (Ceramaseal, New Lebanon, NY). The power supplies are from Spellman High Voltage Electronics (Model RH5R20PN60, Plainview, NY). In general, the voltage applied to the extraction grid is about 500-1500 volts less than the repeller voltage. This combination of voltage settings gives optimal sensitivity and mass

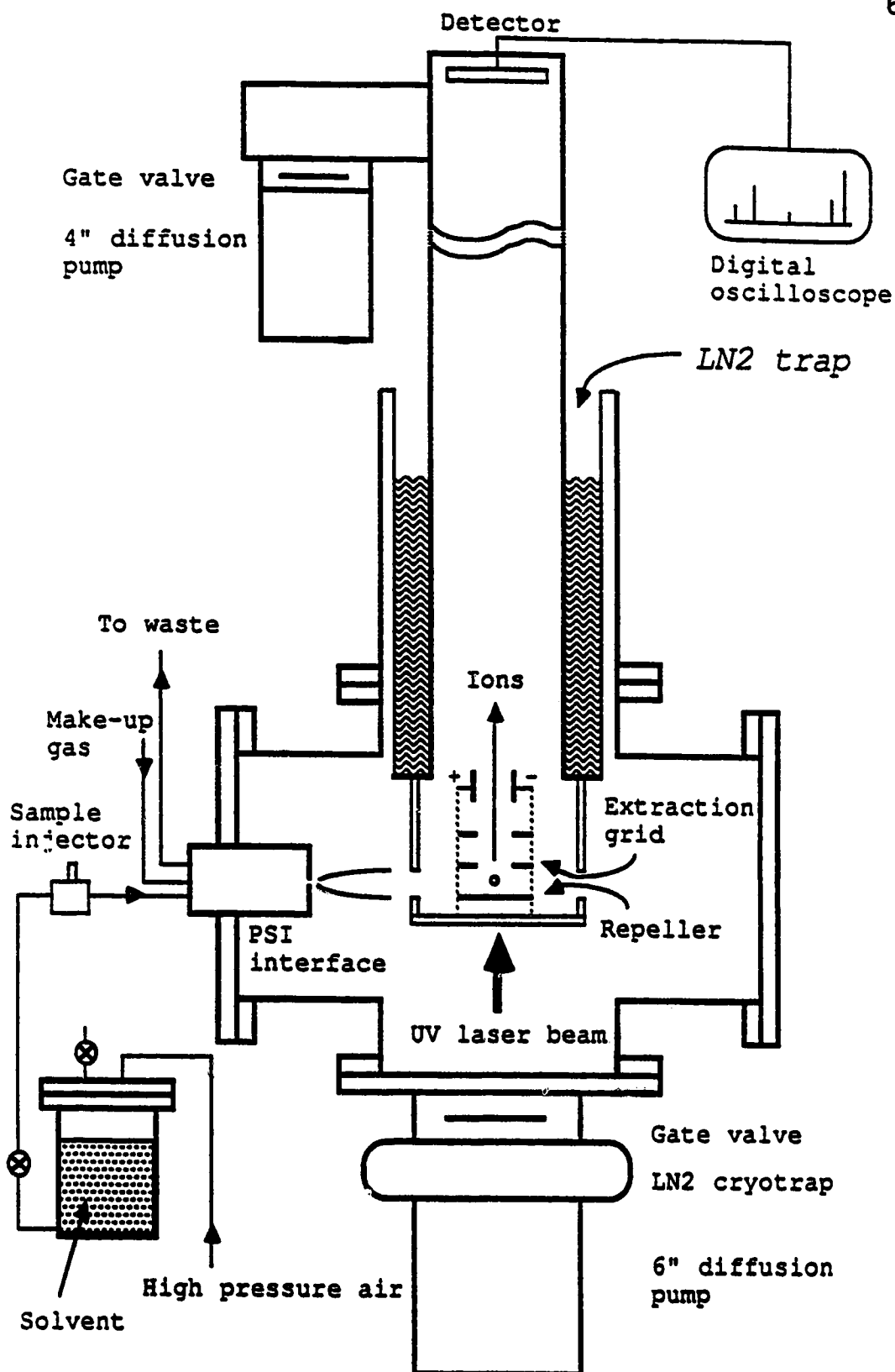


Figure 4.1. Schematic of the linear time-of-flight mass spectrometer for flow injection analysis.

resolution. The ions are detected by a microchannel plate detector (Galleo Electro-Optics Corp., Sturbridge, MA). The mass spectrum is recorded by a LeCroy 9400A digital oscilloscope. Data are then stored in an IBM compatible 386SX PC for processing. The mass resolution of this system is typically about 300.

This PSI interface consists of two important parts. One is the heated capillary tube in which the liquid flow is converted into aerosol droplets and/or supersaturated vapor. These aerosols are then expanded into the sample vaporizer for complete desolvation and vaporization. The heated capillary tube is a 5 cm long, 1.58 mm o.d. and 0.25 mm i.d. stainless-steel tubing wrapped with a Nichrome 60 heating coil (Pelican Wire Co., Naples, FL). The sample vaporizer is part of the nozzle head of a high temperature pulsed nozzle. This nozzle is designed to be used for flow injection analysis based on the earlier version of the high temperature pulsed nozzle used for SJS reported by Li and Lubman [117]. It consists of two components, i.e., the nozzle body and the nozzle head, separated by a water cooling system [117]. The cold nozzle-body contains a solenoid, which is used to drive a plunger for introducing the sample vapor to the mass spectrometer in a pulsed form. The nozzle head is heated during the operation for sample vaporization.

The current design of the nozzle body is similar to the one reported by Li and Lubman [117]. It consists of a solenoid, a spring and a plunger (see cold nozzle-body in Figure 4.2). The solenoid is a modified automobile fuel injection valve (Bosch, part number 0280150035, purchased from a local auto-parts store). The dimensions of the solenoid are 25 mm in diameter and 32 mm in length. The electric feedthrough used to provide the current for driving the solenoid is constructed of Vespel that is threaded so that it screws into the stainless-steel body. A stainless-steel rod is epoxidized into the Vespel using "Torr Seal" (Varian). A copper strip screwed on the rod is used to contact the lead of the solenoid. The power supply for driving this solenoid is similar to that reported [118]. It can generate a 400-V pulse with a duration of $\sim 35 \mu\text{s}$. In this experiment, a 100-V pulse is used to drive the solenoid.

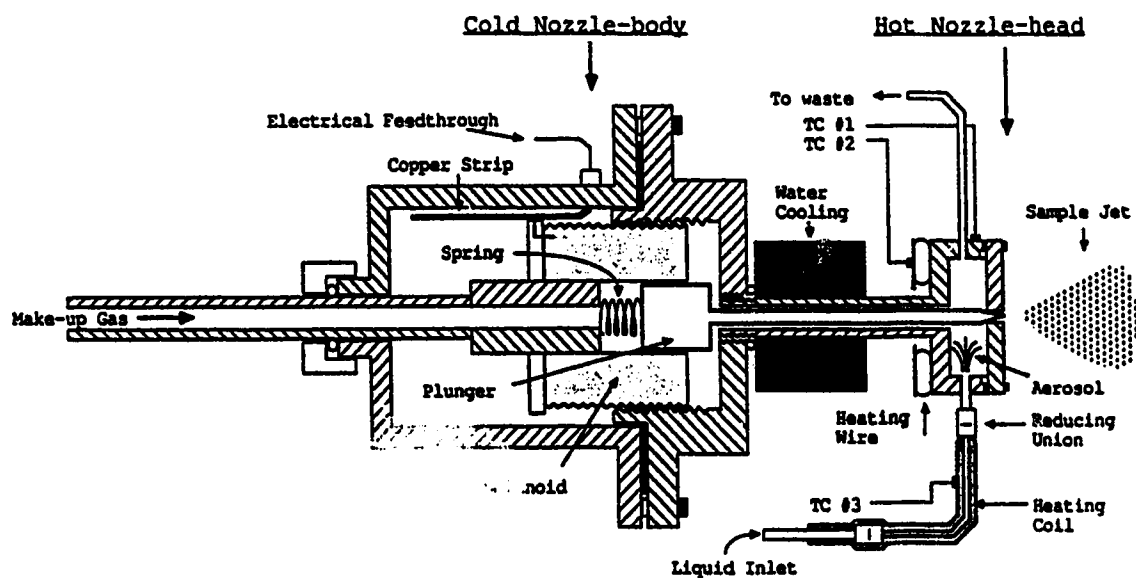


Figure 4.2. Schematic of the design of the pulsed sample introduction interface. Drawing is not to scale. The dimensions of the major components are given in the text.

The plunger is made of a long stainless-steel needle (1.5 mm in diameter and 55 mm in length) which screws into a steel base for magnetic attraction. The other end of the needle forms a metal-to-metal seal against the orifice. During the operation, a voltage is applied to the solenoid to generate a magnetic field that attracts the plunger away from the orifice to form a jet. When the power is off, the spring pushes the plunger against the orifice to make a seal. The leakage from the seal is negligible compared to the gas emitted per pulse. The sample pulse width is measured to be about 1000 μ s FWHM.

The hot nozzle-head contains a sample vaporizer, an aerosol inlet, and an outlet to waste. The sample vaporizer is heated by a coil of thermocoax heating wire (Phillips Electronic Instruments, Norcross, GA). A stainless-steel plate with a 500 μ m diameter orifice is sealed to the nozzle head using a copper gasket and knife edge seal. The dimension of the inner area of the nozzle head in which aerosol expansion and vaporization takes place is 25 mm in diameter and 8 mm in length.

Three type-K thermocouples (TCs) are used to monitor the temperatures of the interface at different regions. In the studies reported here, the temperature of the nozzle front (TC #1 in Figure 2.2) is 425°C. The temperature near the heating wire (TC #2) is 600°C. The temperature of the heating coil (TC #3) is \sim 200°C. The reading of this temperature depends on the position of the TC. In this experiment, TC #3 is located about 5 cm away from the nozzle head.

The FIA system consists of a pump driven by compressed gas, a metering valve for flow rate adjustment, and a sample injector (Rheodyne Model 7125 with a 20- μ L injection loop). Sample and carrier liquid are pumped to the PSI interface through a 1.58 mm o.d. and 1 mm i.d. stainless steel tubing. In this experiment, methanol is used as the carrier liquid with a flow rate of 0.5 mL/min. The flow rate is determined by measuring the volume of methanol consumed in a given time period. All samples are freshly made by using methanol as the solvent. All chemicals were purchased from Aldrich Chemical Co., Milwaukee, WI, or Sigma Chemical Co., St. Louis, MO and used without purification.

4.3. Results and Discussion

Applicability of the interface. Table 4.I lists the compounds studied by this FIA with MPI time-of-flight mass spectrometry. The ionization laser beam is at 266 nm with its power density of $\sim 1\text{-}2 \times 10^6 \text{ W/cm}^2$. The reason for choosing these compounds to demonstrate the applicability of this interface is mainly because they have been extensively studied by MPI in this laboratory with various vaporization/desorption techniques for sample introduction in a TOFMS. Throughout this study the experimental conditions

Table 4.I Compounds Studied by FIA/MPI Mass Spectrometry with the PSI Interface.

Compound	M.W.	M.P. (°C)	Major Ions [m/z (% rel. int.)]
(a) PAHs			
2-Methylanthracene	192	204-206	192(100)
9,10-Dimethylanthracene	206	182-184	206(100)
2-Chloroanthracene	212	221-223	212(100)
9-Chloroanthracene	212	100-101	212(100), 178(99)
1-Aminoanthracene	193	114-118	193(100), 165(36), 139(10), 63(16), 51(7), 39(13), 27(4)
2-Methylnaphthalene	142	34-36	142(100), 115(7), 63(7), 51(3), 39(5)
Triphenylene	228	197-200	228(100)
Carbazole	167	245-247	167(100)
Anthranilic acid	137	146-148	93(100)
(b) Pineal Indoles			
Tryptophan	204	289-290	204(100), 130(47)
Melatonin	232	116-118	232(100), 174(41), 160(53)

5-Methoxytryptamine	190	121-123	190(100), 160(84), 117(9), 30(22)
6-Methoxytryptamine	190	146-147	190(100), 160(49), 117(8), 30(20)
Harmaline	214	232-234	214(100)
5-Hydroxyindole-3-acetic acid	191	161-164	191(100), 146(32)
Tryptophol	161	59	161(100), 130(43), 103(12), 77(22), 51(17)
(c) Catecholamines			
DL-Tyrosine	181	325	181(100), 137(5), 107(35)
Tyramine	137	161-163	137(100), 30(63)
Octopamine*	153	169-171	153(69), 123(100), 30(54)
Syneprhine	167	187	167(24), 123(8), 44(100)
Phenylephrine*	167	143-145	167(7), 123(2), 44(100)
Metanephhrine*	197	175	197(21), 153(9), 44(100)
Phenylpropanolamine*	151	174-176	151(2), 107(3), 77(2), 44(100)
L-Dopa	197	195	197(100), 137(17), 123(24)
Hydrocinnamic acid	150	47-49	150(100)
Vanillic acid	168	210-213	168(100)
4-Hydroxy-3-methoxyphenyl- acetic acid	182	142-145	182(100), 137(33)
3,4-Dihydroxyphenylacetic acid	168	127-130	168(100), 146(71)
4-Hydroxy-3-methoxy- mandelic acid	198	132-134	198(100), 153(5), 65(14)
3-Hydroxy-4-methoxy- mandelic acid	198	132-134	198(100), 153(5), 65(9)

Homovanillyl alcohol	168	40-42	168(100), 137(31)
(d) Neuroleptic drugs			
Desipramine*	266	214	266(100), 208(17), 194(15), 72(20), 58(17), 44(32)
Promazine*	284	181	284(23), 86(8), 58(100), 44(6)
Chloropromazine*	318	194-196	318(20), 274(3), 86(9), 58(100), 44(9)
Imipramine*	280	174-175	280(100), 236(34), 208(9), 194(6), 86(28), 58(52), 44(7)
(e) Volatile molecules			
Phenol	94	43	94(100), 65(10), 39(8)
2-Ethylphenylamine	135	**	135(100), 120(57), 103(4), 77(7), 51(4), 39(3), 27(3)
o-Anisidine	123	6	123(100), 108(31), 80(15), 51(8), 39(4), 27(8)
1-Benzylpiperazine	176	**	176(100)
o-Cresol	108	31	108(100), 91(7), 77(10), 27(10)
3-Ethylphenol	122	**	122(100), 107(48), 77(14), 51(4), 39(6), 27(12)
4-Propylphenol	136	22	136(100), 107(88), 77(10), 27(10)
2-sec-Butylphenol	150	16	150(94), 121(100), 107(3), 91(3), 77(14), 51(10), 39(5), 27(6)

*HCl salt.

**Liquid.

are kept the same. The temperature of the heated capillary tube is 200°C and the temperature near the nozzle orifice is 425°C. A make-up gas of CO₂ is used and its flow rate is optimized to be ~40 mL/min. The use of the make-up gas prevents sample and liquid carrier condensation which may occur due to their feedback from the nozzle's hot head to its cold body. It also provides a means of sweeping the sample and liquid carrier vapors out of the sample vaporizer rapidly, resulting in sharp peaks with less tailing (see below and Figure 4.6).

Figure 4.3 shows some typical MPI mass spectra of molecules studied by this FIA/MPI mass spectrometry. One of the key results is that molecular ions are observed for most compounds studied. In general, no thermal decomposed products are detected. Note that some molecules listed in Table 4.I are considered as thermally labile. For instance, indole-3-acetic acid can be readily decomposed upon heating. Figure 4.4(A) shows the MPI mass spectrum of this compound. This mass spectrum is obtained by placing the solid sample directly into the nozzle and heating the sample up to 150°C. At this temperature, a peak corresponding to methylindole is observed. Further heating only increases the intensity of this peak. No molecular ion peak is observed. This result shows that indole-3-acetic acid, upon directly heating, decomposes into methylindole. However, the mass spectrum in Figure 4.4(B) obtained by using FIA with MPI displays a strong molecular ion peak for indole-3-acetic acid. The lack of thermal decomposition in this study can be attributed to the fact that the sample molecules are rapidly vaporized in the sample vaporizer. Moreover, the probability for the sample to make a contact with the inner wall of the vaporizer is minimized due to the presence of large quantity of hot methanol vapor resulting in the reduction of catalysis action of the metal surface [119]. However, for anthranilic acid as shown in Table 4.I only the thermally decomposed product is observed. This indicates that for thermally very labile compounds this interface involving rapid heating may still cause decomposition.

It should also be noted from Table 4.I that this interface is capable of introducing

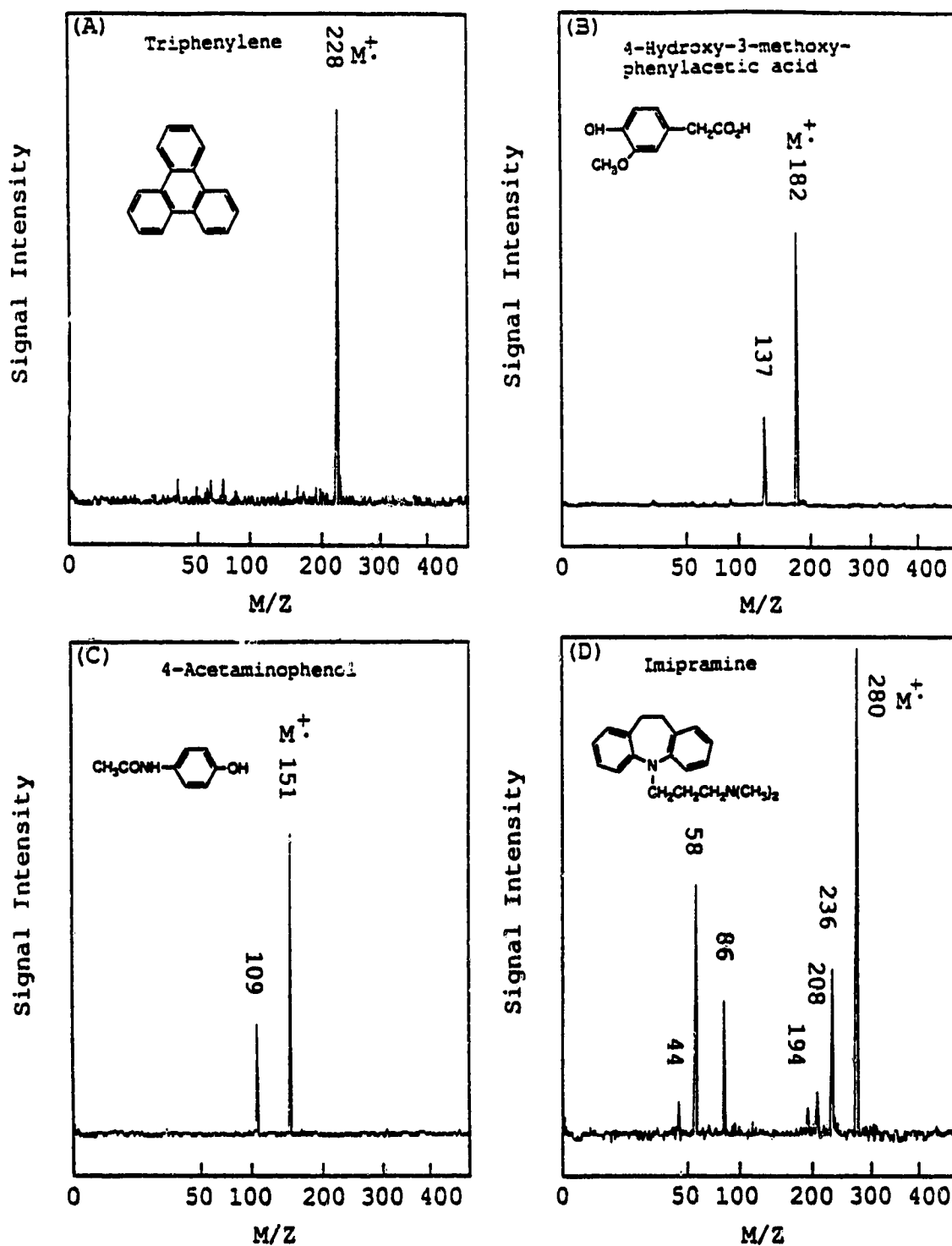


Figure 4.3. MPI mass spectra of (A) triphenylene, (B) 4-hydroxyl-3-methoxyphenylacetic acid(homovanillic acid), (C) 4-acetaminophenol, and (D) imipramine. The ionization laser beam was at 266 nm with its power density $\sim 1 \times 10^6$ W/cm².

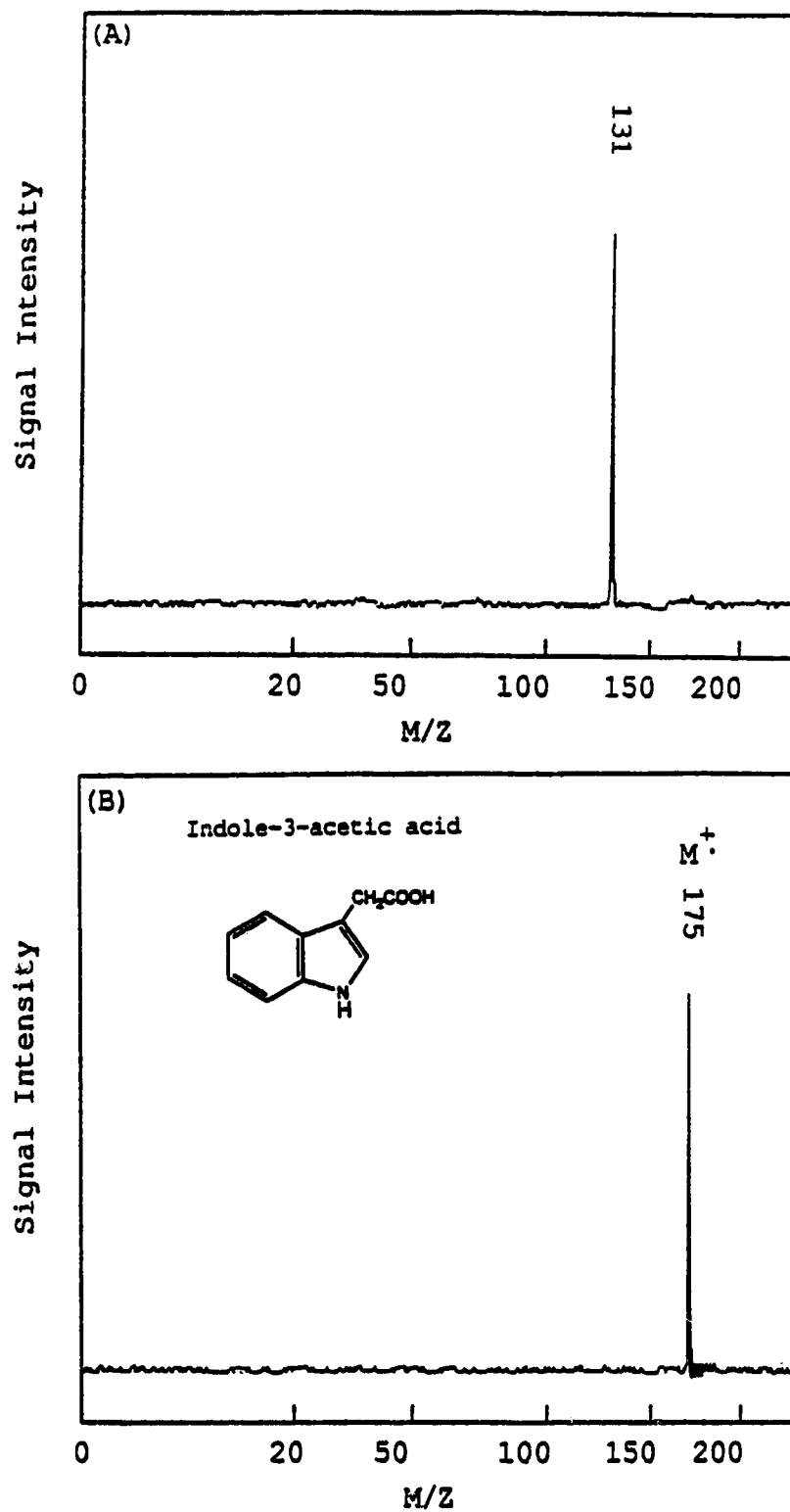


Figure 4.4. MPI mass spectra of indole-3-acetic acid obtained by using (A) direct heating and (B) FIA with MPI. The ionization laser beam was at 266 nm with its power density $\sim 1 \times 10^6 \text{ W/cm}^2$.

both volatile and nonvolatile sample molecules into a TOFMS. The ability of the system to also detect highly volatile species is an important aspect of this interface technique. For nonvolatiles which can be dissolved in methanol, compounds with melting points as high as 325°C (DL-tyrosine) can be transported into the mass spectrometer using the PSI interface.

Background Reduction with a LN₂ trap. In this PSI interface technique, the sample molecules are vaporized and entrained into the ionization region of the TOFMS. Because only a small portion of the gas phase neutral molecules is ionized, most samples will condense on the wall of the lens assembly of the TOFMS. These molecules and their decomposed products will eventually become the background for the analysis of other samples or the same sample in the next run. This cross-contamination can become quite severe in light of the fact that the turn-around-time of the FIA system is usually very short and a large number of samples can be analyzed in a given time period. In the work of interfacing HPLC with MPI, we also anticipate that a severe cross-contamination will occur, especially with the limited pumping capacity we have here. Due to the possible overlapping of the molecular ion and fragments with the background signals, the sensitivity for the detection of molecules of interest is often reduced and the structural information obtained from the mass fragmentation pattern suffers.

A method we have recently developed for background reduction in LD and FAB/MPI [120], based on the ion trajectory differences between the sample ions generated from the jet-cooled molecules and the background ions during the flight from the acceleration region to the detector, can only be applied to a reflectron TOFMS. Thus, the method is not suitable for this work in which a linear TOFMS is used. An alternative method is to use a liquid nitrogen trap to condense the background molecules as well as the solvent vapor. Lubman and Jordan have used this approach to reduce the background in a linear, supersonic beam TOFMS [79]. Later, this method has been used for background reduction in LD/MPI [39]. We show that the liquid nitrogen trap from Jordan Co. can be

used to reduce the background signals very efficiently for this PSI interface.

Figure 4.5(A) shows the MPI mass spectrum of background molecules obtained by using the 266-nm ionization laser beam. This represents a typical background spectrum obtained during the FIA/MPI experiments after several sample injections. It is quite clear that the background signals are very strong. Figure 4.5(B) shows the MPI mass spectrum of aniline along with the background signals. Note that the relative intensities of the individual peaks from the background molecules have been changed. This can probably be attributed to the fact that the sample molecules expand into the vacuum and push some background molecules away, resulting in a variation of the background molecule distribution within the ionization region [120]. Thus, it is difficult to use background subtraction method to eliminate the background peaks. This is particularly true when extensive fragments are produced for structural analysis. Figure 4.5(C) shows the MPI mass spectrum of the background with the LN2 trap filled. All experimental parameters except the vacuum pressure are the same as those used in Figure 4.5(A). As Figure 4.5(C) illustrates, the background signals are now dramatically reduced. Figure 4.5(D) is the mass spectrum of aniline. This figure illustrates that fragment ions from aniline can be clearly identified.

Besides background reduction, the use of a LN2 trap also results in significant reduction of the vacuum pressure. Without LN2 being filled in the trap, the pressure is normally at 5×10^{-7} torr in the detector region when the nozzle is off. However, when the nozzle is open, the pressure rises to 2×10^{-5} torr. After the trap is filled with LN2, the pressures are 1×10^{-7} torr with the nozzle off and 1.5×10^{-7} torr with the nozzle on. It is found that this reduction of the vacuum pressure increases the ion signal intensity. In addition, it allows us to use higher voltages for ion acceleration without any problems such as arcing (see below). It should be noted that when the system is continuously being operated, a full tank of LN2 in the trap (about 4 liters) can last for about 5 hours without refilling.

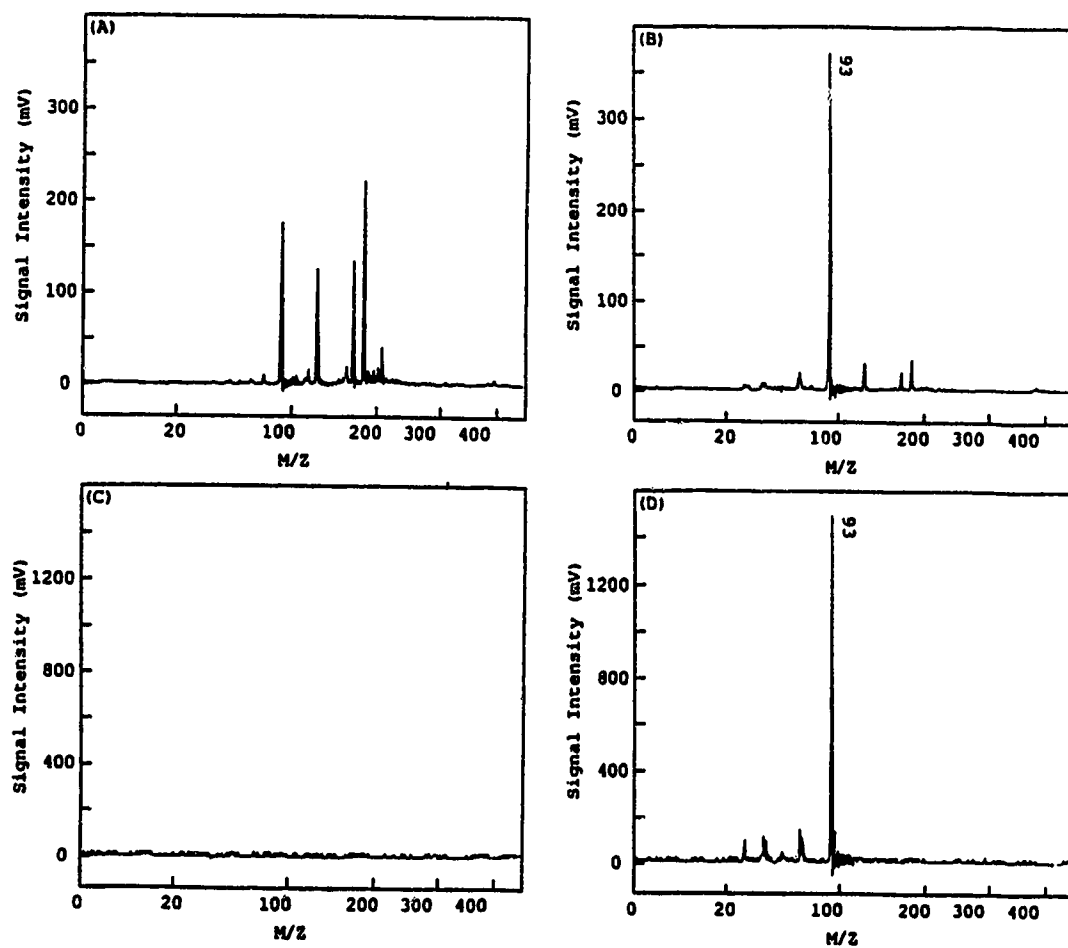


Figure 4.5. MPI mass spectra of (A) background, (B) aniline with background, (C) background with the LN2 trap filled, and (D) aniline with the LN2 trap filled. The ionization laser beam was at 266 nm with its power density $\sim 2 \times 10^6 \text{ W/cm}^2$.

Precision and Memory effects. Figure 4.6 illustrates a series of repeated injections of different concentrations of indole-3-acetic acid. In this experiment, the molecular ion intensity is monitored and integrated by a box-car integrator. The averaged signal is recorded on a chart recorder to produce a flowgram. As Figure 4.6 shows, for five injections at each concentration, the peak areas are quite reproducible. The relative standard deviation (RSD) for each set of peaks is shown above these peaks in the figure. We find that reproducible results can also be readily obtained with this interfacing technique for other compounds. The average RSD is in the range of 4-8%. The key parameters needed to be optimized to achieve reproducible results are the flow rate and the temperature of the heated capillary tube. For this work, the temperature of the tube is optimized at 200°C and the flow rate is 0.5 mL/min. It should be noted that the RSD increases to about 10-20% when the amount of the sample injected is close to the detection limit. Although the reproducibility of the present system is sufficient for many analytical applications, it can be further improved by (1) using a better solvent delivery system to regulate the flow rate more precisely, (2) using feedback control power supplies to control the heating of the interface, and (3) using electronic integration (instead of a chart recorder) with digital filtering or other noise reduction methods.

Figure 4.6 also illustrates that no memory effects were observed at the experimental conditions used. The peak width in terms of time is about 10 s at FWHM. At a flow rate of 0.5 mL/min, this will correspond to a sample volume of 83 μ L. This indicates that peak broadening is observed since we only inject 20 μ L of sample. The extent of interface contribution to this broadening is unknown at present as the carrier transport tube also introduces peak broadening. However, one would expect that peak broadening does occur in this interface, since a large volume change takes place when sample and liquid carrier are vaporized. It takes finite time for the sample vapor to exit the sample vaporizer, resulting in a small tailing in the detected peak as shown in Figure 4.6. Nevertheless, this tailing is not so severe, compared with other interfacing techniques [121]. The fact that no memory

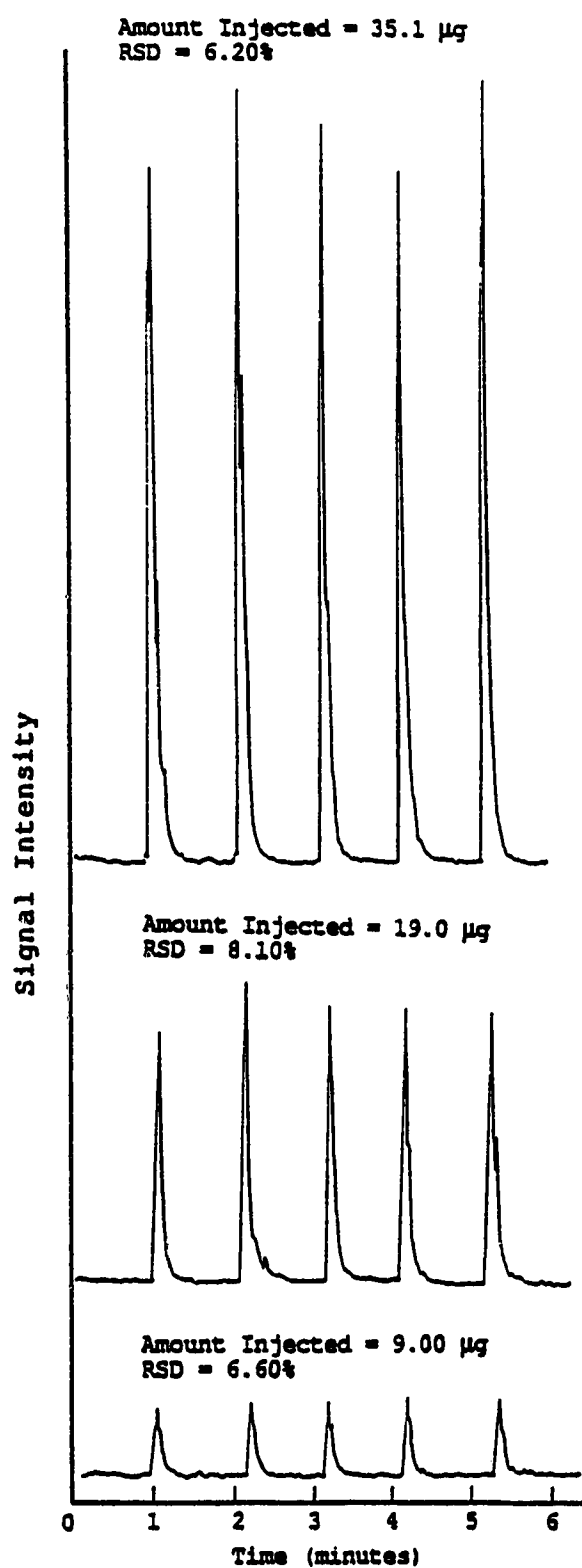


Figure 4.6. Flowgrams for repeated injections of different concentrations of indole-3-acetic acid.

effects and no severe tailing are observed in this interface for FIA/MPI leads us to conclude that it seems feasible to combine HPLC with a TOFMS by using this PSI interface.

Sensitivity and Quantitation. Although the overall sample transmission efficiency for the PSI interface is unknown, the detection limits for several compounds are measured. It is found that for the current system the detection limits are in the nanogram region. For instance, the detection limits at a signal-to-noise ratio of 2 are 3 ng for aniline (b.p. 184°C), 140 ng for indole-3-acetic acid (m.p. 165-169°C), and 4 ng for tryptamine (m.p. 114-119°C). Although these three compounds have different volatility, it appears that the sensitivity of this technique very much depends on only the ionization efficiency for these three compounds. This is because in the MPI studies of indole-3-acetic acid and tryptamine with the use of laser desorption or FAB for sample vaporization, the calibration curves of the molecular ion intensity vs. concentration are similar to that observed here. Aniline has a very high ionization efficiency (~ 25%) [26]. Thus, the detection limit for this compound is lower. However, for chemicals with very low volatility, the sensitivity of the technique may not just depend on the ionization efficiency. Other parameters such as vaporization efficiency are expected to play an important role. Further work is needed to illustrate the effect of various individual parameters on the sensitivity of the system.

The ability to perform quantitation without the use of any internal standards is an important feature of this FIA/MPI method. Figure 4.7(A) shows the calibration curve of tryptamine at high laser power and high acceleration voltages. The data of the peak areas are expressed as an average of five sample injections. The peak areas are integrated by a weighing method and normalized against any variation such as gain in the integrator. As Figure 4.7(A) shows, excellent linearity over more than 2 orders of magnitude is obtained. When the total amount of tryptamine injected is above 2 μ g, molecular ion signal becomes very broad though, indicating that the signal is saturated with the electric detection system used here. However, by decreasing the laser power and acceleration voltages, signal saturation can be eliminated. On the other hand, decreasing the laser power and voltages

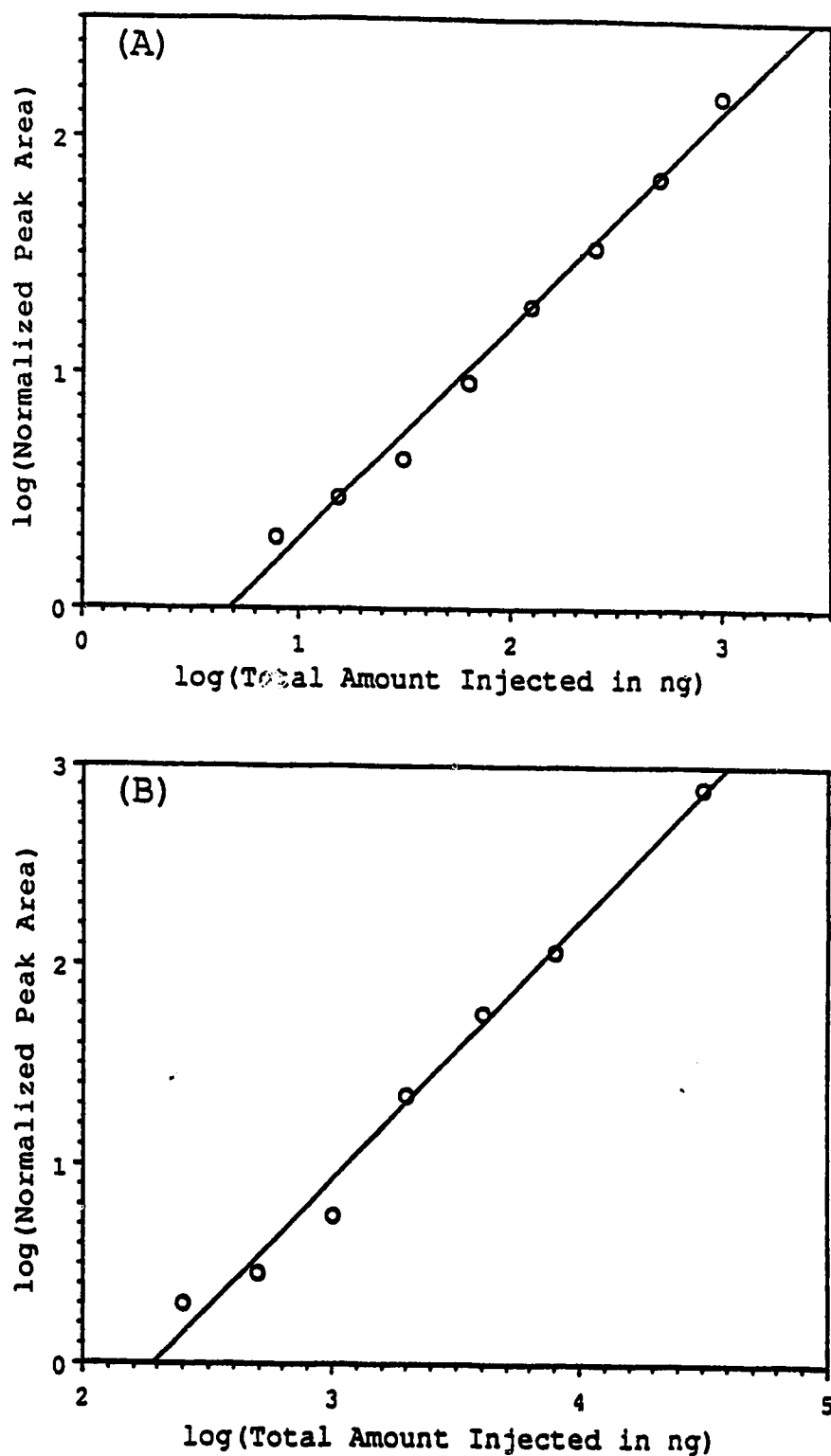


Figure 4.7. Calibration curves of tryptamine. The laser power density is $1 \times 10^7 \text{ W/cm}^2$ and the repeller voltage is 12.5 kV for (A). The laser power density is $\sim 1 \times 10^6 \text{ W/cm}^2$ and the repeller voltage is 5 kV for (B).

reduces the detection sensitivity for the lower concentration samples. Figure 4.7(B) shows the calibration curve of the same compound obtained by using low laser power and low acceleration voltages. This figure illustrates that a linear response over two orders of magnitude can again be obtained, although it is in a different concentration range than that shown in Figure 4.7(A). Thus, it can be concluded that (1) with a fixed laser power and acceleration voltages, 2 orders of magnitude linearity can be achieved for quantitations, and (2) by a proper selection of the laser power and/or acceleration voltages, the linear region can be changed to a different concentration range.

As indicated before, the lower vacuum pressure achieved in the system due to the aid of a LN₂ trap allows us to apply higher voltages for ion acceleration without causing problems such as arcing. We show here that by using 12.5 kV for ion acceleration instead of 5 kV, signals can be generally enhanced about 5 to 10 times for the compounds studied. Figure 4.8 shows the mass spectra of tryptamine obtained by FIA with MPI at 266 nm at different acceleration voltages. The total amount of sample injected is 1 µg. As Figures 4.8(A) and (C) show, the soft ionization of this molecule can be obtained at low laser power. The peak at m/z 130 is from the parent molecule with the loss of $\text{CH}_2\text{-NH}_2$ radical. The hard ionization mass spectra shown in Figures 4.8(B) and (D) reveal that the fragmentation pattern does not change significantly when the acceleration voltage increases. However, the signal intensity is increased when the voltage is changed from 5 kV to 12.5 kV. From the peak areas of the tryptamine flowgram, we estimated that the signal intensity is increased about 8 times.

Clustering. Cluster formation is very likely during the supersonic jet expansion [122]. This is particularly true in the cases where polar solvents are used. Solvents such as methanol and water can interact with sample molecules strongly to form clusters. Cluster formation will reduce the molecular ion peak intensity. In some cases such as the analysis of a mixture, peaks from the cluster ions will also make the molecular ion peak assignment difficult. Thus, for analytical applications, cluster ions are usually undesirable.

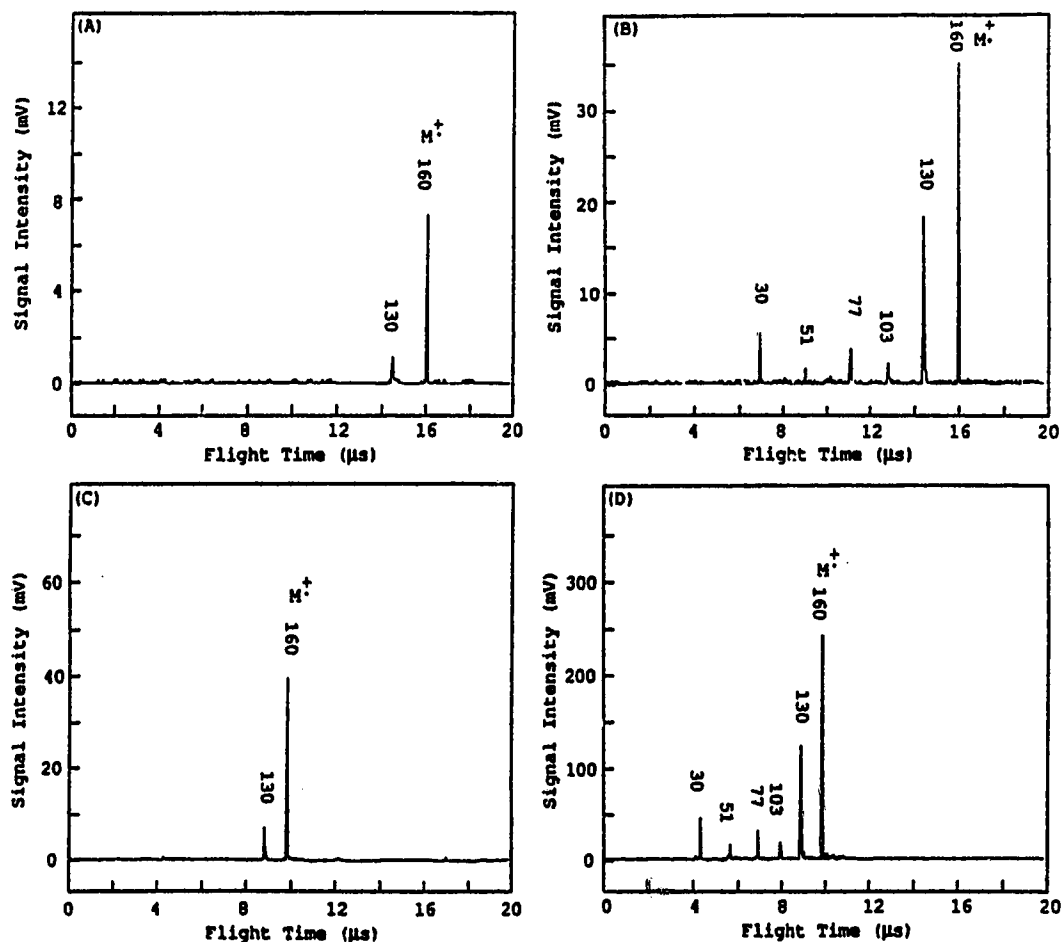


Figure 4.8. Soft and hard MPI mass spectra of tryptamine obtained by FIA with MPI at 266 nm. The repeller voltages are 5 kV for (A) and (B), and 12.5 kV for (C) and (D). The ionization power densities are $\sim 1 \times 10^6$ W/cm² for (A) and (C), and $\sim 1 \times 10^7$ W/cm² for (B) and (D).

Fortunately, in this experimental set-up, we normally do not observe significant amount of clusters. The reason for this is believed to be related to the fact that the temperature of the sample vaporizer of the nozzle is very high. It is known that the reduction of the nozzle temperature energetically favors the formation of clusters while heating the nozzle can reduce the population of clusters [123].

In the cases where we do observe the cluster ions, the variation of the delay time ($\Delta\tau$) between the nozzle opening and the ionization laser pulse can eliminate the cluster ion peaks in the MPI mass spectrum. An example is shown in Figure 4.9. Figure 4.9(A) is the MPI mass spectrum of indole-3-acetic acid at 266 nm with the delay time ($\Delta\tau$) of 660 μs . Figure 4.9(B) is the mass spectrum of the same compound obtained at the same experimental conditions as in Figure 4.9(A), but with the delay time of 540 μs . As Figure 4.9(B) shows, the cluster ions are not detected when the delay time is set properly so that the laser beam intersects the front portion of the sample pulse. This portion of the molecular beam does not contain a significant amount of clusters. This finding is consistent with the results reported by Pang and Lubman [124] where a supercritical NH_3 fluid is used for sample delivery. It should be noted that the front portion of the sample pulse is composed of the coldest molecules in the jet [120]. As a result, an optimal jet-cooled spectrum can be obtained.

4.4. Conclusion

We have developed a pulsed sample introduction interface for combining FIA with a TOFMS. It is demonstrated that this PSI interface can be used to introduce a variety of volatile and nonvolatile molecules into a TOFMS for MPI studies. In most cases, thermal decomposition is not observed. It is also shown that reproducible results can be readily obtained with PSI. No memory effects are found and no severe peak tailing is observed. The detection limits of the present system are in the nanogram region. It is found that excellent linearity over a two orders of magnitude analytical range can be obtained for the

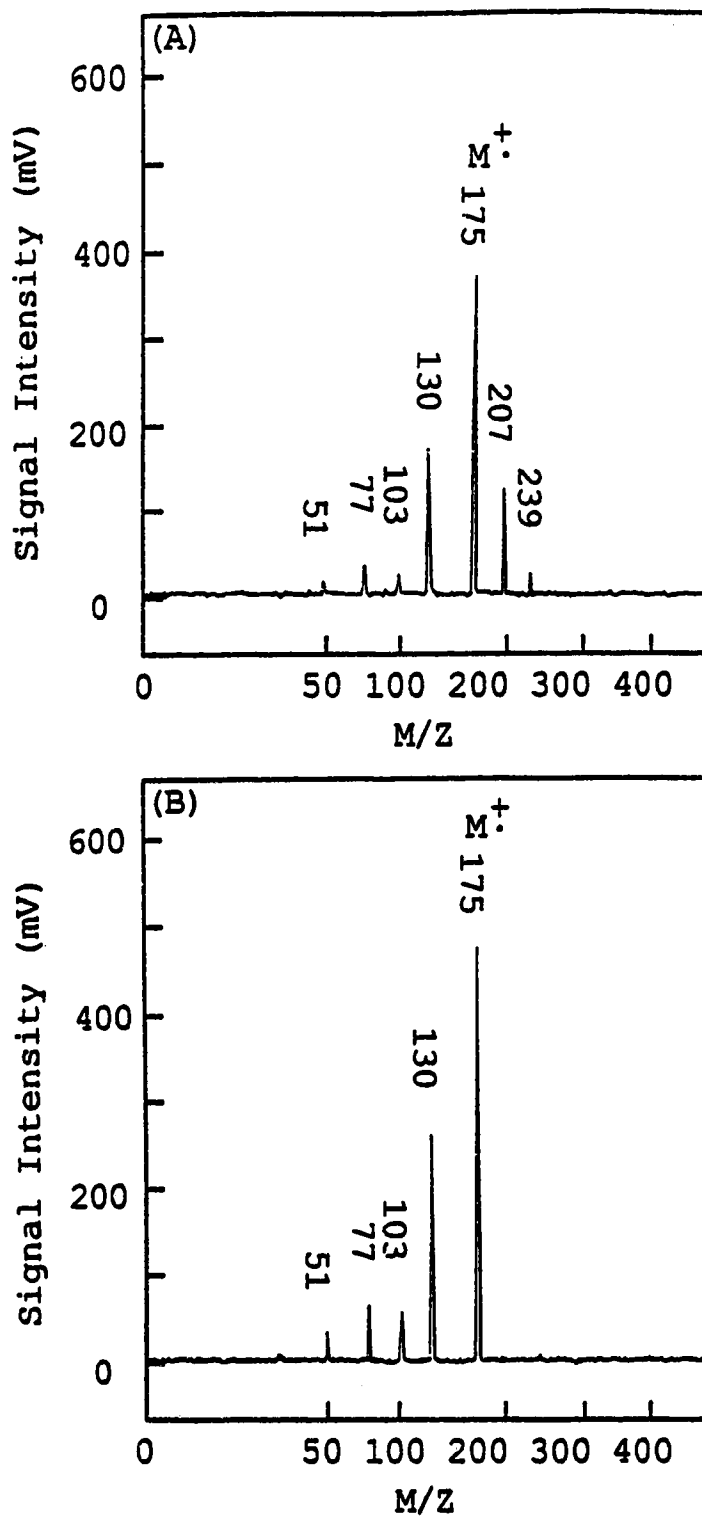


Figure 4.9. MPI mass spectra of indole-3-acetic acid at different delay times: (A) $\Delta\tau = 660 \mu\text{s}$ and (B) $\Delta\tau = 540 \mu\text{s}$. The ionization laser beam was at 266 nm with its power density $\sim 4 \times 10^6 \text{W/cm}^2$.

compounds studied. Another important issue, i.e., clustering, which is unique to the supersonic jet expansion, is studied. It is found that clustering is not a major problem for this interface. For most compounds studied, significant amount of cluster ions are not observed in MPI mass spectra. In the cases where clusters do form, these clusters are found to be formed in the back portion of the sample pulse. Thus, the proper adjustment of the delay time between the nozzle opening and laser pulse allows one to ionize the parent molecules only.

Chapter 5

Liquid Chromatography/Time-of-Flight Mass Spectrometry with a Pulsed Sample Introduction Interface

5.1. Introduction

As described in Chapter 1, mass spectrometry combined with chromatography separation is one of the most powerful techniques for trace analysis. Techniques such as gas chromatography/mass spectrometry (GC/MS) have become a routine method for the detection of organic compounds in a variety of complex matrices. However, many thermally labile and nonvolatile molecules including many highly water-soluble organic pollutants and biochemicals are not amenable to GC/MS. At present, the separation of these molecules is generally done by using high performance liquid chromatography (HPLC). Thus, to extend the MS technique for the detection of these molecules, a powerful on-line LC/MS system should prove very useful.

Almost all current LC/MS systems utilize scanning MS (sectors or quadrupole) for LC detection. To our best knowledge, no suitable interface has yet been developed for combining conventional HPLC capable of handling high flow rates with time-of-flight mass spectrometry (TOFMS). With modern electronics and advanced computer technology, however, TOFMS has the potential to become a very important tool for LC detection with several unique features including its versatility and higher detection sensitivity with no mass limit. Thus, we plan to develop an alternative LC/MS system based on TOFMS with a novel pulsed sample introduction (PSI) interface developed in our laboratory [125]. This interface has been described in a previous chapter.

In this chapter, we report the use of the pulsed sample introduction interface for combining conventional LC with TOFMS. The studies of several important parameters affecting the performance of the LC/TOFMS system are also included. The effective sample transfer efficiency in the PSI interface is reported.

5.2. Experimental

Liquid Chromatography. The LC solvent delivery system consists of a Shimadzu LC-600 programmable liquid pump capable of delivering solvent with variable flow rates ranging from 1 $\mu\text{L}/\text{min}$ to 10 mL/min . For chromatographic work, a Waters Nova-Pak C-18 column (Millipore Ltd., Mississauga, On) is used for separation. A Rheodyne Model 7125 syringe loading injector with a 20 μL sample loop is used for sample injection. In between the column and the PSI interface, a Shimadzu SPD-M6A photodiode array detector is used for obtaining a UV chromatogram. All flow lines are connected with the use of 1.58 mm o.d. and 1 mm i.d. stainless steel tubings.

Pulsed Sample Introduction Interface and Time-of-Flight Mass Spectrometer. The PSI interface and the Time-of-Flight Mass Spectrometer have been described in detail in Chapter 4. All the chemicals were obtained from Sigma Chemical Co. and Aldrich Chemical Co. and used without further purification.

5.3. Results and Discussion

Performance of LC/TOFMS. Figure 5.1 shows the chromatograms of two polycyclic aromatic hydrocarbons (PAHs), namely, triphenylene and benzo[a]pyrene. A mixture of these two PAHs at an amount of 1 μg each is separated by using the C-18 column with 100% methanol as the mobile phase at a flow rate of 1 mL/min . Figure 5.1(A) is the UV chromatogram recorded at 266 nm from the diode array detector. Peak a is from the solvent (benzene). Peaks b and c are from triphenylene and benzo[a]pyrene, respectively. The ion chromatogram obtained by using the LC/TOFMS technique is shown in Figure 5.1(B). For Figure 5.1(B), the gate width of the boxcar integrator is set to monitor the molecular ion peaks of triphenylene and benzo[a]pyrene. The molecular ion peak of the solvent is not monitored. Note that a peak with opposite direction appears in Figure 5.1(B) at the same retention time as benzene. This is due to the electric noise in the boxcar integrator caused by a large ion signal from the ionization of benzene with the 266 nm laser

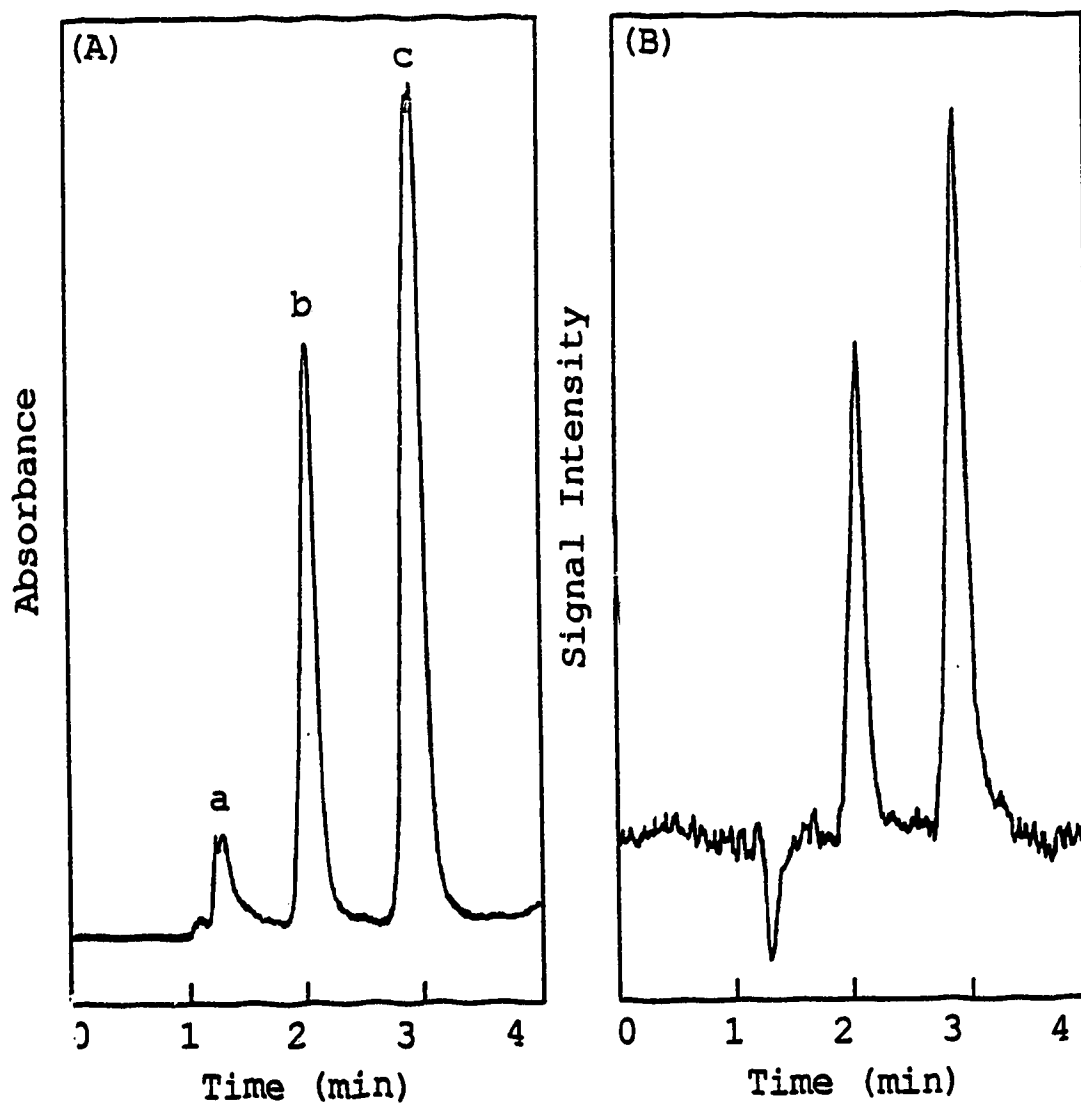


Figure 5.1. (A) UV chromatogram and (B) total ion chromatogram of a mixture of benzo[a]pyrene and triphenylene.

beam. As Figure 5.1 illustrates, the ion chromatogram is almost the same as the UV chromatogram in terms of peak shapes and retention times. No significant peak broadening and other chromatographic distortions are found.

Another example is shown in Figure 5.2 for the chromatograms of three indole derivatives, namely, indole-3-acetic acid, tryptamine, and tryptophol, with an injection of a mixture of 3 μ g each in methanol. The separation is carried out under the isocratic condition with a mobile phase containing 40% water and 60% methanol at a flow rate of 1 mL/min. Figure 5.2(A) is the UV chromatogram and Figure 5.2(B) is the ion chromatogram obtained by monitoring the intensities of three molecular peaks simultaneously with the boxcar integrator. Clearly, under the experimental conditions used, the separation of indole-3-acetic acid and tryptamine is incomplete. However, by monitoring the intensity of the individual molecular ion peak, a selected ion chromatogram can be obtained. Figures 5.2(C), (D) and (E) are the selected ion chromatograms for indole-3-acetic acid, tryptamine, and tryptophol, respectively. Since the UV spectrum for these three compounds are almost the same in the solution, it is not possible to selectively detect individual component by tuning the detection wavelength in the UV diode array detector. It is obvious that TOFMS is superior for the detection of coelutes for LC, compared with a UV detector. More importantly, this example demonstrates that peak distortion is not observed even for coelutes with different molecular properties.

Parameters affecting the LC/TOFMS performance. The above two examples demonstrate that the PSI interface is well suited for combining LC with TOFMS. Next we study the parameters affecting the performance of the LC/TOFMS system. These include the flow rate and the composition of the mobile phase, the temperatures of the sample vaporizer and the capillary tube, and the flow rate of the makeup gas which is introduced into the sample vaporizer directly by passing through the solenoid and the long channel used for holding the plunger.

Figure 5.3 shows the results obtained with a series of injections of 1 μ g of indole-3-

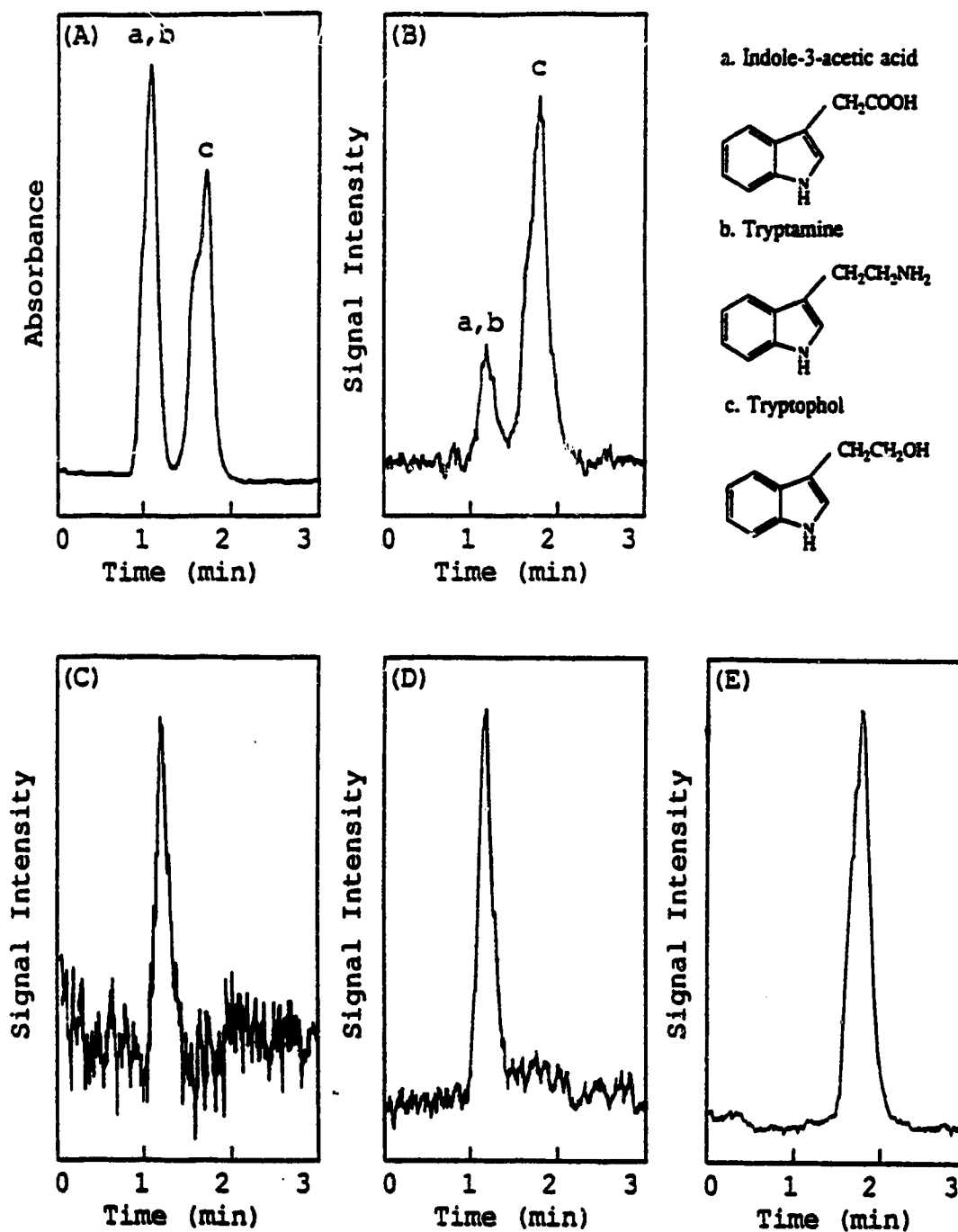


Figure 5.2. (A) UV chromatogram and (B) total ion chromatogram of a mixture of indole-3-acetic acid, tryptamine, and tryptophol. The selected ion chromatograms of (C) indole-3-acetic acid, (D) tryptamine, and (E) tryptophol are obtained by monitoring the individual molecular ion peak only with the use of a linear integrator.

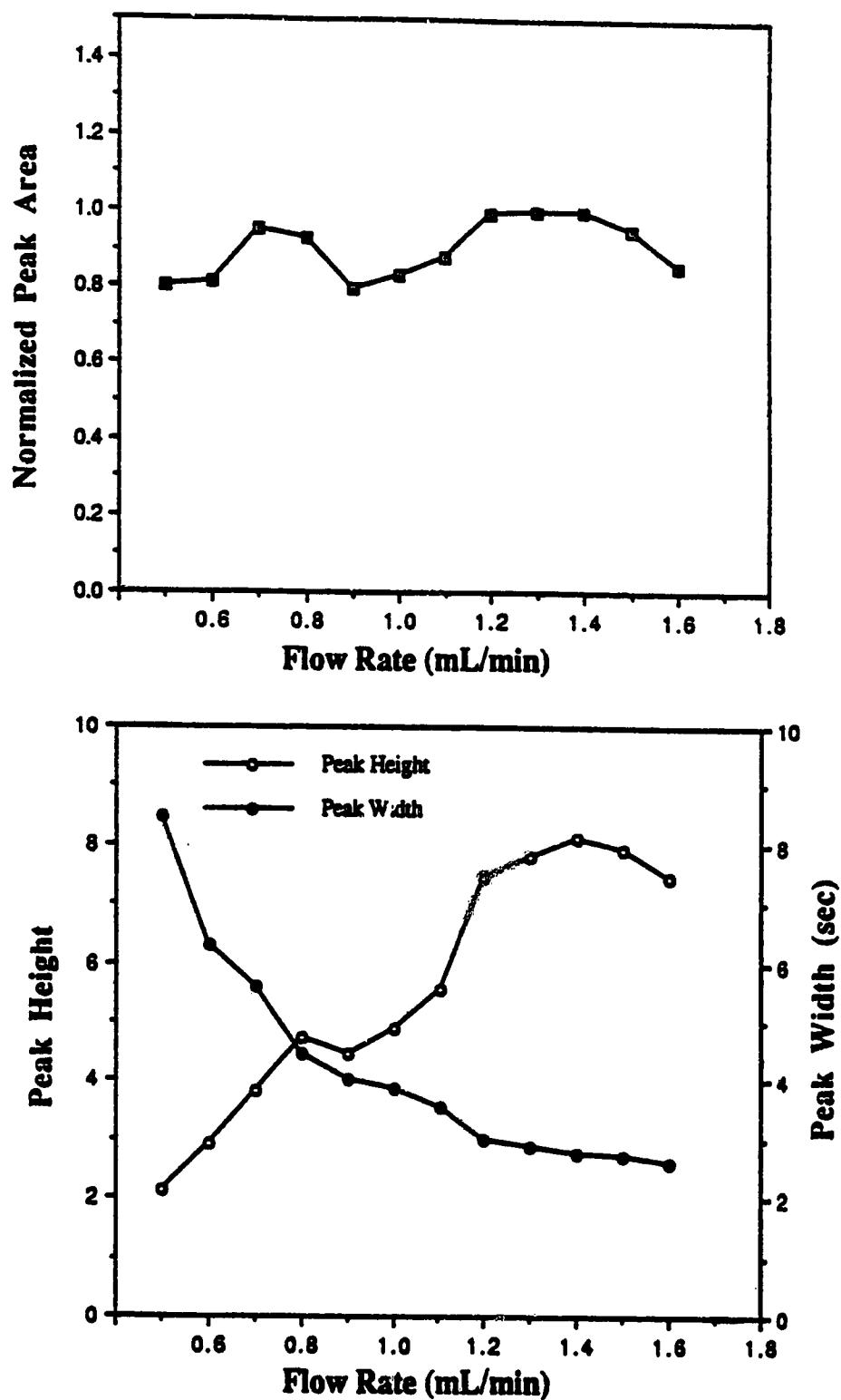


Figure 5.3. Mobile phase flow rate dependence on the performance of the PSI interface. Indole-3-acetic acid is used as the test sample. Methanol is used as the mobile phase.

acetic acid into the methanol stream at different flow rates. All experimental conditions except the flow rate are kept constant. In particular, careful adjustment is made each time when the flow rate is changed to ensure the temperatures of the sample vaporizer and the capillary tube remain constant. As one would expect it, higher flow rate requires more heating power. As Figure 5.3 indicates, the peak height increases and the peak width decreases as the flow rate changes from 0.5 to 1.6 mL/min. However, the peak area which is related to the amount of the sample injected does not vary significantly across the entire flow rate range used. This study indicates that the PSI interface is capable of introducing high flow rate LC effluent, comparable to the flow rate used in conventional LC, into the time-of-flight mass spectrometer.

Various organic solvents including methanol, acetonitrile, hexane, and acetone have been tested for suitability for the PSI interface. It is found that these solvents and mixtures of them with differing proportions can be used without the need of changing the interface conditions. Water can also be used as the mobile phase. However, in this case the detection sensitivity generally decreases as the water content increases, as shown in Figure 5.4. Figure 5.4 plots the scaled peak areas for tryptophol, indole-3-acetic acid, and tryptamine, separated by using a C-18 column, as a function of water content in the mobile phase. (A typical chromatogram is shown in Figure 5.2 where a mixture of 40% water and 60% methanol is used as the mobile phase.) Note that, with 100% water used for separation, the scaled peak area for tryptophol is not shown in Figure 5.4. This is because under this condition the peak of tryptophol in the chromatogram becomes too broad to calculate its area.

Several other compounds have also been studied with or without a column. We find that about one order of magnitude reduction in sensitivity is generally observed when the mobile phase is changed from an organic solvent to pure water. This sensitivity reduction is mainly due to the pressure increase in the vacuum chamber. When water is used, the pressure rises from $<5 \times 10^{-7}$ to $\sim 5 \times 10^{-6}$ torr. It appears that even with the

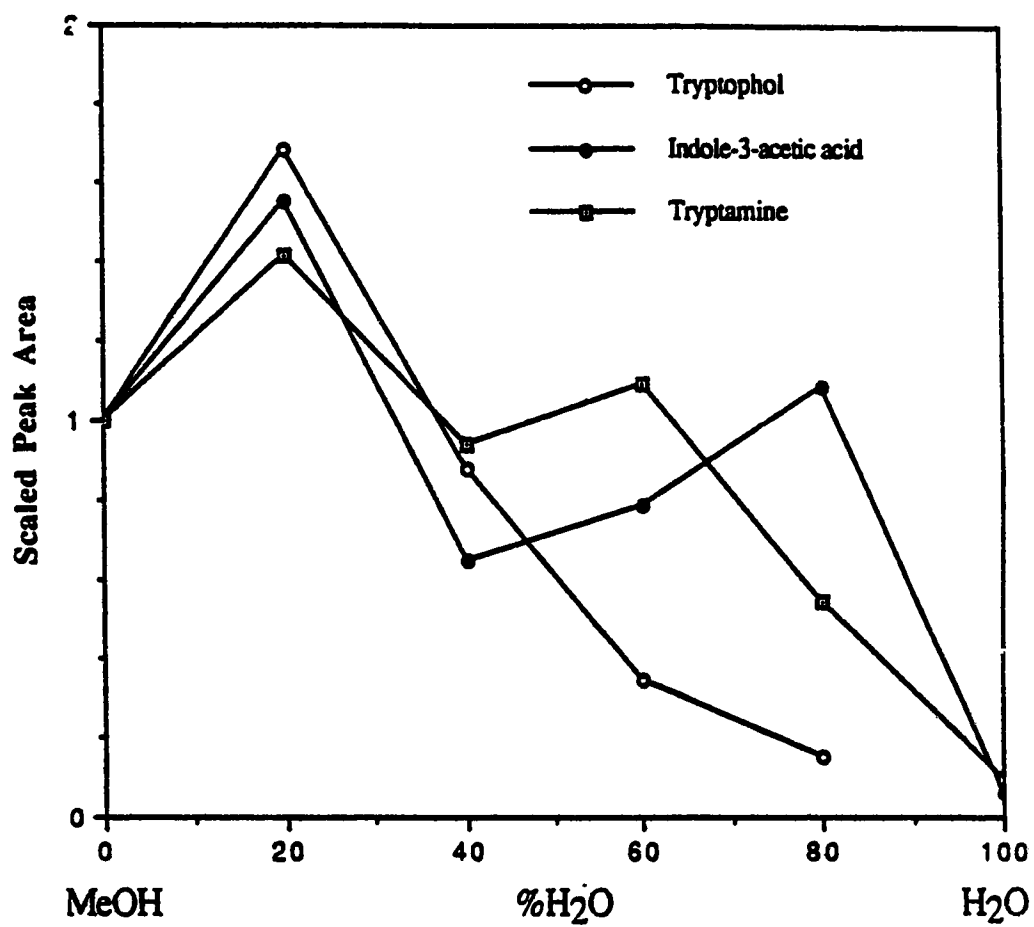


Figure 5.4. Scaled peak area as a function of the water content in the methanol/water mobile phase. The flow rate is kept constant at 1 mL/min.

liquid nitrogen trap, the present vacuum pumping system is not capable of removing water very efficiently. A larger pump and/or an additional trap may overcome this problem. Nevertheless, our study indicates that most common mobile phase used in HPLC can be used for the PSI interface. At present, we are limited to the isocratic conditions due to the lack of an additional liquid pump and a gradient controller for performing high pressure mixing gradient experiments. Future work in this area will include the feasibility study of gradient elution and the suitability of the use of various buffers for the interface.

To optimize the performance of the interface, the temperatures of the sample vaporizer and the capillary tube are found to be critical to enhance the signal stability and the detection sensitivity. Figure 5.5 shows the peak area of indole-3-acetic acid as a function of the sample vaporizer temperature. The temperature is measured near the nozzle front. Methanol is used as the mobile phase. As Figure 5.5 indicates, the peak area increases as the temperature rises. A sharp increase in sensitivity is observed when the temperature exceeds about 480°C. This sharp rise might be attributed to the fact that a threshold temperature exists and has to be reached for complete desolvation and vaporization. Thus, in LC/TOFMS with the PSI interface, the temperature of the sample vaporizer is always kept at maximum. The maximal temperature attended in the present system is limited by the heating capacity of the thermal coaxial heating wire. We are currently experimenting with the use of a block heater to increase the heating capacity. It should be noted that the use of even higher temperature for sample vaporization will not significantly increase the possibility of thermal decomposition. Recent study in this laboratory [126] finds that once a minimum heating rate is reached for a particular compound, the degree of thermal decomposition is independent of heating temperature used in the range from 200 to 550°C.

Another important parameter is the temperature of the capillary tube where the liquid converts into fine aerosols. Figure 5.6 plots the peak area of indole-3-acetic acid at different tube temperatures. When the temperature reaches above ~ 150°C, peak area does

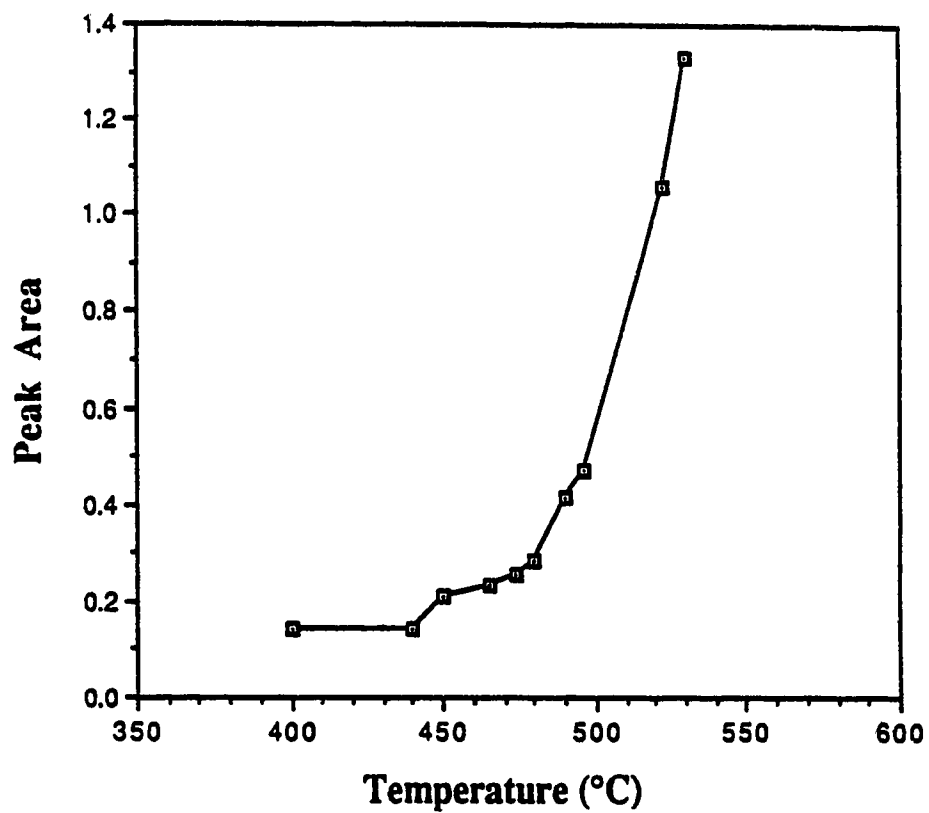


Figure 5.5. Peak area as a function of the temperature of the sample vaporizer. Indole-3-acetic acid is used as the test sample. Methanol is used as the mobile phase at a flow rate of 1 mL/min.

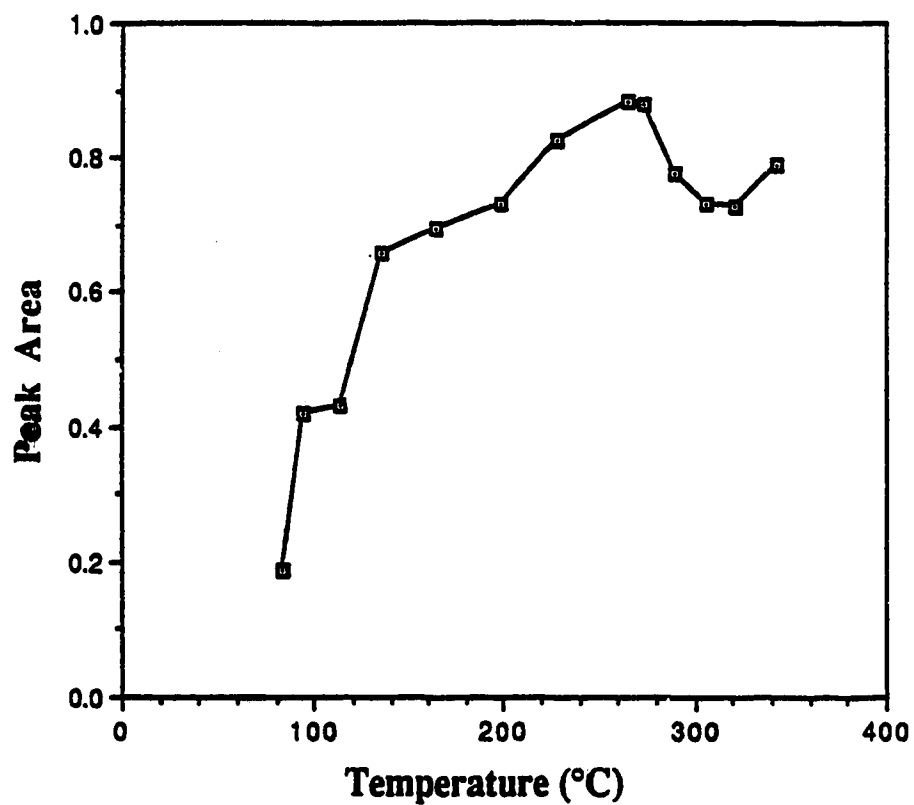


Figure 5.6. Peak area as a function of the temperature of the capillary tube. The LC conditions are the same as those used in Figure 5.5.

not vary significantly. Thus, the temperature of the capillary tube is normally set at 200°C. The use of higher temperature sometimes results in the deposition of the sample inside the tube and thus causes clogging of the tube. Also, it is found that the use of long capillary tube (>5 cm) is not necessary to generate stable signals. The shorter the tube the less the tube clogging problem is. With a 5 cm long tube, tube clogging rarely occurs.

We have also studied the flow rate dependence of the makeup gas on the performance of the interface. Figure 5.7 shows the peak area of indole-3-acetic acid as a function of the CO₂ flow rate. The mobile phase is methanol at the flow rate of 1 mL/min. Similar results are obtained when the mobile phase flow rate is in the range of 0.5 to 1.6 mL/min. It is found that the increase of the flow rate reduces the sensitivity of the system. However, the peak width is independent of the makeup flow rate in the working range examined. It appears that the main function of the makeup gas in the interface for LC/TOFMS is to prevent the feedback of the hot vapor into the cold solenoid. The minimum flow rate needed to prevent the feedback is dependent on the mobile phase flow rate. It is our experience that when the CO₂ flow rate used is less than 100 mL/min at the mobile phase flow rate of 1 mL/min, the hot vapor feedback can sometimes occur during the experiment. Thus, the flow rate of the makeup gas is always kept above 100 mL/min, although the sensitivity may not be at its optimal as shown in Figure 5.7. Other makeup gases such as helium and argon are also tested and similar results are observed. However, CO₂ is chosen here since it can be readily trapped by the liquid nitrogen trap once it is expanded into the vacuum system, resulting in low operational vacuum pressure.

Sample transfer efficiency in the PSI interface. Now that the major parameters affecting the performance are determined, a fundamentally important question is what is the sample transfer efficiency associated with the PSI interface? An ideal interface would introduce all samples into the ionization region of the mass spectrometer and, subsequently, be ionized and detected. With a pulsed ion detection system such as TOFMS, one of the major goals in designing the PSI interface is to introduce a large

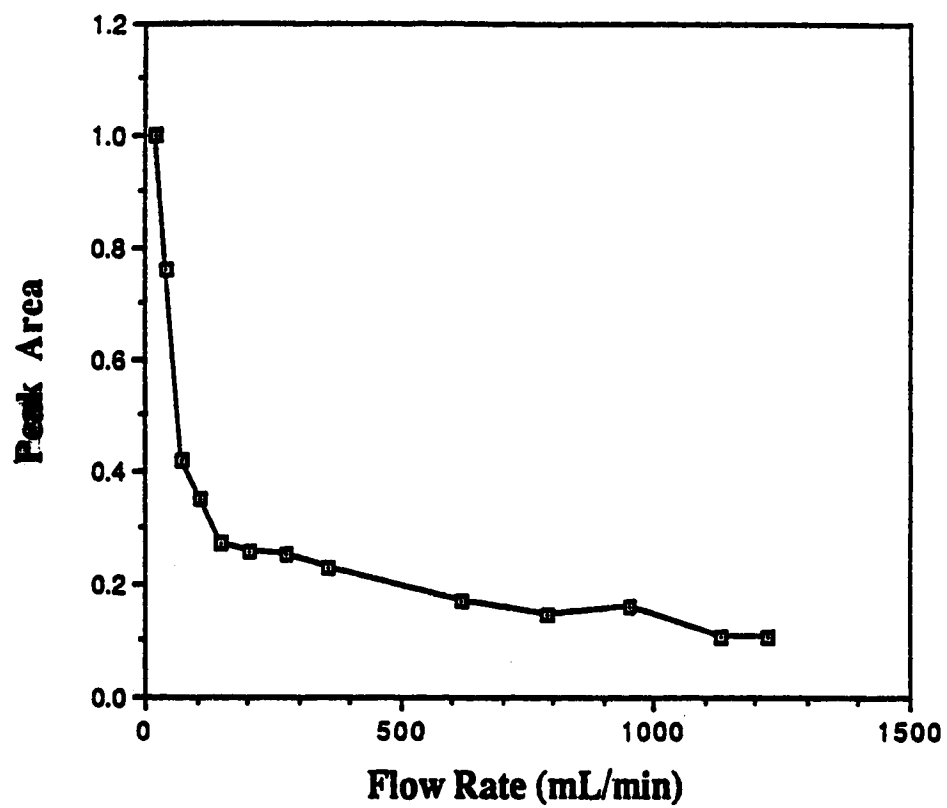


Figure 5.7. Peak area as a function of the makeup gas flow rate. The LC conditions are the same as those used in Figure 5.5.

amount of sample in a number of pulses to allow us to construct a chromatogram with a large peak area. The peak area is ultimately used for the determination of the sample concentration.

The following experiment is performed to determine the sample transfer efficiency in the PSI interface. A liquid nitrogen cooled sample collector is placed about 2 cm away from the orifice of the PSI interface. A known amount of sample is injected into the interface and vaporized. After the gas phase molecules exit the orifice, they are condensed onto the sample collector. The amount of the sample collected is then determined by using HPLC with a UV detector. The results of this measurement for several compounds are listed in Table 5.I. In this table, the sample transfer yield (Y) is defined as the ratio of the amount of the sample collected (N_{col}) and the amount of the sample injected (N_{inj}). It appears that the variation in transfer yield from compound to compound is very small. This small variation could be due to the differences in vaporization efficiency and the ability to generate fine aerosols among the compounds examined.

Table 5.I Sample transfer efficiency of the pulsed sample introduction interface.

Compound	m.p. (°C)	Transfer Yield (%)	Effective Transfer Efficiency (%)
Tryptophol	59	0.52	61
Pyrene	149–151	0.38	45
Indole-3-acetic acid	165–169	0.31	37
Acetaminophen	169–172	0.61	72
Triphenylene	197–200	0.53	62
Vanillic acid	210–213	0.44	52
Chrysene	252–254	0.38	45

In order to make a direct comparison of the sample transfer efficiency between a continuous sample introduction interface and a pulsed sample introduction interface, we can use a term, effective sample transfer efficiency (E), to characterize the interface. Since quantitation in LC is based on the peak area of the chromatogram, we can define E as A_p/A_t , where A_p is the sample peak area of the chromatogram generated from the actual sample introduced by the interface in a continuous or pulsed form to the mass spectrometer and A_t is the peak area of the chromatogram obtained by assuming the total sample injected being continuously transferred into the mass spectrometer system. In a continuous sample introduction interface, the calculation of the effective sample transfer efficiency is quite straightforward. Here, the peak area (A) is directly proportional to the total amount of the sample being detected (N). A is equal to kN , where k is a constant related to the properties of the detector and the recorder. The peak area (A_p) from the chromatogram with an injection of N_{inj} moles of sample is equal to kN_{col} , if only N_{col} moles of sample are transported by the interface to the mass spectrometer and the collected in the sample collector. However, the peak area (A_t) would be kN_{inj} if all of the sample injected were introduced into the mass spectrometer. Thus, the effective sample transfer efficiency is equal to N_{col}/N_{inj} or the sample transfer yield.

Now in the PSI interface the sample introduced into the system is concentrated into a few numbers of pulses. From each sample pulse, an ionization signal or a data point can be generated. In the end, a chromatogram is constructed from these data points. Therefore, the size of the peak area in this chromatogram is dependent on the intensity of the individual data point. The intensity of the data point is in turn directly related to the amount of the sample contained in each individual sample pulse. Although the total amount of the sample pulsed into the mass spectrometer over the entire peak elution time is small in the PSI interface, the amount of sample per pulse can be quite high, resulting in a large peak area. Clearly, in the calculation of the effective sample transfer efficiency for the PSI interface, A_p is not equal to kN_{col} . However, A_t is still equal to kN_{inj} as defined above.

Thus, $E = A_p/(kN_{inj})$. In reality, A_p (in arbitrary units) can be easily calculated from the chromatogram and N_{inj} is known.

To find out the k value, we need to examine carefully how we construct the chromatogram. From the experiment, we know that the individual sample pulse profile is close to a rectangular shape with a width of about 1 ms. Now if we assume that the chromatogram is constructed by using a continuous ion detection technique, then the peak in the chromatogram will consist of a series of rectangles (A_i) and its area can be readily estimated by multiplying the height (H_i) by 1 ms and it will be equal to kN_i , where N_i is the amount of sample contained in the sample pulse. Thus, $N_i = A_i/k = H_i \times 1/k$. Since the amount of sample introduced into the mass spectrometer in several pulses, we have $N_{col} = \sum N_i = \sum A_i/k$ or $k = \sum A_i/N_{col}$. Thus, $E = A_p/(kN_{inj}) = A_p/(\sum A_i/N_{col} \times N_{inj}) = A_p/\sum A_i \times N_{col}/N_{inj} = Y \times A_p/\sum A_i$.

To calculate the peak area, a curve fitting method is used. Figure 5.8 shows a typical flow injection peak (dot line) obtained by injecting indole-3-acetic acid into the LC/TOFMS system. The solid line is generated from a curve fitting program, Matlab (The Mathworks Inc.S.Natick.MA). The experimental data fits well to an exponentially modified Gaussian function [127, 128]. This function is used to determine the peak area as well as the peak height. The latter is then used to calculate the area of an individual sample pulse at a given elution time according to the equation, $A_i = H_i \times 1$. The ratio between the peak area (A_p) in Figure 5.8 obtained by the fitting function and the area sum of individual sample pulses ($\sum A_i$) is determined to be 118. Thus, for indole-3-acetic acid, the effective sample transfer efficiency is $0.31\% \times 118$ or 37%. This simply means that although only 0.31% of the sample or LC effluent is introduced into the vacuum system with PSI interface, it would be equivalent to transfer 37% of the sample into the mass spectrometer with a continuous sample introduction interface. However, without a sample enrichment device, it is difficult to introduce 37% of the LC effluent into the vacuum without overloading the pumping system.

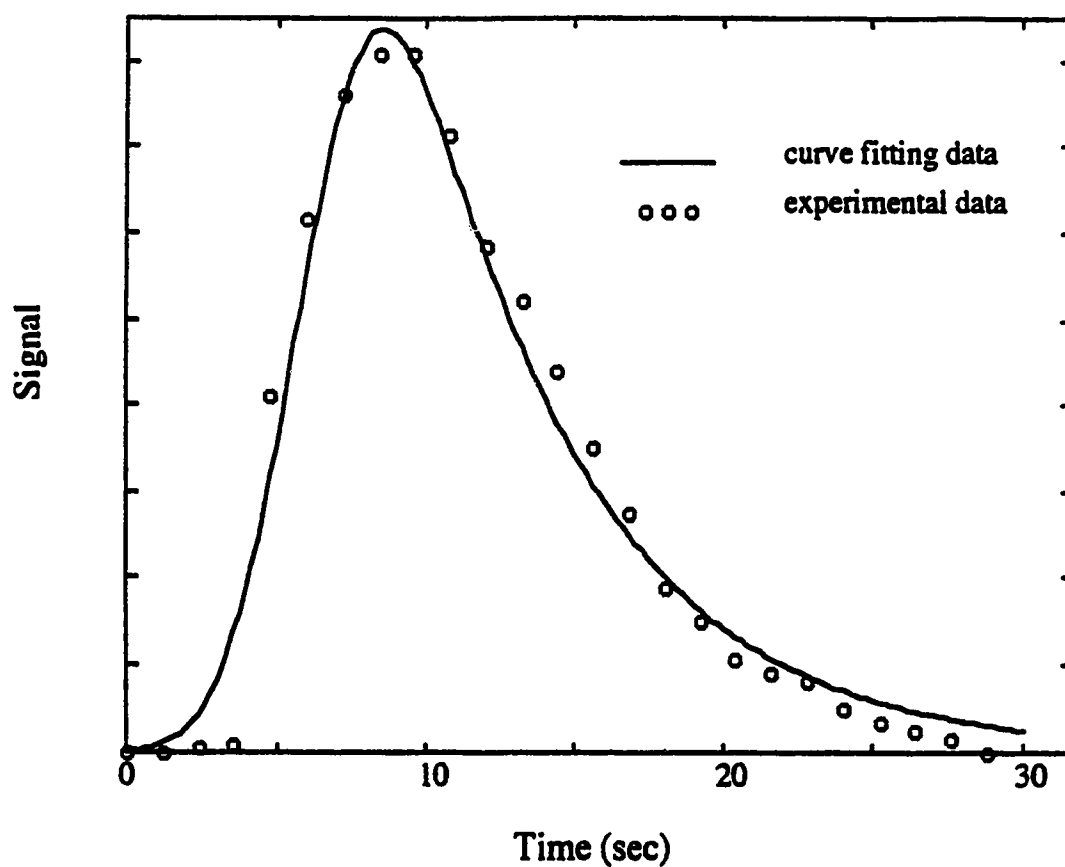


Figure 5.8. A typical peak obtained by the LC/TOFMS system. The dot line is the experimental result from the injection of indole-3-acetic acid. The solid line is generated from the curve fitting program.

Since other compounds examined give similar peak profiles as shown in Figure 5.8, the E values are simply calculated by multiplying Y and 118. Table 5.I shows that the effective sample transfer efficiency ranges from 37% to 72% for the compounds examined. This demonstrates that the PSI interface provides an efficient means of introducing LC effluent into the mass spectrometer. Combined with a pulsed ion detection system, it should provide high detection sensitivity. However, the overall sensitivity of the LC/TOFMS system is related to not only the sample transfer efficiency but also other factors such as the background noise level, the ionization volume, the ionization efficiency, and the ion detection efficiency. Currently the detection limit of the system is compound dependent, ranging from pg to ng. For example, the detection limits for aniline and tryptamine are about 10 pg and 100 pg, respectively.

5.4. Conclusion

We have shown that conventional liquid chromatography can be combined with time-of-flight mass spectrometry by using the PSI interface. It is found that the ion chromatograms obtained by using LC/TOFMS are similar to the UV chromatograms. The interface does not introduce significant peak distortion. Various experimental parameters affecting the performance of the LC/TOFMS system are investigated. It is found that high flow rate of mobile phase, ranging from 0.5 mL/min to 1.6 mL/min, can be used. Furthermore, it is shown that a number of organic solvents and water or a mixture of these can be used as the mobile phase. In addition, it is demonstrated that the temperature of the sample vaporizer should be kept as high as possible to achieve efficient sample vaporization. The temperature of the capillary tube in which the LC effluent is converted into aerosol is also found to be important. An optimal temperature range should be used to generate stable signals and also avoid the sample deposition which may cause the clogging of the sample transfer tube. The function of the makeup gas appears to be merely for preventing the hot gas from feedbacking into the cold solenoid. Finally, it is shown that

the effective sample transfer efficiency is quite high with the PSI interface. By pulsing only 0.31% to 0.61% LC effluent into the mass spectrometer, a chromatogram can be obtained with its peak area equivalent to that obtained by introducing 37% to 72% sample continuously. This important finding indicates that LC/TOFMS with the PSI interface could become a very sensitive means of molecular detection.

Chapter 6

Conclusion and Future Work

MPIMS has been widely used for chemical analysis, particularly resonant two-photon ionization (R2PI) SJ-MPIMS which can provide a two-dimensional detection scheme that allow unique identification of chemicals based on the mass spectra and the wavelength spectra. SJ-MPIMS has several unique features over other ionization techniques, such as higher sensitivity and higher selectivity. My research has mainly focused on the development of this technique for complex mixture analysis. In particular, a novel interface technique has been developed to combine LC with SJ-MPIMS.

In Chapter 2, two main problems associated with SJ-MPIMS, namely sensitivity and background, were studied. A method to enhance sensitivity by using a cylindrical lens improved signal sensitivity from 4 to 16 times without any loss in terms of mass resolution and supersonic jet cooling. The method developed to reduce background is based on the intrinsic construction of the mass spectrometer. Here, we apply a voltage to the deflector plate that will alter the ion trajectory of the background ions and sample ions. This results in spatial separation of the sample and background ions so that we can selectively detect sample or background ions.

Chapter 3 described the development of FAB as a means of sample vaporization for SJ-MPIMS. A variety of biological molecules as well as polycyclic aromatic hydrocarbons can be desorbed. The detection limit is typically in the low nanogram regime. We have shown that it is possible to use this technique to selectively ionize the active substance in a drug tablet with no sample preparation. We have demonstrated that FAB can be used to introduce samples into supersonic jet expansions without affecting the jet cooling. In addition, we have shown that tryptamine can be selectively desorbed from a mixture of indole-3-acetic acid and tryptamine by adding NaOH to the mixture.

In real analysis, the components of interest always exist in a complex matrix. Even though the MPI technique can selectively ionize particular components, it is always advantageous to have sample separation prior to the mass analysis. Since most biochemicals are separated with the use of high performance liquid chromatography (HPLC), we are involved in developing LC/SJMPIMS. The goal is to develop a convenient interface to combine conventional LC with TOFMS.

Most of the mass spectrometers used for LC detection belong to the sector or scanning type. These detectors always have problems such as lower ion transmission, limited mass range and longer time to acquire a mass spectrum. However, time-of-flight mass spectrometer can overcome these problems. In my research, a pulsed sample introduction interface has been developed for LC/TOFMS. Both Chapter 4 and Chapter 5 described the development of the LC/TOFMS with the PSI interface. In Chapter 4, the design of the interface has been shown. In addition, the performance of PSI in terms of its applicability, sensitivity, memory effect, peak tailing, and reproducibility have been studied. In Chapter 5, the applications of this PSI interface for on-line LC/TOFMS have been shown. The parameters affecting the performance of the LC/TOFMS system have been studied in detail.

The future development of this LC/TOFMS involves two stages. In the first stage, the sensitivity optimization of our current system will be addressed. Although picogram detection limits have been demonstrated, the sensitivity of the LC/TOFMS system with MPI can be enhanced by several means. They include (1) the use of a larger diameter orifice (e.g. 1 - 2 mm) to increase the throughput, (2) the use of a slit nozzle for sample introduction, and (3) the use of a cartridge heater to provide better heating in the sample vaporizer of the high temperature nozzle.

A data acquisition system is also under development for LC/TOFMS. This system will be able to collect spectra at maximum 20 Hz, store in a PC computer, and allow us to do data manipulation later to generate chromatograms and obtain the mass spectra of

eluted peaks.

In the second stage, this LC/TOFMS will be applied for real sample analysis such as the analysis of residues from drugs, antibiotics and pesticides. During these analyses, the problems of the PSI interface will be identified and further improvements of the interface can be made. Problems related to the chromatographic separation conditions such as high salt buffers and gradient elution that may affect the performance of the PSI, will be studied.

In addition, combining supersonic jet spectroscopy (SJS) with LC/TOFMS is underway. This spectroscopic technique will enhance the detection specificity of TOFMS. This technique provides a two-dimension detection scheme based on mass spectra and wavelength spectra which is particularly useful for isomer identification.

In order to extend the applicability of this LC/TOFMS to a wider range of compounds, an EI source will be developed. The main advantage of incorporating EI to our system is its low cost, simplicity, and availability of EI spectra for unknown identification. Mass resolution will also be improved from the current 300 to above 2000 by incorporating a reflector to this linear TOFMS. It is our hope that this PSI-LC/TOFMS system will provide complementary information to existing LC/MS for the detection of thermally labile and nonvolatile molecules.

All the works covered in this thesis have been published or submitted for publication. A summary of publications is given in Table 6.I.

Table 6.I Publications

Authors	Title	Journal
Alan P.L. Wang; J.Y. Zhang; D.S. Nagra; and Liang Li	Signal Enhancement by Using a Planar Laser Beam for Multiphoton Ionization in a Supersonic Jet/Reflectron Time-of-Flight Mass Spectrometer	Applied Spectroscopy 45, 304 (1991)
Liang Li; Alan M. Hogg; Alan P.L. Wang; Y.J. Zhang; and D.S. Nagra	Pulsed Fast Atom Bombardment Sample Desorption with Multiphoton Ionization in a Supersonic Jet/Reflectron Time-of-Flight Mass Spectrometer	Analytical Chemistry 63, 974 (1991)
Alan P.L. Wang and Liang Li	A Method for Background Reduction in a Supersonic Jet/Multiphoton Ionization Reflectron Time-of-Flight Mass Spectrometer	Applied Spectroscopy 45, 969 (1991)
Alan P.L. Wang and Liang Li	Pulsed Sample Introduction Interface for Combining Flow Injection Analysis with Multiphoton Ionization Time-of-Flight Mass Spectrometry	Analytical Chemistry 64, 769 (1992)

Authors	Title	Journal
Alan P.L. Wang and Liang Li	Liquid Chromatography/Time-of- Flight Mass Spectrometry with a Pulsed Sample Introduction Interface	Submitted to Analytical Chemistry

Bibliography

1. Johnson, P. M., Berman, M. R., and Zakheim, D. *J. Chem. Phys.* 1975, 62, 2500.
2. Petty, G., Tai, C., and Dalby, F. W. *Phys. Rev. Lett.* 1975, 34, 1207.
3. Johnson, P. M. *J. Chem. Phys.* 1975, 62, 4562.
4. Rava, R. P., and Goodman, L. *J. Am. Chem. Soc.* 1982, 104, 3815.
5. Nieman, G. C., and Colson, S. D. *J. Chem. Phys.* 1978, 68, 5656.
6. Robin, M. B., and Kuebler, N. A. *J. Chem. Phys.* 1978, 69, 806.
7. Antonov, V. S., Knyazev, I. N., Letokhov, V. S., Matjiuk, V. M., Moshev, B. G., and Potapov, V. K. *Opt. Lett.* 1978, 3, 37.
8. Boesl, U., Neusser, H.J., Schlag, E. W. *Z. Naturforsch. A.* 1978, 33, 1549.
9. Krogh-Jespersen, K., Rava, R. P., Goodman, L. *Chem. Phys.* 1979, 44, 295.
10. Fisanick, G.J., Eichelberger, IV, T.S., Heath, B. A., Robin, M. B. *J. Chem. Phys.* 1980, 72, 5571.
11. Duncan, M.A., Dietz, T.G., Smalley, R. E. *Chem. Phys.* 1979, 44, 415.
12. Boesl, U., Neusser, H.J., Schlag, E. W., *J. Chem. Phys.* 1980, 72, 4327.
13. Frueholz, R., Wessel, J., Wheatley, E. *Anal. Chem.* 1980, 52, 281.
14. Seaver, M., Hudgens, J. W., DeCorpo, J. J. *Int. J. Mass Spectrom. Ion Phys.* 1980, 34, 159.
15. Johnson, P.M. *Acc. Chem Res.* 1980, 13, 20 and references cited therein.
16. Reilly, J. P., and Kompa, K.L. *J. Chem. Phys.* 1980, 73, 5468.
17. Zandee, L., Bernstein, R. B., and Lichtin, D. A. *J. Chem. Phys.* 1978, 69, 3427.
18. Zandee, L., and Bernstein, R. B. *J. Chem. Phys.* 1979, 70, 2574.
19. Zandee, L., and Bernstein, R. B. *J. Chem. Phys.* 1979, 71, 1359.
20. Bernstein, R. B. *J. Phys. Chem.* 1982, 86, 1178.
21. Lubman, D. M., Naaman, R., and Zare, R. N. *J. Chem. Phys.* 1980, 72, 3034.

22. Cooper, C. D., Williamson, A. D., Miller, J. C., and Compton, R. N. *J. Chem. Phys.* 1980, 73, 1527.
23. Dietz, T. G., Duncan, M. A., Liverman, M.G., and Smalley, R. E. *Chem. Phys. Lett.* 1980, 70, 246.
24. Dietz, T. G., Duncan, M. A., Liverman, M.G., and Smalley, R. E. *Chem. Phys. Lett.* 1980, 73, 4816.
25. Rettner, T. G., and Brophy, J. H. *Chem. Phys.* 1981, 25, 53.
26. Boesl, U., Neusser, H. J., and Schlag, E. W. *Chem. Phys.* 1981, 55, 193.
27. Wessel, J. E., Cooper, D. E., and Klimcak, C. M. In *Laser Spectroscopy for Sensitive Detection*, Gelbwach, J. A. Ed., Proc. Society of Photo-Optical Instrumentation Engineers: Bellingham, WA, 1981, p 286.
28. Lubman, D. M., and Kronick, M. N. *Anal. Chem.* 1982, 54, 660.
29. Sack, T. M., McCrery, D. A., and Gross, M. L. *Anal. Chem.* 1985, 57, 1290.
30. Rhodes, G., Opsal, R. B., Meek, J. T., and Reilly, J. P. *Anal. Chem.* 1983, 55, 280.
31. Irion, M. P., Bowers, W. D., Hunter, R. L., Rowland, F. S., and McIver, Jr. R. T. *Chem. Phys. Lett.* 1982, 93, 375.
32. Carlin, T. J., and Freiser, B. S. *Anal. Chem.* 1983, 55, 955.
33. Tembreull, R., and Lubman, D. M. *Anal. Chem.* 1984, 56, 1962.
34. Gobeli, D. A., Yang, J. J. and El-Sayed, M. A. *Chem. Rev.* 1985, 85, 529.
35. Tembreull, R., Sin, C. H., Li, P., Pang, H. M., and Lubman, D. M. *Anal. Chem.* 1985, 57, 1084.
36. Tembreull, R., Dunn, T. M., and Lubman, D. M. *Spectrochimica Act.* 1986, 42A, 899.
37. Tembreull, R., and Lubman, D. M. *Anal. Chem.* 1986, 58, 1299.
38. Tembreull, R., and Lubman, D. M. *Anal. Chem.* 1987, 59, 1003.
39. Tembreull, R., and Lubman, D. M. *Anal. Chem.* 1987, 59, 1028.

40. Tembreull, R., and Lubman, D. M. *Appl. Spectros.* 1987, 41, 431.
41. Engelke, F., Hahn, J. H., Henke, W., and Zare, R. N. *Anal. Chem.* 1987, 59, 909.
42. Hahn, J. H., Zenoba, R., and Zare, R. N. *J. Am. Chem. Soc.* 1987, 109, 2842.
43. Grotemeyer, J., Boesl, U., Walter, K., and Schlag, E. W. *Org. Mass Spectrom.* 1986, 21, 595, *Org. Mass Spectrom.* 1988, 23, 388.
44. Grotemeyer, J., Boesl, U., Walter, K., and Schlag, E. W. *Org. Mass Spectrom.* 1986, 21, 645.
45. Grotemeyer, J., Boesl, U., Walter, K., and Schlag, E. W. *J. Am. Chem. Soc.* 1986, 108, 4233.
46. Lubman, D. M. *Anal. Chem.* 1986, 59, 31A.
47. Hager, J. W., and Wallace, S. C. *Anal. Chem.* 1988, 60, 5.
48. Brophy, J. H., and Rettner, C. T. *Opt. Lett.* 1979, 4, 337.
49. Boesl, U., Neusser, H. J. and Schlag, E. W. *J. Chem. Phys.* 1980, 72, 4327.
50. Fluendy, M. A. D., and Lawley, K. P. *Chemical Applications of Molecular Beam Scattering*, Chapman and Hall: London, 1973, Chapter 3.
51. Kantrowitz, A., and Grey, J. *Rev. Sci. Instrum.* 1951, 22, 328.
52. Anderson, J. B., Andres, R. P., and Fenn, J. B. *Adv. Chem. Phys.* 1966, 10, 275.
53. Anderson, J. B. In *Molecular Beams from Nozzle Sources in Molecular Beams and Low Energy Gasdynamics*, Wegener, P.P., Ed., M. Dekker: New York, 1974.
54. Smalley, R. E., Wharton, L., and Levy, D. H. *Acc. Chem. Res.* 1977, 10, 139.
55. McClelland, G. M., Saenger, K. L., Valentinin, J. J., and Herschbach, D. R. *J. Phys. Chem.* 1979, 83, 947.
56. Miller, T. A. *Science* 1984, 223, 545.

57. Levy, D. H. *Sci. Amer.* 1984, 250, 96.
58. Hayes, J. M., and Small, G. J. *Anal. Chem.* 1983, 55, 565A.
59. Hayes, J. M. *Chem. Rev.* 1987, 87, 745.
60. Arpino, P.J., and Guiochon, G. *Anal. Chem.* 1979, 51, 682A.
61. Guiochon, G., and Arpino, P.J. *J. Chromatogr.* 1983, 271, 13.
62. Markey, S. P. *Anal. Chem.* 1970, 42, 306.
63. Games, D. E. *Adv. Chromatogr.* 1983, 21, 1.
64. Allison, J., Holland, J. F., Enke, C. G., and Watson, J. T. *Anal. Instrumentation* 1987, 16, 207.
65. Niessen, W. M. A., and van der Greef, J. In *Liquid Chromatography- Mass Spectrometry*, Cazes, J. Ed., M. Dekker: New York, 1992, Chapter 3.
66. Tal'roze, V. L., Skurat, V. E., Gorodetskii, I. G., and Zolotai, N. B. *Russ. J. Phys. Chem.* 1972, 46, 456.
67. Karas, M., and Bahr, U. *Trends Anal. Chem.* 1990, 9, 321.
68. Li, L., and Lubman, D. M. *Rev. Sci. Instrum.* 1988, 59, 557.
69. Lubman, D.M., and Li, L. "Resonant Two-Photon Ionization Spectroscopy of Biological Molecules in Supersonic Jets Volatilized by Pulsed Laser Desorption", In *Lasers and Mass Spectrometry*, D.M. Lubman, Ed., Oxford: New York, 1990, Chap. 16, p354.
70. Grotemeyer, J., and Schlag, E. W. *Angew. Chem. Int. Ed. Engl.* 1988, 27, 447.
71. Li, L., Hogg, A.M., Wang, A.P.L., Zhang, J.Y., and Nagra, D.S. *Anal. Chem.* 1991, 63, 974.
72. Nagra, D. S., Zhang, J. Y., Li, L. *Anal. Chem.* 1991, 63, 2188.
73. Mamyrin, B. A., Karataev, V. I., Schmikk, D. V., and Zagulin, V. A. *Sov. Phys. JEPT (Engl. Trans.)*, 1973, 37, 45.

74. Walter, K., Boesl, U., and Schlag, E. W. *Int. J. Mass Spectrom. Ion Processes* 1986, 71, 309.
75. Yang, M., and Reilly, J. P., *Anal. Instrumentation* 1987, 16, 133.
76. Li, L., and Lubman, D. M. *Appl. Spectrosc.* 1988, 42, 418.
77. Li, L., and Lubman, D. M. *Anal. Chem.* 1988, 60, 2591.
78. Li, L., and Lubman, D. M. *Appl. Spectrosc.* 1989, 43, 543.
79. Lubman, D.M., and Jordan, R.M. *Rev. Sci. Instrum.* 1985, 56, 373.
80. R.M. Jordan Co., 990 Golden Gate Terrace, Grass Valley, CA.
81. Deluca, M.J., and Johnson, M.A. *Chem. Phys. Lett.* 1989, 162, 255.
82. Sin, C.H., Pang, H.M., Lubman, D.M., and Zorn, J.C. *Anal. Chem.* 1986, 58, 487.
83. Rizzo, T.R., Park, Y.D., Peteanu, L., and Levy, D.H. *J. Chem. Phys.* 1985, 83, 4819.
84. Cable, J.R., Tubergen, M.J., and Levy, D.H. *J. Am. Chem. Soc.* 1987, 109, 6198.
85. Barber, M., Bordoli, R.S., Elliott, G.J., Sedgwick, R.D., and Tyler, A.N. *Anal. Chem.* 1982, 54, 545A.
86. Hogg, A.M. *Int. J. Mass Spectrom. Ion Phys.* 1983, 49, 25.
87. Alexander, A.J., and Hogg, A.M. *Int. J. Mass Spectrom. Ion Phys.* 1986, 69, 297.
88. Rizzo, T.R., Park, Y.D., Peteanu, L.A., and Levy, D.H. *J. Chem. Phys.* 1986, 84, 2534.
89. Li, L., and Lubman, D.M. *Anal. Chem.* 1989, 61, 1911.
90. *Chemical Analysis of Polycyclic Aromatic Compounds*, Tuan, V-D. Ed., John Wiley & Sons, Inc.: New York, 1989.
91. Caprioli, R.M., Fan, T., and Cottrell, J.S. *Anal. Chem.* 1986, 58, 2949.
92. Li, L., and Lubman, D.M. *Rapid Commun. Mass Spectrum.* 1989, 3, 12.

93. Beavis, R.C., Linder, J., Grotemeyer, J., and Schlag, E.W. *Chem. Phys. Lett.* 1988, 146, 310.
94. Anderson, W.R., Jr., Frick, W., and Daves, G.D., Jr. *J. Am. Chem. Soc.* 1978, 100, 1974.
95. Freas, R.B., Ross, M.M., and Campana, J.E. *J. Am. Chem. Soc.* 1985, 107, 6195.
96. Van Breemen, R.B., Snow, M., and Cotter, R.J. *Int. J. Mass Spectrom. Ion Processes* 1983, 49, 35.
97. Cotter, R. *Anal. Chem.* 1980, 52, 1767.
98. Campana, J.E., and Freas, R.B. *J. Chem. Soc. Chem. Commun.* 1984, 1414.
99. Wang, A.P.L., Zhang, J-Y., Nagra, D.S., and Li, L. *Appl. Spectrosc.* 1991, 45, 304.
100. Caprioli, R.M. *Anal. Chem.* 1983, 55, 2387.
101. Scott, R., Scott, C., Munroe, M., and Hess, Jr. J. *J. Chromatogr.* 1974, 99, 395.
102. Tal'Rose, V., Karpov, G., Gordoetshii, I., and Skurat, V. *Russ. J. Phys. Chem.* 1968, 42, 1658.
103. Baldwin, M., and McLafferty, F. *Org. Mass Spectrom.* 1973, 7, 111.
104. Henion, J.D. *Anal. Chem.* 1978, 50, 1687.
105. Blakley, C.R., and Vestal, M.L. *Anal. Chem.* 1983, 55, 750.
106. Willoughby, R.C., and Browner, R.F. *Anal. Chem.* 1984, 56, 2626.
107. Carroll, D.I., Dzidic, I., Stillwell, R.N., Haegele, K.D., and Horning, E.C. *Anal. Chem.* 1975, 47, 2369.
108. Thomson, B.A., Iribarne, J.V., and Dziedic, P.J. *Anal. Chem.* 1982, 54, 2219.
109. Whitehouse, C.M., Dreyer, R.N., Yamashita, M., and Fenn, J.B. *Anal. Chem.* 1985, 57, 675.

110. See for examples, (a). Crowther, J.B., Covey, T.R., and Henion, J.D. In *Detectors for Liquid Chromatography*, Yeung, E.S., Ed., John Wiley & Sons: 1986, New York, Chapter 8, pp292-330. (b). *Liquid Chromatography/Mass Spectrometry, Applications in Agricultural, Pharmaceutical, and Environmental Chemistry*, Brown, M.A., Ed., American Chemical Society: 1990, Washington, DC.
111. Imasaka, T., Yamaga, N., and Ishibashi, N. *Anal. Chem.* 1987, 59, 419.
112. Anderson, B.D., and Johnston, M.V. *Appl. Spectrosc.* 1987, 41, 1358.
113. Lubman, D.M. *Mass Spectrometry Reviews* 1988, 7, 535-554 and 559-592.
114. Ruzicka, J., and Christian, G.D. *Analyst* 1990, 115, 475.
115. Stewart, K.K. *Anal. Chem.* 1983, 55, 931A.
116. Pang, H.M., Sin, C.H., and Lubman, D.M. *Appl. Spectrosc.* 1988, 42, 1200.
117. Li, L., and Lubman, D.M. *Rev. Sci. Instrum.* 1989, 60, 499.
118. Sin, C.H., Pang, H.M., and Lubman, D.M. *Anal. Instrumentation* 1988, 17, 87.
119. Beuhler, R.J., Flanigan, E., Greene, L.J., and Friedman, L. *Biochem. Biophys. Res. Commun.* 1972, 46, 1082.
120. Wang, A. P. L., and Li, L. *Appl. Spectrosc.* 1991, 45, 969.
121. Vestal, M.L., Winn, D.H., Vestal, C.H., and Wilkes, J.G. In *Liquid Chromatography/Mass Spectrometry, Applications in Agricultural, Pharmaceutical, and Environmental Chemistry*, Brown, M.A., Ed., American Chemical Society: 1990, Washington, DC., Chapter 14, pp215-231.
122. Levy, D.H., Wharton, L., and Smalley, R.E. In *Chemical and Biochemical Applications of Lasers*, Moore, C.B., Ed., Academic: 1977, New York., Vol. II, pp1-41.
123. Bartell, L.S. *J. Phys. Chem.* 1990, 94, 5102.
124. Pang, H.M., and Lubman, D.M. *Rev. Sci. Instrum.* 1988, 59, 2460.

125. Wang, Alan P. L., and Li, L. *Anal. Chem.* 1992, 64, 769.
126. Nagra, D.S., Zhang, J.Y., and Li, L. manuscript in preparation.
127. Groshka, E. *Anal. Chem.* 1972, 44, 1733.
128. Foley, J.P. *J. Chromatogr. Sci.* 1984, 22, 40.